Final Report
Brayton Cycle Demonstration Unit

December 7, 2018

Team 1A

Jacob Barker
Samm Metcalfe
Ashley Shumaker

ME 486C – Fall 2018

Instructor: Sarah Oman
Faculty Advisor: David Willy

DISCLAIMER

This report was prepared by students as part of a university course requirement. While considerable effort has been put into the project, it is not the work of licensed engineers and has not undergone the extensive verification that is common in the profession. The information, data, conclusions, and content of this report should not be relied on or utilized without thorough, independent testing and verification. University faculty members may have been associated with this project as advisors, sponsors, or course instructors, but as such they are not responsible for the accuracy of results or conclusions.

EXECUTIVE SUMMARY

The design team was challenged by David Willy, a Mechanical Engineering Instructor at Northern Arizona University, to design and build an in-class demonstration unit to demonstrate a specific Thermodynamic Cycle. The chosen cycle was left to the discretion of the team (with final approval by the client), but the client had several specific requests for the design team:

- Safe for classroom setting
- No combustion
- Demonstrate at least 1 application
- Mounted on Cart
- Powered by wall outlet or self-powered
- Collect and analyze data
- Easily identifiable subsystems
- User's manual and supporting literature

After discussing possible alternatives with the client, the team settled on the Brayton Cycle for the working cycle, as it is one of the most important cycles taught in NAU Thermodynamics II courses. The team began by researching different applications of the Brayton Cycle in the real world, and ultimately chose to replicate a turbojet as it is the simplest application of the Brayton Cycle and would streamline both construction of and instruction with the unit.

The team analyzed the Customer Requirements, generated related Engineering Requirements to meet these Customer Requirements, and completed a House of Quality to determine the most important Engineering Requirements for the project. Research and Analyses were also conducted for the three primary components of a turbojet model: the compressor, the combustion chamber, and the turbine.

Next the team worked on creating numerous possible designs, and selected the best design using a Pugh Chart and Decision Matrix. After initial selection, the chosen design was slightly modified to improve performance. The final design uses a simplified turbojet model consisting of the three components mentioned above. These components were 3D printed from PLA, and mounted on an aluminum shaft. This assembly sits inside of an acrylic tube, which is split in half and hinged to allow for maintenance and hands-on interactivity. The device uses heated compressed air in place of combustion, provided by an air compressor and two compressed air tanks fed through a heat exchanger consisting of a band heater and cast-iron pipe. The model is mounted on a cart with equipment to measure temperature and pressure at four states. Temperature data is collected by 4 Thermocouples and a National Instruments DAQ, and pressure data is taken by two pressure transducers and a manifold system. The final product is shown in Figure I below.

Figure I: Brayton Cycle Demonstration Unit

ACKNOWLEDGEMENTS

The design team would like to thank everyone who provided us guidance over the past year. First and foremost, we would like to thank our client and first-semester instructor Mr. David Willy, for challenging us to complete this project and providing helpful input every step of the way. We would also like to thank our lecturer, Dr. Sarah Oman, for providing valuable feedback and making design suggestions. Amy Swartz, the class TA for both semesters of the project, helped the team complete several assignments, offered design ideas, and reviewed our work on many occasions. Several other faculty members also met with our design team to provide advice. Dr. Thomas Acker helped the team in their initial aerodynamics work, and Dr. Heidi Feigenbaum made suggestions for blade deflection analyses using finite element analysis and beam analysis. Finally, we would like to thank the Mechanical Engineering Department and CEIAS at Northern Arizona University for sponsoring the project.

Table of Contents

1 BACKGROUND

1.1 Introduction

A hands-on classroom experience can be vital for a college student's understanding of course material. This project's main goal was to help bridge the gap between figures and equations on paper to a functioning model that a student can interact with. The Brayton Cycle is of particular interest in Thermodynamics as it is the working cycle used in gas turbine engines such as those found in airplanes. Current NAU engineering students are taught the theory and mathematics behind Brayton Cycle, but their exposure to this cycle's applications in the real world is limited to textbook illustrations and online videos. In order to enhance student understanding of the Brayton Cycle, the team was tasked with designing and manufacturing a Brayton Cycle Demonstration Unit which can be used in Thermodynamics courses.

1.2 Project Description

Thermodynamics II (ME392) classes need in-class demonstration equipment to help teach specific topics. This project will aide in the understanding of a specific cycle that will be determined by the client and team. For this project, one or more working benchtop examples are required to help with instruction. An example of a system within the design space that the client has in mind can be found here: https://www.youtube.com/watch?v=6rX4xv5-NvE&feature=youtu.be. Note that this is just an example and should NOT be directly copied. Client Requirements

- Must be able to operate in a safe manner for classroom demonstration
- Must not function from combustion (compressed air or electrical source is acceptable)
- Must be able to demonstrate at least one application (turbofan, etc)
- Must be mounted onto a cart for ease of transport in and out of the classroom
- Must be powered from typical wall outlet sources or be self powered
- Should be able to collect data to analyze performance
- The system does not have to work exactly as in the real world, but a user should be able to convert the testing results so it can be compared to a real world system
- Should be able easy to identify subsystems and functions of those subsystems within the demo unit

Client Based Deliverables

- At least one functioning system with data collection
- User's manual for operation
- Supporting Literature for system and subsystem functionality
- Short video demonstration in support of the User's Manual

2 REQUIREMENTS

As noted previously, the customer for this project is David Willy, an Instructor at NAU, who intends to use this model as an in-class teaching tool. In designing this device, we wanted to ensure first and foremost that it meets his wants and needs for his intended usage. Thus, as a starting point, we first met with our client several times to determine what was most important to him. Using these client needs as well as the project description, we generated a list of customer requirements, and subsequently a list of engineering requirements to ensure these customer requirements were met.

2.1 Customer Requirements (CRs)

After meeting several times with Mr. Willy, reviewing the project description, and discussing the problem, the team came up with the following list of customer requirements (CRs), presented in Table 1 for reference. The important of each requirement was weighted on a scale from one to five, which was used in constructing the House of Quality in Section 2.5

Table 1: Customer Requirements

Requirement	Weight
Scaled	3
Portable	4
Interactive	2
Educational	5
Usable in a lecture	5
Safe	5
Wall outlet or self-powered	4
Instructions for use	3
Durable/Reliable	3

The client's biggest priority was for the model to be educational. To accomplish this, he had several specific requests. The model must take temperature and pressure measurements at the four key states in the thermodynamic cycle, and it must be transparent to allow students to see its inner-workings. Our team generated several more customer requirements based on this request: educational and usable in a lecture. For this model to be beneficial it must add a teaching element that a lecture alone cannot accomplish. Furthermore, the model must operate within the timeframe of a lecture, so its operation time cannot be exceedingly long. It must also be scaled, portable, and fit on a cart for transport into and out of a classroom. The model must also include instructions so that any instructor or student is easily able to operate it. The model must be reliable, so that it operates the same way every time, and durable, so that it lasts for many semesters of instruction. A model that only works intermittently or breaks after just a few uses would not be a worthwhile investment. Finally, the model needs to be safe for both the instructor and the students. To ensure safety and compatibility in the classroom, the model must receive power from a standard wall outlet or be self-powered.

2.2 Engineering Requirements (ERs)

With the list of customer requirements established the team sought to create measurable Engineering Requirements (ERs) to meet all customer needs. Table 2 provides a summary of these requirements.

Table 2: Engineering Requirements

ER	Target
Size	≤ 2’ x 3’
Weight ≤100 lbs.	≤ 100 lbs.
Data Acquisition	Pressure and Temperature values at every stage
Demonstration time	≤ 15 min
Outer Casing	Must be clear
Power source	120V 60 Hz AC and/or compressed air
Safety	Minimize exposure to dangerous/moving parts
Lifespan	≥ 10 semesters

To make the model scaled and portable, the team decided that the model should fit within a 2’x3’ perimeter and should weigh less than 100 pounds. This was a rough estimate based on an average cart size that would be suitable in the classroom. The weight was a large overestimate but ensured the model would be movable by a single person when placed on a cart. The ER describing the ability to measure temperature and pressure at every state came directly from a customer request. This makes the model interactive and adds to its educational value. In analyzing Brayton Cycle problems, pressure and temperature are the first pieces of information needed, so these measurements are crucial to the effectiveness of this model.

To further enhance the educational aspect of the design, the team decided that the outer casing must be constructed from clear material to allow students to visualize how the model runs and how the cycle operates. To ensure the model is usable within a lecture, the team limited its total operation time to 15 minutes. The team also decided the model should be powered by 120v, 60Hz electrical power and/or compressed air, so that it can be easily and safely powered in the classroom. To further enhance safety, the team also agreed that there should be minimal exposure to any dangerous or moving parts; all moving components or those carrying electricity would be properly covered.

To address reliability and durability, the team created the ER that the model must last 10 semesters minimum. Ideally the model would last much longer, but the team felt that a five-year period would allow the model to fulfill its purpose and provide sufficient time for the investment costs to be recuperated.

2.3 Testing Procedures

The team also developed a set of procedures to test each requirement to ensure they are met. Some of the engineering requirements are quite easy to measure, such as size and weight. These can be measured with a simple tape measure and scale, although to measure weight the team will likely measure large components (turbine, cart, air compressor, etc.) separately, then sum the weights to calculate a total. Temperature and pressure measurement are also simple to test; the team will simply verify each sensor is collecting a reading that compares well with expectations (e.g. the ambient temperature and pressure should match local data).

To test demonstration time, the team will run through an entire cycle of the device, from initial startup to data acquisition, to verify the cycle can be completed in the allotted 15 minutes.

To test safety, our team created a two-part test. First, the team will perform a visual inspection of the device to make sure everything is installed and fastened down correctly. If necessary, the team will adjust fasteners and joints. Next, we will enclose the testing area in a thin material, most likely tissue paper, and start up the device, allowing it to run through the cycle. If the device damages the lining, it will be evident that there is a safety issue somewhere in the design. However, if the paper remains undamaged, the device should be safe to use. The only issue with this test may be the exhaust at the turbine exit, so we may need to alter this test somehow in this location.

Testing reliability will be more difficult, as we will only be able to test the device when it is new. However, to predict reliability, we will simply perform numerous test cycles of the device to monitor its performance over time. The team set a goal for the device to last about 10 semesters. This device will most likely only be used about 4-5 times per semester, for a total of about 50 uses. To test this, the team will run through 25 test cycles with the device. We will watch to ensure all parts operate correctly, and check measurements to verify that they do not change over time, indicating a sensor error.

Finally, our team plans to test performance characteristics of the device, such as wind speed and/or thrust, and heat transfer of the heating element during operation. Ideally, this model should provide temperature and pressure differentials large enough to provide useful data, as well as a work output in the form of thrust. Measuring the efficiency of the combustion chamber will be done with an infrared thermometer, and wind speed and thrust will be measured using an anemometer and potentially a strain gauge.

2.5 House of Quality

After generating a list of engineering requirements, a Quality Functional Deployment (QFD) or “House of Quality” was used to determine which were most important. To begin, the team rated each customer need on its level of importance on a scale from one to five. Next, each engineering requirement was rated based on its effect in meeting the customer needs. A score of 1 indicates a weak relationship, 3 indicates a moderate relationship, 9 indicates a strong relationship, and a blank indicates no relationship. These relative scores were multiplied by the respective weights for each customer need and summed to calculate the Absolute Technical Importance. The Relative Technical Importance is simply an ordinal ranking of the engineering requirements based on their absolute technical importance. Figure 1 displays the completed QFD.

Customer Requirement	Weight	Engineering Requirement	Size constraint	Weight	Measure inputs/outputs	Operation time	Outer casing	Power source	Minimize exposure to moving parts	Lifespan
1. Scaled	3		9	3				1		
2. Portable	4		9	9		1				
3. Interactive	2		1		9	1	9			
4. Eductational	5				9	3	9			1
5. Safe	5							1	9	
6. Usable in a Lecture	5		3	1	3	9	3	1		3
7. Wall outlet or self-powered	4							9		
8. Instructions for use	3									1
9. Durable/Reliable	3							1		9
Absolute Technical Importance (ATI)			80	50	78	62	78	52	45	50
Relative Technical Importance (RTI)			1	5	2	3	2	4	6	5
Target ER values			2' x 3'	<100 lb	>2	≤15 min	clear	AC/air	n/a	≥5 yr

Figure 1: Completed QFD

The QFD revealed that the most important engineering requirements were the size constraint, temperature and pressure measurements, and clear outer casing. This was expected, as all these engineering requirements ensure the educational aspects of the final design.

3 EXISTING DESIGNS

Before beginning our own design, our team first began researching current systems that already exist. For this project, we decided to focus on two main areas of research. First, we researched the general processes behind the Brayton Cycle, as well as real word applications of this cycle. Next, we researched small-scale, simplified model units that would be more similar to what we intended to build.

3.1 Design Research

The team began research by investigating real-world applications of the Brayton Cycle. While there are countless variations of Brayton Cycle engines, they can be categorized into four main types: turbojets, turboprops, turbofans, and turboshafts. All four of these engines share the same core element: a gas generator consisting of a compressor, combustion chamber, and turbine section [1]. The turbojet is the simplest of the four types and is essentially just the gas generator described above with an inlet and exhaust nozzle added. The compressor, driven by the turbine, compresses air into the combustion chamber, where combustion adds a heat to the flow. The heat and pressure are converted into rotation to power the compressor, and the remaining energy is then used to create thrust in the exhaust section. A turboprop operates on the same principle, except the excess energy remaining after powering the compressor is used to power another turbine section, attached to a propeller through a gearbox [1]. In a turboprop, the propeller generates most of the thrust rather than the exhaust nozzle in a turbojet engine. A turboshaft engine is nearly

identical to a turboprop engine, except that the output shaft is not connected to a propeller. Instead, it can be used to power the rotor blades of a helicopter or connected to a generator such as in a power plant [1].

The turbofan engine is the most widely used type of engine for aircraft propulsion [1]. In a turbofan, excess shaft power is used to drive a fan ahead of the main compressor. The air from this fan passes around the inner core of the engine through a separate nozzle, which provides most of the thrust [1].

Our client initially requested that our group avoid building a turbofan model, so we debated between the other three types. Initially we intended to design a turboprop style model. However, given the small size of our design team, we ultimately decided it would be best to focus on the simplest type: the turbojet, which would provide a model of the Brayton Cycle without the added complexities of an additional gearbox and propeller.

3.2 System Level

3.2.1 Real-World Applications

Most modern-day aircraft have abandoned the turbojet engine in favor of the turbofan engine design. However, one application where turbojets are still frequently used is small unmanned aerial vehicles, like drones and cruise missiles. The compact size and relative simplicity of a turbojet engine makes it useful in these applications. Today, one of the leading manufacturers of turbojet engines is Safran, who produces the Microjet engine line. There are several different variations in this engine range, so the team decided to focus one type, the Microturbo TRI 60, to get an idea of turbojet engine specifications. The Microturbo TRI 60 is shown in Figure 2 [2].

Figure 2: Microturbo TRI 60 Turbojet Engine [2]

There are also several variations within the TRI-60 product line, but all variants share similar specifications. This turbojet engine is approximately 26 inches long, 13 inches in diameter, and weighs between 108 and 135 pounds. It makes use of a three-stage, axial turbine, with a compressor pressure ratio ranging from 3.83:1 to 5.58:1. The combustor is an annular smokeless type, with 12 nozzles and a single spark igniter housed in a stainless-steel casing. The turbine is a single stage, axial design, and mates directly to the compressor through a single shaft. The turbine inlet temperature is approximately 1,850 °F [2]. These design specifications yield thrust ratings of between 787 and 1,200 lbst depending on the model variation.

The Microturbo TRI 60 engine has been used in many applications, from Anti-ship missiles to Drones [2]. This research was very surprising to the team. The TRI 60 turbojet is small enough to meet the target size specified in our engineering requirements and can still generate over 1000 pounds of static thrust. While

this engine is far more complex than anything our team could produce, it was valuable in determining some design criteria for our design. It also reveals how compactly turbojet engines can be manufactured.

3.2.2 Existing Demonstration Units

One of the most interesting products discovered during our research was the MiniLab Gas Turbine Lab made by Turbine Technologies [3]. This is a self-contained turbojet engine demonstration unit, which essentially has the same intended use as our project. As shown in Figure 3, the MiniLab Gas Turbine Lab consists of a small-scale SR30 Turbojet engine, mounted inside of an enclosed workbench. The apparatus is mounted on wheels to allow for easy transportation and is shielded to protect users from heat and moving parts.

Figure 3: MiniLab Gas Turbine Lab [3]

This product measures temperature and pressure at every state, which is an essential customer need for our design. It also includes its own software program, which can be used to display these pressure and temperature readings, as well as fuel flow, thrust, and engine speed, shown below in Figure 4. Additionally, the software allows users to plot any of the measurable parameters to learn how the performance reacts to the operating conditions.

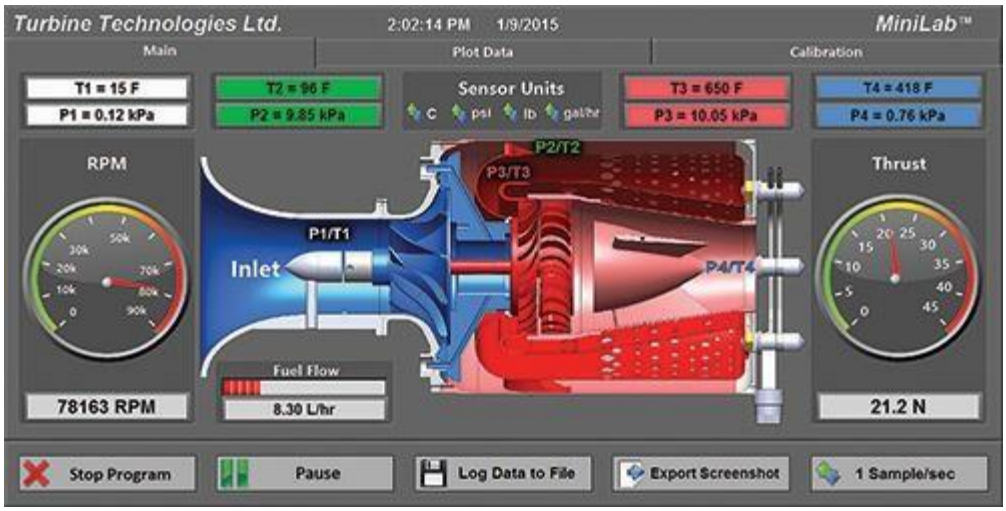

Figure 4: MiniLab Interactive Virtual Instrument Panel [3]

This product is essentially the ideal version of a Brayton Cycle demonstration unit and meets or exceeds all customer needs given to our design team save for its large size. Unfortunately, this device was far more complex than any design our team could produce and also far too expensive. However, it provided a valuable benchmark which demonstrates how a model like this should operate. Additionally, the team also felt that there were several ways this design could be improved upon. For example, given that the MiniLab uses a real turbine engine, the user cannot see any of the moving parts inside of the turbojet engine. While our design is not as realistic as this product, it does have one advantage in that the clear outer casing allows students to visualize what is actually happening during the operation of the Brayton Cycle. Additionally, it is much smaller and more portable, and significantly more affordable.

3.2.3 Other Applications

During research our team also found that there are fully-functional scale models of turbine engines used for model airplanes. These small replicas function as real engines and use actual fuel and combustion. At the time of this research, the team was still planning on building a turboprop engine, and focused on this type of engine. One example of a model turboprop is the Wren Power Systems Model 54 turboprop engine, which is shown in Figure 5.

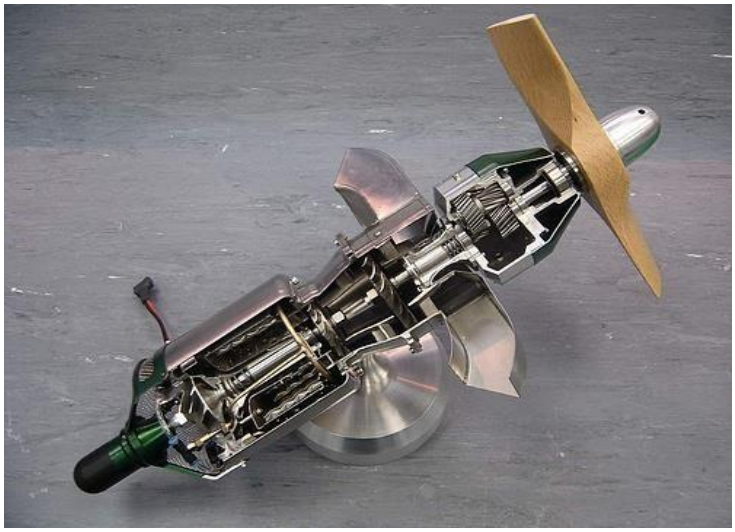
Figure 5: Wren 54 turboprop cutaway [4]

The engine utilizes a single compressor and two turbine stages. The first turbine is used only to power the compressor. There is a second, separate shaft with a single turbine that drives the gearbox for the propeller. This design is called a two-stage engine because of the separated turbine stages, which can be seen in Figure 5 above. In this model, the intake is on the opposite end of the propeller, which is a less common design. Real turboprop engines usually have the intake behind the propeller to help force more air in the compressor. Because of this engine's size it is extremely sensitive to foreign particles and the reversed design is preferable, as the intake will be inside the cab of the plane and will allow cleaner air to enter the compressor. This two-stage design is less efficient than a single-stage design where the output shaft of the turbine is directly connected to the gearbox. This is because the second turbine is an impulse turbine relying on the air being exhausted to spin the shaft causing greater losses than if the shaft was directly connected to the gearbox [5]. Another peculiarity of this design is the use of a radial compressor rather than a typical axial compressor. In this application, the radial compressor is advantageous, as it can be implemented using a single stage. This parameter is discussed in more detail in the Compressor section.

These model turbines are visually impressive and the cutaway shown above would make an excellent teaching tool. Unfortunately, however, they are very expensive; Wren Power Systems website lists the model shown above costs around $4,000, which was far outside of our team's budget [5]. Still, it was beneficial to find this model, as it showed an example of a Brayton Cycle model very different from the typical design. This showed our team that we could alter the standard design to better suit our application.

3.3 Subsystem Level

As mentioned previously, all Brayton Cycle engines, including turbojets, turbofans, turboprops, and turboshafts, share a similar core element known as the gas generator, which consists of a compressor, combustion chamber, and turbine section. Thus, in performing subsystem design research, the team decided to focus on these three elements.

3.3.1 The Compressor

The compressor is the first component in a Brayton Cycle engine. It connects through a shaft to the turbine, from which it receives its power. The purpose of the compressor is to compress the air and raise its pressure before combustion to stretch the pressure vs. volume (P-V) diagram as well as the Temperature vs. Entropy (T-S) diagram, increasing work output.

There are several ways to compress air in a Brayton Cycle engine. The standard type seen in most jet engines today is the axial compressor. This configuration is composed of radial vanes (or blades) that are mounted like discs on a central hub, which directs the flow through the compressor parallel to the shaft [6,7]. Figure 6 shows a simple diagram of an axial flow compressor with stator vanes, which will be discussed later.

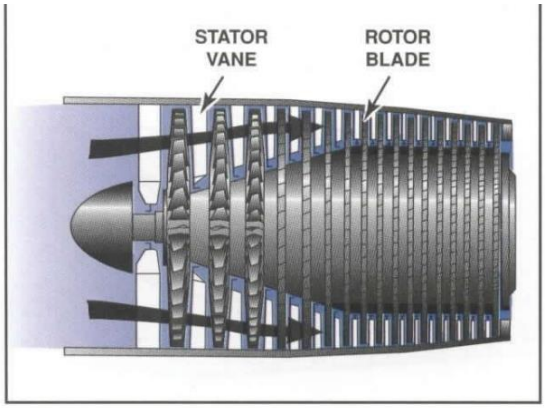

Figure 6: Cross section of an Axial Compressor [7]

As shown above, the rotor blades look similar to fan blades, and rotate to draw air into the engine. As the flow moves further into the engine, the area between the rotor hub and outer casing decreases, which compresses the air. This compressed air flow is then directed to the combustion chamber.

The stators do not rotate with the rest of the blades, and while a functioning compressor can be made without them, stators increase the efficiency and effectiveness of each stage. A single compressor stage is defined to have one set of rotors and one set of stators [8]. The rotating blades will cause the flow to swirl in the direction of rotation, which causes the compressor to be less efficient. A simple diagram of one rotor in a cylindrical housing and how the flow swirls can be seen in Figure 7 below.

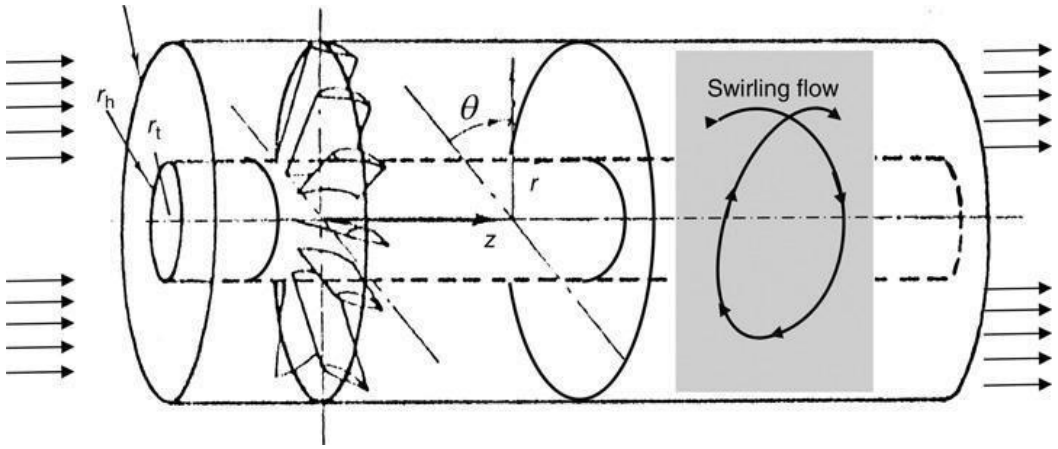

Figure 7: Flow swirl due to rotor [9]

Adding stator blades redirects the flow to be parallel to the axis of rotation. This decreases turbulence in the flow, increases the static pressure of each stage, and directs the flow perpendicular to the blades of the next stage.

The decrease of area between the inner hub and outer casing is an essential part to effectively compressing flow in an axial compressor. To achieve this area-decrease, the diameter of the hub can change, the outer diameter of the casing can change, or both can vary; the design in Figure 6 uses a combination of both to accomplish the area decrease. The first section, closest to the inlet on the left, has a constant outer casing diameter while the hub has a converging cross section. Next, the center section has a combination of a changing outer casing and inner hub radii. Lastly, the far right section has a constant hub radius with a converging outer casing. A more in-depth look at the relationship between the hub and outer casing can be seen in the turbine section.

Another compressor configuration is the radial, or centrifugal, compressor. Unlike the axial compressor, this configuration relies on the swirling of air to function, which forces the air away from the rotor and down to the combustion chamber. This configuration is mainly used in turbochargers in the automotive industry, though it can be used in a Brayton Cycle engine as seen in the model turboprop shown in Figure 5. It was also implemented in early jet engines [6]. Figure 8 shows the rotor and housing of a radial compressor.

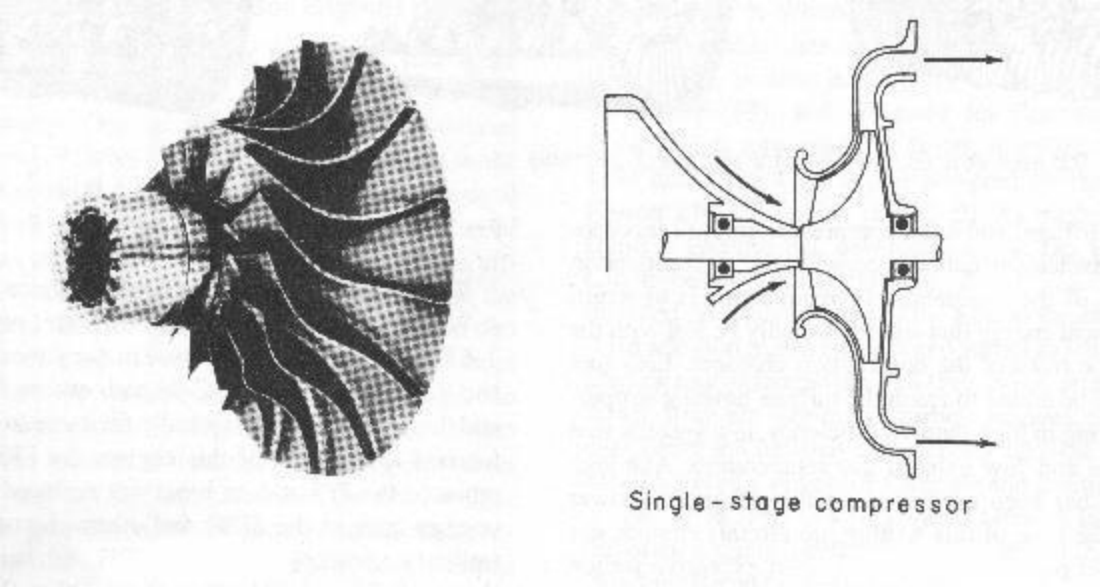

Figure 8: Cross section of Radial Compressor

As Figure 8 demonstrates, the vanes of a radial rotor direct the air from the center of the rotor to the outer edges. This configuration is ideal when using only one compressor stage as one radial stage is much more effective at compression than a single axial stage [6]. One NASA article states that an average axial compressor stage can increase the pressure by about 1.2 times, where a similar single-stage radial compressor stage can compress the air by a factor of 4 [6]. Though they are simpler and more efficient, radial compressors cannot be placed in series the same way as axial compressor stages. To place radial compressor stages in series, the flow must be redirected to the center of the next stage for the rotor to be effective.

Based on this research, our team decided an axial compressor would likely be the best option for our design. This is detailed in the design selection stage, which is later in the report. Because our design is to be used as an educational tool, and is supposed to represent how an actual Brayton Cycle engine works, we decided against the radial compressor, as they are rarely used in actual jet engine applications.

3.3.2 The Combustion Chamber

The main purpose of the combustion chamber is to add heat to the system before the working fluid enters the turbine. This increased temperature gradient increases the potential work output from the turbine. In a typical design, air is mixed with a fuel source and ignited in the chamber. There are typically three different geometric shapes for combustion chambers [10]. The Can Combustor, Figure 9, is made of several different chambers through which air flows [10]. Each chamber has outer and inner tubes; the inner tube is where the combustion takes place and the air flows through the tube by louvers in the inner dome [10]. The outer tube is used to regulate air flow [10].

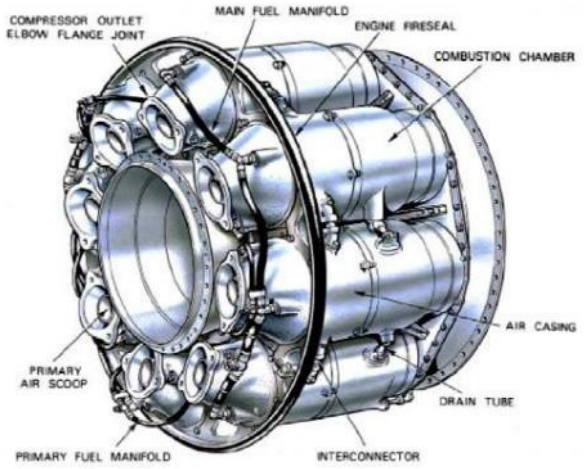

Figure 9: Can Combustor

An annular combustor, Figure 10, has a single chamber with walls inside to control the air flow into the combustion zone [10]. There are two areas where the compressed air is mixed with the fuel. The primary air supply is fed into the combustion chamber to mix with the fuel source and combusted [10]. The secondary air is used to cool the air-fuel mixture before entering the turbine to prevent damage to the turbine blades [11].

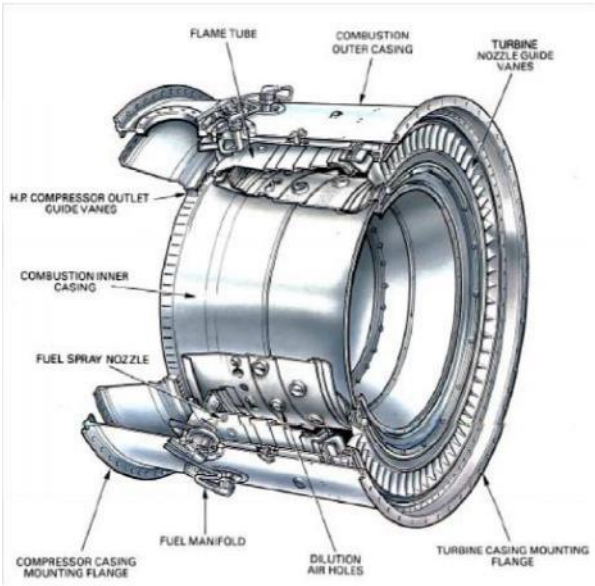

Figure 10: Annular Combustor

The third type of combustion chamber is the Can-Annular combustor, which combines the two previous types as the name suggests [10]. This combustor takes the several chambers of a can combustor and incorporates an annular combustor in each chamber [10]. This is shown below in Figure 11.

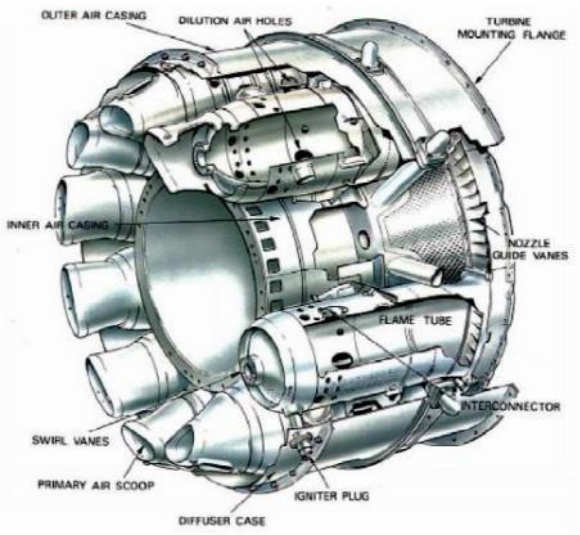

Figure 11: Can-Annular Combustor

For any combustion chamber to work properly, the air velocity coming into the chamber must be decelerated with a diffuser to ensure a stable combustion [10]. Too much air in the combustion chamber will cause a lean mixture, preventing the engine from operating at maximum efficiency. The air-fuel ratio that will yield the best efficiency is approximately 1:15 [11].

For safety reasons the team cannot create a model with a functional combustion chamber. The team decided to research outside sources to simulate the effect of an actual combustion chamber. There are several methods of accomplishing the effects of a combustion chamber. One way is to add more compressor stages to increase pressure. Another option would be to have an outside heating source pump in heated air or to have heated coils in place of the combustion chamber. The engine would still benefit from the use of a diffuser before the simulated combustion chamber to create the most heat transfer into the system.

In both a real or simulated combustion chamber, the design must be such to keep the total pressure loss at a minimum. In any design there will be losses due to friction [11]. Designing for minimal pressure loss could include making the surfaces of the combustion chamber as smooth as possible and making the air flow as streamlined as possible. For an actual combustion chamber, pressure losses are usually around 2-7 percent [11].

3.3.3 The Turbine

The turbine sits behind the combustion chamber and is mounted on the same shaft as the compressor. Its primary task is to power the compressor, by converting the heat and pressure energy from the combustion chamber into mechanical shaft power [12]. The use of the remaining power depends on the type of application, which heavily influences the final design. However, there are several design options used no matter the application.

The Turbine stage of a gas generator contains two primary types of components: the turbine nozzle, or stator, and the turbine rotor. The turbine nozzle is a row of stationary blades mounted ahead of the rotating rotor. Because it is stationary, the stator cannot do any work. Instead, it has two main functions. First, it converts the potential energy in the hot, high-pressure gas into kinetic energy by adding swirl to the flow [12,13]. Second, the turbine nozzle changes the direction of the flow, in order to maximize the force it can impart onto the turbine rotor. Generally, a turbine nozzle is placed ahead of each rotor to redirect the flow before each stage. An illustration of this configuration is shown in Figure 12 below.

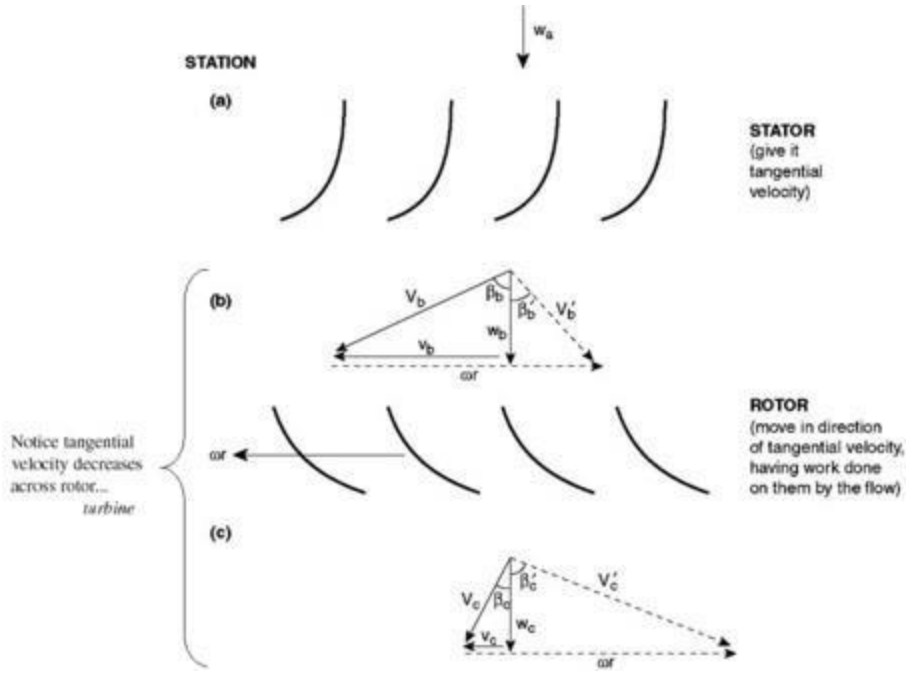

Figure 12: Turbine Stator/Rotor arrangement [13]

However, particularly for our design application, the turbine stator presented a manufacturing challenge. The stator stage must be mounted concentrically between the rotor stages but must be held stationary. In a real gas turbine, the stator can be incorporated into the outer casing of the engine, as shown in Figure 13 [14].


Figure 13: Turbine Stator [14]

However, because our design is intended for use as a demonstration tool, the engineering requirements dictate that the outer casing must be transparent. Most 3D printers can only produce opaque objects even with clear filament. Thus, we decided to use pre-manufactured acrylic tubing, which makes it difficult to install fixed stator sections. Initially, we to avoid this issue by using a stator-less turbine design. As the name suggests, a stator-less turbine removes the nozzle guide vanes, and the flow exiting one turbine rotor passes directly to the next rotor without the use of a stator in between [15]. While this design simplifies manufacturing, it adds complexity to the rotor blade design. Ultimately, we decided to incorporate stators using a press-fit design, which is detailed later in the report.

There are two major classifications for turbines: Impulse, or constant pressure turbines, and Reaction Turbines [12]. In an Impulse Turbine, gas expansion occurs only in the stator, or turbine nozzle, which converts potential energy in the gas from heat and pressure into kinetic energy. As the gas passes through the nozzle guide vanes, it is accelerated rapidly while its temperature and pressure decreases. The gas then exits the turbine nozzle, impacting the turbine blades, and imparting rotation through momentum exchange [12]. As the gas passes through the rotating stage of the turbine, its pressure remains constant, hence the "constant pressure" name. After each turbine stage, velocity is lower than at the nozzle exit, as energy has been extracted from the flow and converted into shaft work. This process can be observed in the plot on the upper left of Figure 14, which illustrates how pressure, temperature, and velocity change as the flow progresses through the different stages of the turbine [12].

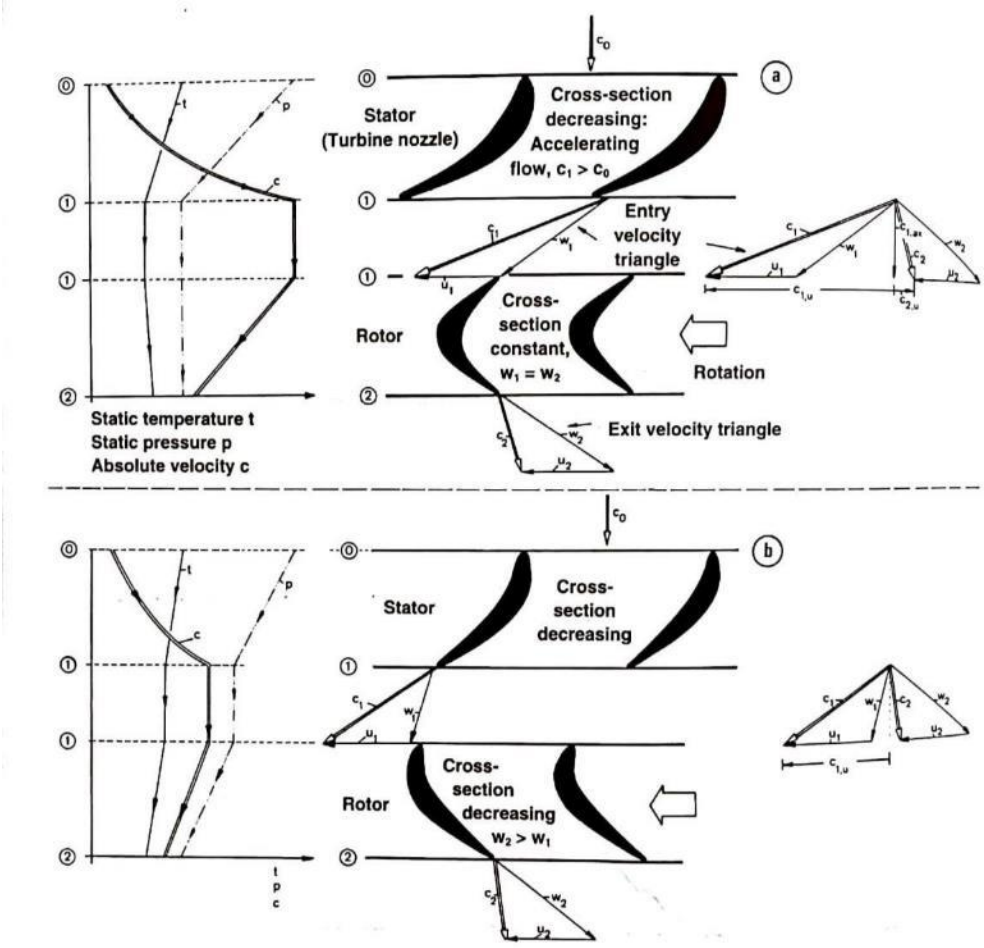

Figure 14: Impulse vs. Reaction Turbine [12].

Alternatively, in a Reaction Turbine, gas expansion takes place in both the stationary nozzle and the rotating turbine [12]. In the rotor section, the gas expands and accelerates similar to the Impulse Turbine, but to a lesser degree. This expansion continues in the turbine section, where the rotating blades share a more similar profile to the guide vanes. Due to the nature of the blade profile design, the air flow creates an aerodynamic force on the turbine blades, much like the lift force on a wing, which causes the turbine to rotate [12]. However, there is still a momentum exchange between the gas and the blades, much like in the Impulse Turbine.

A comparison of these two designs and their respective blade profiles is provided in Figure 14. The plots on the left of the figure compare the differences in pressure, temperature, and velocity through the different sections. Both of these designs have their own benefits. The Reaction Turbine is generally more efficient, but an impulse turbine has a higher power output, which can reduce the number of turbine stages required [12].

Given the benefits of each design, most turbines use a combination of the two. In a turbine, circumferential velocity increases radially outward, from a minimum at the hub to a maximum at the blade tip. However, it is beneficial to have a constant velocity profile across the entire length of the blade. To accomplish this, turbine blades are generally designed as constant-pressure type at the base, gradually changing to the reaction-type at the tip [12].

Another consideration of turbine design is the profile of the hub and casing. These choices can affect mass flow rate, power production, and turbine efficiency [16]. Again, there is endless variability in designing these parameters. However, the options can be divided into three main categories: constant tip radius with variable hub radius, constant hub radius with variable tip radius, and variable hub and tip radius [16]. These three designs are presented in Figure 15 for comparison.

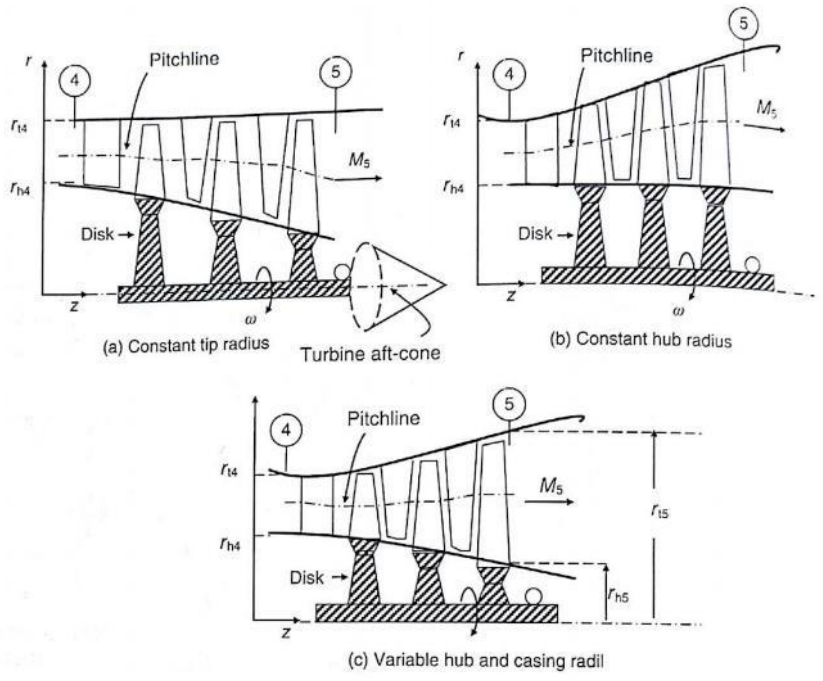

Figure 15: Turbine Hub and Casing Options [16]

Each of these designs offer their own distinct advantages. For instance, a constant tip radius can be beneficial in a turbofan. In a turbofan engine, the hot exhaust is mixed with the "cold" stream from the outer

flow. In this scenario, using a constant outer radius can lead to better integration of the cold and hot air streams [16]. A constant outer radius also reduces centrifugal stresses in the rotor blades, and can reduce the weight and frontal area of the engine. In aircraft engines, a tapered hub radius can also be advantageous, as the hub can be integrated with the exhaust cone, which is used to direct exhaust flow at the turbine exit [16].

A constant hub radius also has several benefits, particularly in stationary gas turbines used in power plants. This design choice can integrate with an exhaust diffuser, and also reduces manufacturing cost and complexity since all turbine rotor disks share the same inner diameter. Using both a variable hub and tip radius can allow for a constant pitchline. However, it is also the most complex design, the most difficult to manufacture, and generally increases both cost and weight [16].

As mentioned earlier, our design uses pre-manufactured acrylic tubing for turbine housing. Because of this, it was not possible to use a variable casing radius design. Thus, our design uses a variable hub radius to accomplish area reduction in the compressor and expansion in the turbine. The hub radius is easily changed using 3D printing, allowing the outer casing to remain constant and completely transparent for easy viewing.

4 DESIGNS CONSIDRED

In the initial decision process, we decided to focus on the main structure of the design. Though there are just three main subsystems to any Brayton Cycle engine, there are many ways to build each subsystem. Each team member researched one subsystem and generated a few variations that could be used in our design. The team then worked to create different combinations of these subsystem designs to create a total of 15 different concepts, summarized in Table 3. Most of these designs combined different design elements discussed in the above subsystem research. The design team considered compressor and turbine type, hub and casing geometry, shaft configurations, and different options for combustion chamber substitutes. We sketched each of the 15 concepts, which can be seen in Appendix A.

Table 3: Design Descriptions

Design description
1. Radial compressor and turbine, no heating
2. constant hub radius, no heating, statorless
3. constant hub radius with preheat, statorless
4. Constant tip radius with preheat, statorless
5. Constant tip radius with heating in chamber, statorless
6. constant tip radius with heating around outside of chamber, statorless
7 .Concentric shaft, 2 separate stages of comp. and turb. with preheat, statorless
8. Front Diffuser, constant tip radius with preheat, statorless
9. Stator compressor and turbine, constant tip radius with preheat
10. Stator compressor turbine, constant tip radius with in chamber heat
11.Statorless, constant hub radius, with heating around outside of chamber
12. Statorless, constant hub radius, with in chamber heating
13. Constant inner and outer radius, statorless, no heating
14. Stator compressor and turbine, constant hub radius, with preheat
15. Stator compressor and turbine, constant hub radius, with pre-chamber heating

Design 13 is highlighted in yellow as it was chosen as the datum when used in design selection, discussed further in Section 5.1. The chosen datum was the simplest design possible, which used constant a constant hub and tip radius, stator-less blades, and no added heating in the combustion section. The design sketch for the datum can be seen in Figure 16 below.

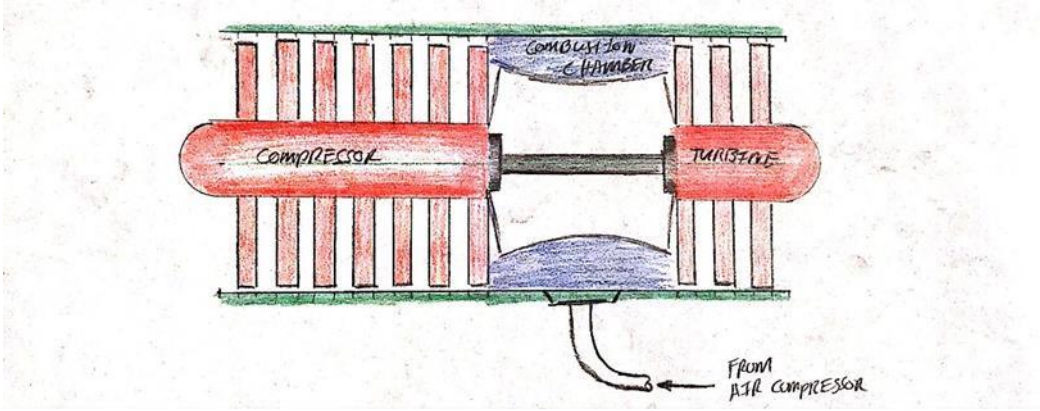

Figure 16: Detailed Sketch of Datum

Each concept utilized a different combination of the subsystem variations. For example, Figure 17 shows a sketch of Design 14, which used stators on the compressor and turbine. Figure 18 shows a sketch of Design 3 without stators.

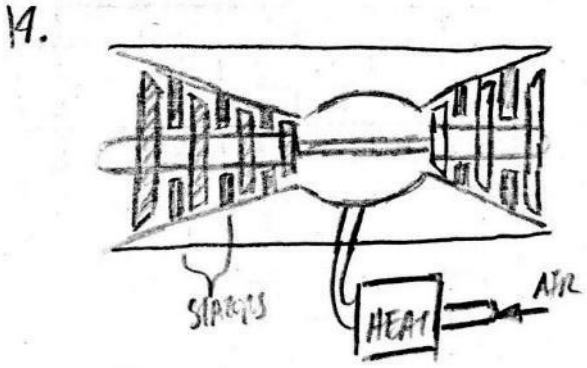

Figure 17: Design 14 Sketch

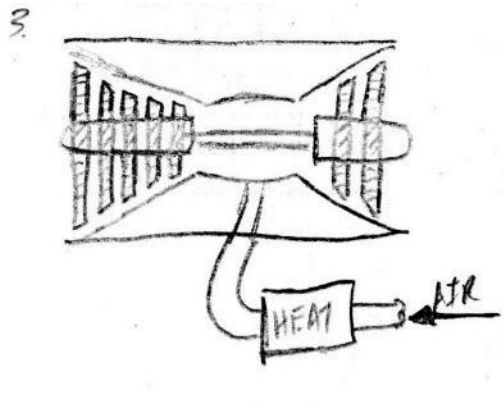

Figure 18 Design 3 Sketch

In Figures 17 and 18 above, both designs made use of a "pre-chamber" to heat the incoming air, and both designs utilize the constant hub radius design. To illustrate the different heating designs, Figure 19 below depicts Design 5 with the in-chamber heating, and Figure 20 below shows Design 11 with the heating around the outside of the chamber.

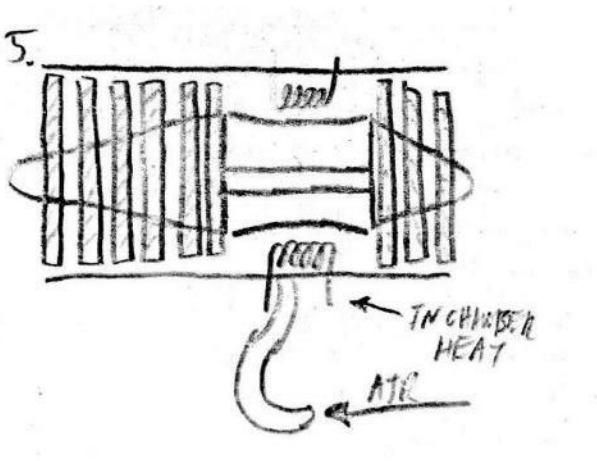

Figure 19: Design 5 Sketch

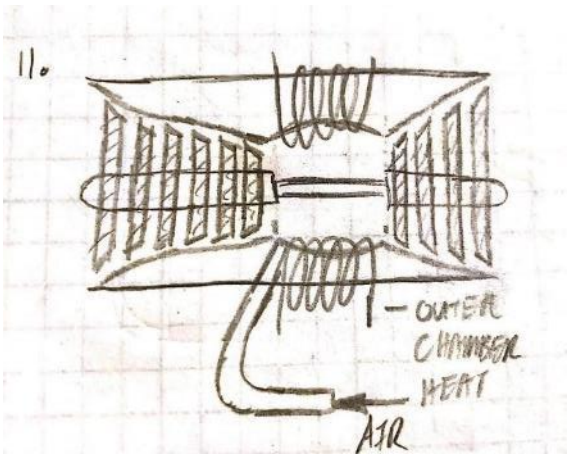

Figure 20: Design 11 Sketch

In the above figures it can also be seen that Design 5 utilizes the constant tip radius and Design 11 utilizes the constant hub radius.

5 DESIGN SELECTED

Having created many potential concepts, our team needed a way to objectively choose the best design. This section details the decision-making processes implemented by the team to choose a final design from the initial fifteen concepts, as well as a brief discussion of the results of these methods. It then describes the finalized design in detail including engineering calculations used in the analysis.

5.1 Rationale for Design Selection

To reduce the number of potential designs, the team first compiled the 15 designs into a Pugh Chart and scored each against the engineering requirements and the datum to find the top four designs. The entire Pugh Chart can be seen in Appendix B. Below in Table 4 is small portion of our Pugh chart showing our requirements and how the first 4 designs scored.

Table 4: Pugh Chart showing designs 1-4

Criteria	1	2	3	4
Portable	-	s	s	s
Interactive	-	-	-	+
Educational	-	-	+	+
Durable	+	-	-	s
Reliable	-	s	-	-
Fit in 2x3 foot perimeter	s	s	s	s
Total weight < 100lbs	-	s	s	s
Demo < 15 minutes	s	s	-	-
Visability	-	-	-	s
120v AC, 60Hz, and/or compressed air	-	s	s	s
Minimize exposure	-	s	s	s
Feasibility	-	-	-	-
Efficiency	-	+	+	+
Cost	-	-	-	-
Total -	11	6	7	4
Total +	1	1	2	3
Total s	2	7	5	7

The red highlighting above the first three concepts indicates that they were eliminated in the first round of concept selection. The green highlight on the fourth design shows that it scored well enough to proceed to the next step in the process.

To decide on a final design, our team placed the four remaining designs into a Decision Matrix. The Decision Matrix used the same criteria as the Pugh Chart. However, several criteria were rated at “S” or same for all designs, so these were eliminated from the Decision Matrix to streamline the process. After narrowing the criteria, our team assigned a weight to each, based on its importance in meeting the customer needs. The criteria were weighted on a scale from zero to one, with the sum of all criteria weights summing to one. Next, each design was rated on a zero to 100 scale based on its competence for each of the evaluation criteria. Because the designs were highly conceptual at this point, most of these ratings were subjective. We found it most effective to compare the designs against one another when assigning scores. For instance, adding a heating element to the design will increase its educational value and efficiency, but will reduce its reliability and longevity.

After scoring all four designs, these raw scores were multiplied by the weight of each category, and summed to determine the strongest design. The completed Decision Matrix is shown in Table 5.

Table 5: Decision Matrix

	Concept	9		11		13		15	
Criteria	weight	raw score	wtd score	raw score	wtd score	raw score	wtd score	raw score	wtd score
Educational	0.2	65	13	80	16	50	10	80	16
Visability	0.18	80	14.4	65	11.7	80	14.4	80	14.4
Minimize exposure	0.13	50	6.5	50	6.5	50	6.5	50	6.5
Cost	0.13	80	10.4	75	9.75	85	11.05	75	9.75
Feasibility	0.1	50	5	70	7	90	9	70	7
Interactivity	0.17	60	10.2	60	10.2	70	11.9	80	13.6
Reliability	0.03	60	1.8	60	1.8	80	2.4	60	1.8
Durability	0.03	60	1.8	60	1.8	80	2.4	60	1.8
Demo time	0.02	80	1.6	80	1.6	90	1.8	80	1.6
Efficiency	0.01	85	0.85	70	0.7	50	0.5	70	0.7
Total	1		65.55		67.05		69.95		73.15

As shown above, all four final designs scored very closely, as all had many similarities. However, based on these criteria, Design 15 was the strongest concept. This is illustrated below in Figure 21.

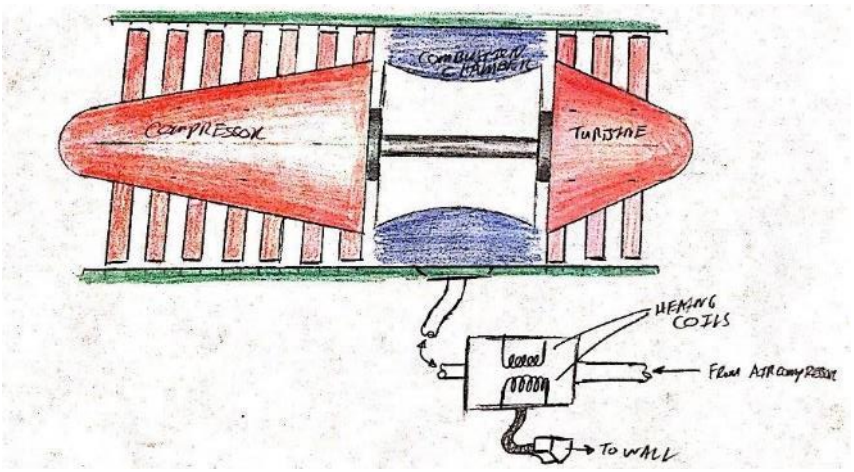

Figure 21: Winning Concept

This design functioned without any combustion, as did most others. It featured a stator-less compressor and turbine, with a constant blade tip radius and variable hub radius. Compressed air was used in place of combustion to add energy to the flow in the form of pressure. This design also implemented an in-line heater for the compressed air stream to further enhance the energy added during this stage.

The team saw numerous benefits in this chosen design. First, the elimination of combustion made this unit much safer to use in a classroom setting. Use of compressed air would sufficiently increase flow energy and adding a heater helped to differentiate further between measurements at different states. Heating the air before it enters the "combustion chamber" is also beneficial, as it prevents the plastic from being heated directly, theoretically reducing thermal strain and increasing longevity. Finally, a stator-less compressor and turbine were chosen with constant tip radius for simplifying manufacturing.

Ultimately, as the project progressed, many aspects of this design were changed based on later variables. However, this served as the starting point for the design, and many aspects in the final design are similar to this initial concept. Next, first iteration of the final design is presented, as well as additional analyses completed by the team.

5.2 Design Description

Figure 22 shows an isometric view of the final CAD model, while Figure 23 shows an assembly drawing. For detailed drawings of all components, please refer to Appendix C.

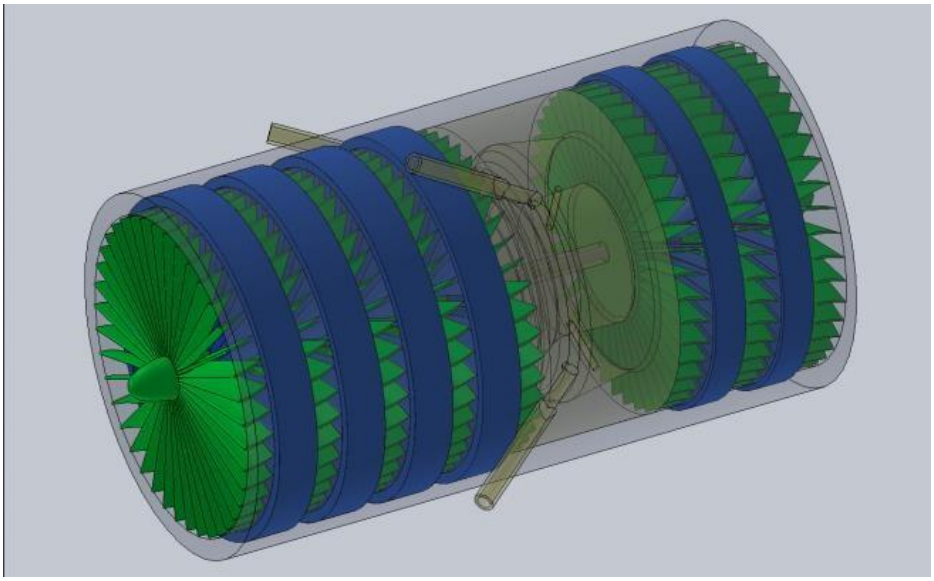

Figure 22: Final CAD Model

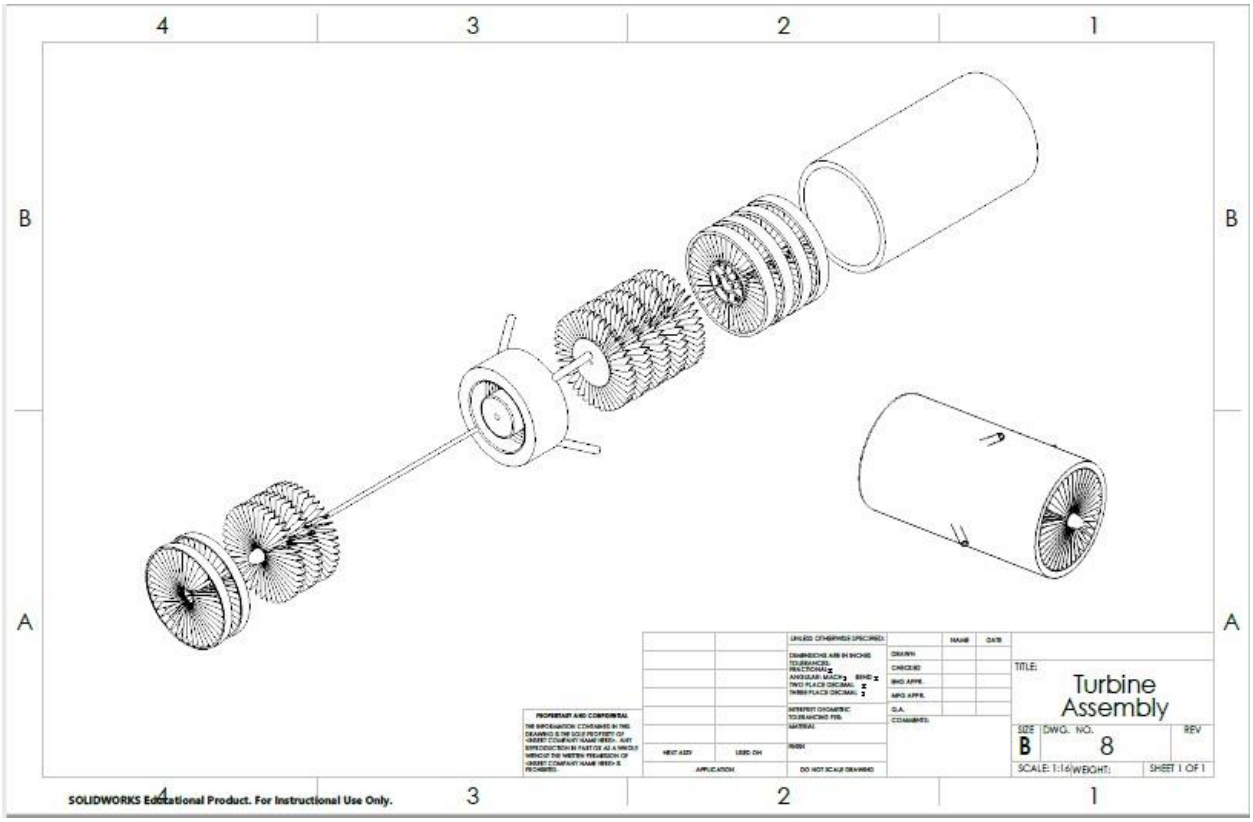

Figure 23: Final Assembly Drawing

As seen above, this design was very similar to the design chosen through the formal decision process. It uses a clear, outer casing of constant radius to allow for easy viewing of internal processes. While it is difficult to see in the above figure, it implements a variable hub radius to effectively compress air through the compressor section, and expand it through the turbine section; for a better look at this feature, refer to the detailed part drawings in Appendix C. In the middle "combustion chamber" section, heated compressed air is added to replace actual combustion. This is one area that was refined during the design process. In the initial concept shown in Figure 21, the compressed air was injected through a single port. This design would concentrate the flow in one location. To better distribute the flow throughout the cross section, the design was changed to have four ports evenly spaced throughout the combustion chamber. These ports are also aligned at an angle, to better direct the flow into the turbine section.

Another change to the design was the addition of stators, shown in blue, after rotor sections, shown in green. These were initially eliminated as the team thought they would make the design too difficult to manufacture. However, after more thorough research on compressor and turbine design, we determined that they would be necessary to better direct the flow through each stage, and to improve the efficiency of the model. All blade sections in the final design have an outer diameter of 16 centimeters, while the model has a total length of 30 centimeters.

5.2.1 Engineering Calculations

As noted earlier, each team member was assigned a subsystem of the design to analyze. These analyses were discussed in broad terms in the subsystem breakdown section above. A summary of the calculations performed for each subsystem is summarized below.

5.2.1.1 Compressor Calculations

A detailed description of the calculations performed for the compressor section can be seen in Appendix D. To summarize the calculations performed, first we calculated the Reynolds number for the inlet, assuming a turbulent flow. We estimated the sizes of the blades and the acrylic pipe that will contain everything. Using those assumptions, a Reynolds number was calculated across the blades and an airfoil shape was chosen to suit these numbers. The next step was to assume the speed at which the unit will rotate to start developing velocity triangles to figure out the angle of attack and geometric twist for the blades at each stage.

5.2.1.2 Combustion Chamber Calculations

The heated air flow for the combustion chamber was treated as an internal flow problem to calculate the amount of heat entering the system. The air flow comes from an air compressor running through a band heater for a simulated combustion chamber. The assumptions made for this design problem were the flow is fully developed, the flow will be treated as a laminar flow and the heat flux is constant. The final outcome for the design problem is the final temperature for the system. The Reynolds number for the air compressor was the first calculation made. Then the amount of heat flux can be calculated with the constant Nusselt number for a laminar flow. Then the mass flow rate can be calculated for the final temperature calculations. The amount of heat flux depends on the initial and final temperatures; however, the final temperature is the unknown so several iterations are needed so the numbers match. Appendix E provides the equations used in these calculations.

5.2.1.3 Turbine Calculations

Similar to the compressor, the main parameter of interest in the turbine section is the angle of attack of the turbine blades. Currently, the team still has many unknowns which will affect the angle of attack of the turbine blades. In order to accommodate for these parameters, a MATLAB code was created to allow a user to input parameters such as volumetric flow rate, angular velocity, number of blade elements, and desired

angle of attack. Using this information, the program outputs the pitch angle required at each blade location to maintain the desired angle of attack, as well as a plot representing the results. An example output, as well as a detailed breakdown of the MATLAB code and the calculations used within the MATLAB code, refer to Appendix F.

6 PROPOSED DESIGN—FIRST SEMESTER

Most of the fundamental parts of the design, including the rotor and stator blades, will be 3D printed because they are a custom design. The components will be mounted on a shaft, with the rotors mounted on bearings to allow free rotation. The outer casing of the unit will be a clear acrylic tubing that will allow students to see through to each stage. Ports will be drilled in various locations along the model to allow for several key components. The most important of these are the ports outside of the combustion chamber for compressed air. As noted earlier, heated compressed air will be injected at this stage to simulate the combustion process. This will be accomplished using a Porter Cable air compressor and tank, and a 100-Watt band heater wrapped around the air hose between the air compressor and combustion chamber.

As previously discussed, one of the vital engineering requirements was temperature and pressure measurement, derived from the client's request for interactivity. To thoroughly analyze the thermodynamic Brayton Cycle, four temperature and pressure measurements are needed: one at the entry to the compressor, a second at the entry to the combustion chamber, a third at the exit of the combustion chamber, and a fourth at the exit of the turbine. Ideally, the team would utilize separate measurement instruments for each of the four locations. However, due to a limited budget of just $500, a compromise had to be made in this area. Rather than using four pressure transducers, a single pressure transducer was to be used to monitor all four locations. We intended to design a valve system to allow each port to connect to the same transducer; the measurement location will be changed by opening the valve for the desired port and closing the other three. The pressure transducer was to be mated to a National Instruments NI-6009 14-bit data acquisition (DAQ) device for data acquisition, provided by the client, Professor David Willy.

Temperature measurement was also compromised slightly due to budget constraints. Thermocouples are inexpensive, so one J-Type thermocouple was specified at each of the locations of interest. However, the budget only allows for a single-input temperature measurement DAQ device, the National Instruments USB-TC01. Each thermocouple had its own male adapter, to allow the user to easily switch between measurements. Both DAQ devices are controlled by LabVIEW Virtual Instrument (VI) software, which allows for data collection and manipulation. Table 6 shows a complete Bill of Materials for the final design.

Table 6: Bill of Materials

Bill of Materials						
Item	**Quantity**	**Cost per unit**	**Manufacturer**	**Item #**	**Vendor**	**Hyperlink**
Acrylic Tubing	1 ft	$13.43	U.S. Plasic Corp	44550	U.S. Plastic Corp	https://goo.gl/rmKMEm
3D Printed Compressor Blades	255 g	$25.50	MakerBot	N/A	NAU Cline Library	See Part Drawing
3D Printed Compressor Stator Blades	292 g	$29.20	MakerBot	N/A	NAU Cline Library	See Part Drawing
3D Printed Turbine Blades	152 g	$15.20	MakerBot	N/A	NAU Cline Library	See Part Drawing
3D Printed Turbine Stator Blades	213 g	$21.30	MakerBot	N/A	NAU Cline Library	See Part Drawing
3D Printed Combustion Chamber	208 g	$20.80	MakerBot	N/A	NAU Cline Library	See Part Drawing
Ceramic 608 Bearings	2	$8.99	Acer	SK8	Acer Racing	https://goo.gl/5BpiMh
Air compressor with tank	1	$89.00	Porter Cable	C2002	CPO Commerce	https://goo.gl/KRQu8p
Band Heater	1	$28.50	Tempco	NHL00100	Grainger	https://goo.gl/WnqnU8
J Type Thermocouple Wire	7.62 m	$0.60	TIP Industries	TIPWRJ008	TIP Industries	https://goo.gl/PiFj3X
Thermocouple Connectors	1	$3.05	Omega	OST-U-M	Omega	https://goo.gl/bAjo9v
Thermocouple DAQ	1	$107.00	National Instruments	USB-TC01	National Instruments	https://goo.gl/U5soAU
Pressure Transduser	1	$49.00	Transducers Direct	TDH30BG025003B004	Transducers Direct	https://goo.gl/ZAUC21
Pressure Transduser DAQ	1	$250.00	National Instruments	USB-6009	National Instruments	https://goo.gl/xaw9sP
	Total:	**$661.57**				

At this stage, the team was still working on finalizing the design. In order to stay on schedule, the team created a simplified agenda outlining the remaining major milestones and the approximate date by which they should be completed. This schedule is summarized in Table 7.

Table 7: Implementation Schedule

Milestone	**Target completion date**
Perform testing with Thermo 1B team device	September 9
Finalize design details	September 16
Order remaining parts	September 19
Complete 3D printing	October 7
Complete testing procedures	November 3
UGRADS Poster	November 5
Final Report/CAD Package	December 3

7 IMPLEMENTATION

All the work discussed thus far was completed during the first semester of the project. After taking a break for the summer, the team resumed work in the fall semester. Section 7.1 details the team's initial plan for the second semester, and as such, is written in future tense. However, as will be seen, many changes were made along the way to alter this plan; section 7.2 describes how implementation actually occurred. Comparing these two sections is a useful summary of the difference between planning and implementation.

7.1 Manufacturing

Most of the manufacturing necessary for this is 3D printing. For the device to function properly, it is important that the 3D printed parts fit together with close tolerances. To ensure this, the team designed a test ring to compare with the inner diameter of the tubing used for the outer casing. After the correct sizing is determined, the CAD model can be adjusted and the final iterations of the blades can be sent for printing. These blades will be used for the first testing of the system to ensure size and functionality of the model. After the team knows the blades are fully functional, the CAD drawing will be sent to the NAU RapidLab for a higher print quality.

The only other custom manufacturing necessary will be the rotating shaft to which the blades will be attached. The diameter of the shaft will be determined by the bearings. The team selected 608z ball bearings because they are common in many products and are easy to find in many variations. Further, ungreased, ceramic bearings will be the best option for this design because they have minimal friction. These bearings are designed to fit on a shaft with an 8-millimeter nominal diameter. Finding an 8-millimeter shaft might prove difficult and expensive, so finding a shaft that is close in size and machining it to the desired size is the best option. One of the team members has access to and experience using a lathe, so the team does not have to outsource machining for the shaft.

The majority of the remaining parts will be purchased off the shelf. As noted earlier, the 3D printed blades and shaft will be mounted in acrylic tubing, which will be ordered online. This assembly will be mounted to a cart to allow for easy transportation into and out of the classroom. The cart will contain all other equipment necessary to run this experiment. A key aspect of this will be the data collection system, which utilizes thermocouples and pressure transducers to measure temperature and pressure. The client requested that these variables be measured at four points: the compressor inlet and outlet, and the turbine inlet and outlet.

At the beginning of the semester the team learned that the previous capstone team purchased two pressure transducers that were available to use. Thus, the team intends to design a manifold type system to allow four pressure measurements to be taken using just two transducers. Each manifold will have two “branches” that will go to the separate points, each branch being controlled by a valve that will allow switching between different points.

Additionally, the team intends to purchase the cart mentioned above, thermocouple wires, connectors, and a data acquisition system (DAQ) for the thermocouples. All the components have been sourced and will be ordered online or purchased locally in Flagstaff. Many of these components were changed since last semester. An updated Bill of Materials is presented for reference in Appendix G. (Note, this Bill of Materials was later updated again; a final version is presented in Appendix J).

Finally, the team also needs to design a simple LabVIEW program to collect the temperature and pressure measurements. This will be controlled by a laptop which can be mounted on the cart next to the model turbojet. The client requested that this program also be able to visually display the collected data, preferably through graphs. The team intends to meet with him to finalize the details of this program.

Once 3D printing is finished and all necessary components arrive, the team should be able to assemble the device relatively quickly. However, it is likely many variations will need to be made once the device is assembled and tested. The updated implementation schedule is presented in Table 8 but is still expected to change. The table is color coordinated: blue assignments are assigned to Samm, green assignments to Jacob, and yellow to Ashley. White rows are expected to be equally shared by all team members.

Table 8: Updated Implementation Schedule

Milestone	Target completion date
Perform testing with Thermo 1B team device	September 9
Finalize design details	September 16
Order remaining parts	September 19
Complete 3D printing	October 24
Device manufacturing/assembly	October 28
Complete testing procedures	November 11
Iterate and redesign	November 16
UGRADS poster	November 30
Operation and Assembly Manual	November 30
Final Report/CAD Package	December 5

7.2 Design Changes

This section describes how manufacturing actually occurred, and outlines changes that took place during this stage. Section 7.2.1 details individual analyses completed by the team members testing different aspects of the design, and how these results influenced the design. The team also made many design changes based on initial testing of previous iterations of the project and issues and ideas encountered during implementation. These are separated into two sections. Section 7.2.2 addresses design changes made before manufacturing, while section 7.2.3 details design changes made after real implementation began.

7.2.1 Individual Analyses

Before beginning manufacturing, the team wanted to study a few key aspects of the design. To do this, each team member picked a key component, and performed an analysis of this component to test different design parameters. The results of these analyses are presented below.

7.2.1.1 Blade Deflection and Stress Analysis

After printing prototype blades and studying another teams' version of this project, the team noted that blade deflection was an issue. The 3D printed blades were often very weak and ductile, and deflected a significant amount under slight pressure. To avoid this problem, we used a thicker blade profile and shorter blade length in our CAD models. However, we needed a way to predict whether these changes would be enough to sufficiently reduce blade deflection.

As discussed earlier, blade profiles are a complex shape and curve as they extend radially outward. Thus, to be truly accurate, a finite element analysis (FEA) approach would be ideal. However, for the purpose of this project, it was determined that a simplified beam analysis should be sufficient. The complex profile of the blade was simplified to a straight beam, shown in Figure 24, and the two components of wind, discussed in detail in Appendix F, were separated and simplified as shown in Figure 25, to produce the beam loading shown in Figure 26 and 27. Figure 26 represents the load due to tangential wind speed, and Figure 27

represents the load due to axial flow. In these figures, L is the length of the blade, c is the chord length, or length of the chord line in Figure 26, and t is the blade thickness

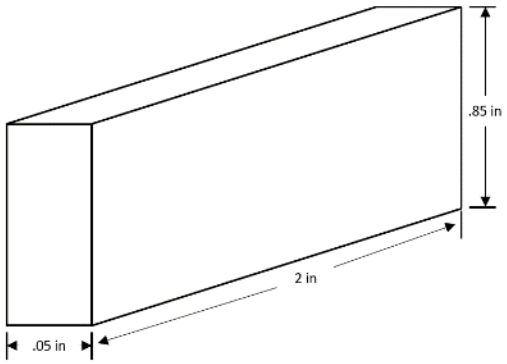

Figure 24: Simplified Beam Model

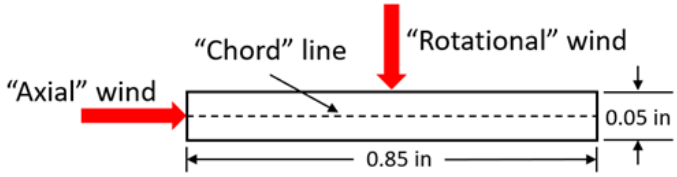

Figure 25: Simplified Wind Flow

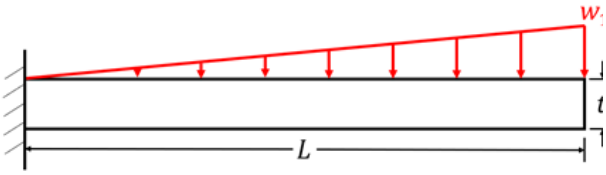

Figure 26: Loading from Tangential Wind

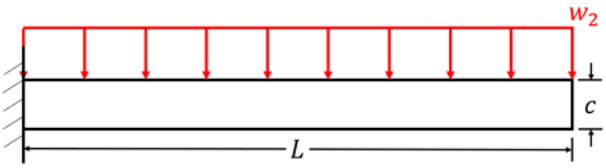

Figure 27: Loading from Axial Wind

These models were analyzed using the equations

$$\delta_1 = \frac{11 w_1 L^4}{120 EI} \tag{1}$$

For Figure 26, and

$$\delta_2 = \frac{w_2 L^4}{8 EI} \tag{2}$$

For Figure 27. Based on these calculations, it was determined that the changes made to the blades were sufficient to prevent deflection. After printing, these conclusions were verified, as the blades required a significant force, much larger than those experienced during normal operation, to produce noticeable deflection. A MATLAB code was also written to automate these calculations, available in Appendix H.

7.2.1.2 Shaft Sizing Analysis

As noted earlier, the design uses a shaft to which all blades are mounted. The goal was to use the most light-weight shaft possible to decrease inertia and increase blade speed. The system is driven by how much back work that can be achieved by the turbine, so having minimal resistance is ideal. After looking at a previous teams' shaft design and testing their system, the team knew the shaft needed to have a smaller diameter and

ideally use a lighter material. Based on material availability and cost, the two best options were steel and aluminum.

Finding the rotational force of a shaft is governed by the equation

$$\tau = I\alpha \tag{3}$$

where τ is the rotational force or torque, I is the moment of inertia and α is the angular velocity of the shaft. The moment of inertia formula for a cylinder about the center axis is given by

$$I = mr^2 \tag{4}$$

where m is the mass of the shaft and r is the radius.

As another point of comparison, the shaft of the summer team was also compared with these equations. The results of the calculations showed that reducing the diameter from 3/4" to 8 mm reduced the rotational force by a factor of ten, confirming the team needed to reduce the shaft diameter for better efficiency. Furthermore, comparing different materials showed an 8 mm shaft of aluminum needed three times less rotational force to spin. These calculations guided the team to use an aluminum shaft over a steel shaft.

7.2.1.3 Heat Exchanger Analysis

To improve safety, the team decided to replace combustion with an electric heat exchanger as discussed previously. Analyzing the heating pre-chamber is important so the maximum amount of heat is added to the incoming air. A MATLAB code was created with the intention of allowing a user to change multiple parameters to find the ideal size and length of the pre-chamber. An anemometer was used to measure the average velocity of the air coming out of the air line. For these calculations it was assumed that the entire chamber would be at steady state and have the same temperature as the heater band; it was also assumed that there was no contact resistance between the band and the chamber. To start the calculations, a 20-degree temperature increase was assumed across the chamber. The resistive network of the heat transfer into the air flowing through the chamber was simplified into conduction through the metal pipe, and convection into the air passing through. When finding the convective heat transfer coefficient, an issue was encountered, and which resulted in two unknown variables. Thus, we would need to gather some actual data from a prototype pre-chamber and gather the missing variables. The prototype chamber constructed was six inches long and had a 1 ½-inch diameter. This design worked quite well and there was a temperature increase after the combustion chamber of about 20 °F. Due to the acceptable performance, the team decided not to alter the design and used the prototype heating pre-chamber in the final design with only slight modification.

7.2.2 Design Changes Based on Initial Testing

This semester, the team began by testing the prior iteration of the design created by the previous capstone team. Based on this testing, we decided to make several changes to our design. The most significant change was to reduce the outer casing diameter from 6 inches to 4.5 inches. In our testing, we noted that the compressed air tank selected for the design ran empty too quickly. Changing the diameter decreases the mass flow rate and rotational inertia of the blades, which allows for a longer run time. It also decreases the cost of 3D printing and acrylic tubing. The team also decided to decrease the number of stages in the compressor and the turbine. With this design change, the team saved on cost, made more space on the cart, and reduced the rotating mass.

The team also reviewed the first design and made a few changes that should further improve performance. The previous iteration of the design utilized a combustion chamber with four inlets. This was redesigned to

accept one inlet from a compressed air source, and then diffuse the air in a manner modelled after a Dyson fan. Having only one air inlet will simplify manufacturing, and the new diffuser design will distribute the heated air more efficiently. An updated CAD model is shown below in Figure 28.

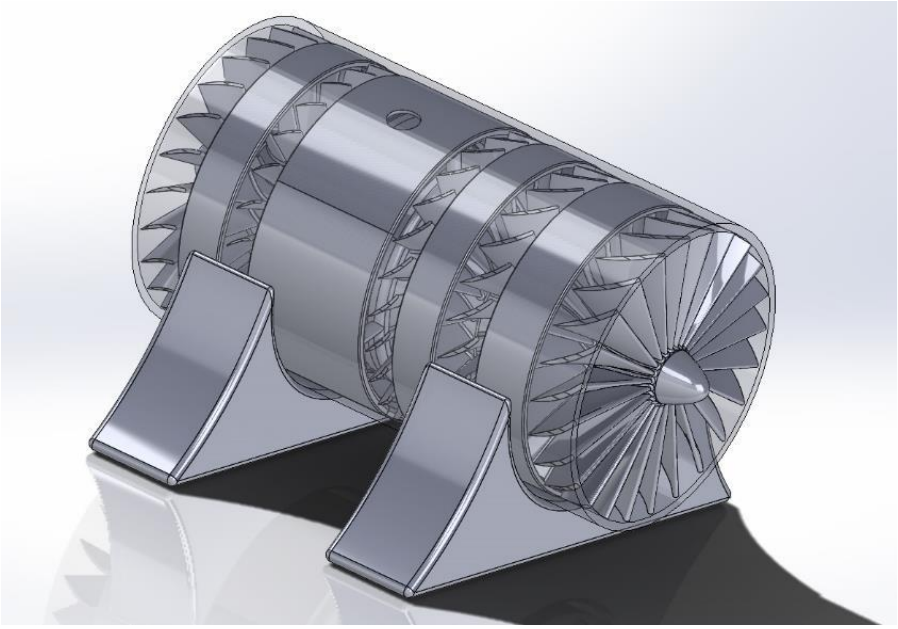

Figure 28: Current CAD model

The first step of manufacturing was ordering all the parts needed from the respective vendors. Once the premade items were on the way, the test piece previously mentioned in the manufacturing plan was designed and printed. This fixture tested blade and stator fitment, shaft fitment, and bearing fitment, and is shown below in Figure 29. While difficult to see in the figure, the outside diameter has steps to test different blade diameter fitments in the acrylic tubing. The smaller circles on the inside test bearing and shaft fitment.

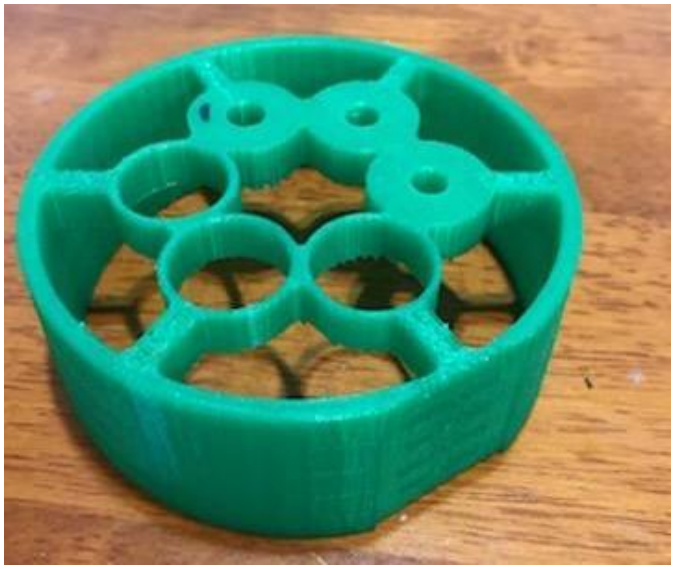

Figure 29: Blade Fitment Test Fixture

Unfortunately, after testing this component in the purchased acrylic tube, the team found it was too small, so another had to be printed with larger outer diameter sizes. The newer version had the correct sizing,

which allowed the team to determine the correct sizes for the stators and blades. Based on these findings, slight adjustments were made to the blade and stator diameters in the CAD model to ensure a tight fit. The updated CAD models were sent to the NAU MakerLab for printing. Two of the stator sections are shown below in Figures 30 and 31.

Figure 30: First Stator Section

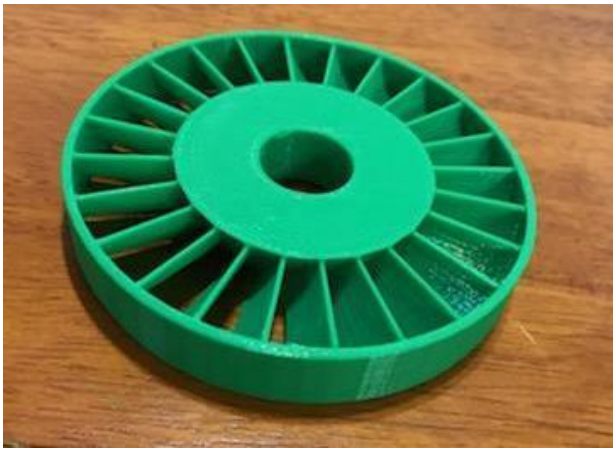

Figure 31: Second Stator Section

The team also had to make a slight adjustment to the combustion chamber design to accommodate 3D printing. The new design has a thin, internal slit along its circumference to evenly distribute the air. This presents a challenge as the support material required during 3D printing would be very difficult to remove. For testing purposes, the team decided to cut the combustion chamber into four pieces to facilitate removal of the support material. This is shown in Figures 32 and 33 below. However, for the final version, this design was changed once again, which is addressed in the next section. We also printed the "saddle" pieces shown in Figure 28 that are used to mount the acrylic tube to the cart.

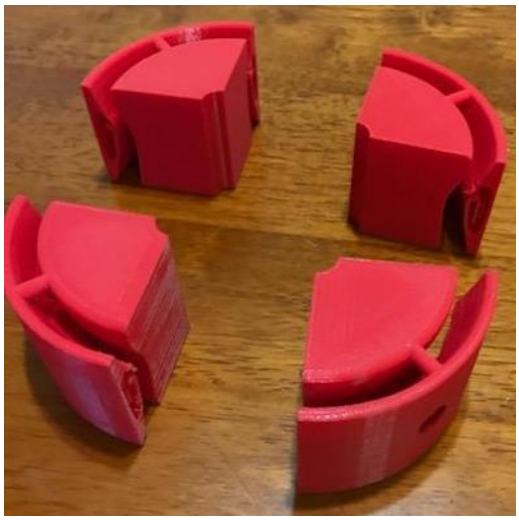

Figure 32: Combustion Chamber Cut Sections

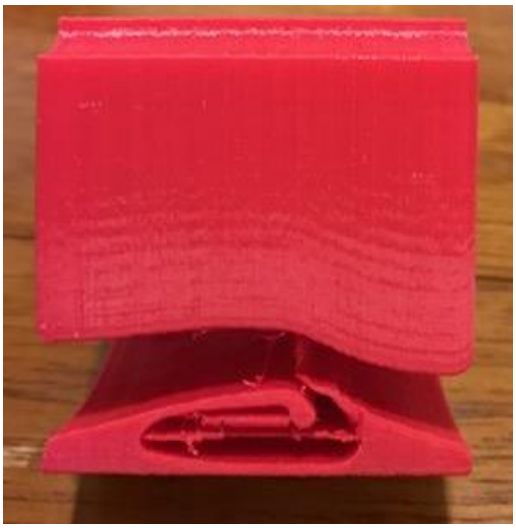

Figure 33: Support Material in Diffuser

The team underestimated how long the prototype 3D printing would take, which slowed progress, as assembly could not occur without the blades. However, a few other subsystems were worked on in the meantime. First, the purchased shaft was machined from ⅜ in to 8 mm for tight fitment with the bearings. This is shown below in Figure 34.

Figure 34: Shaft Machining

The team also created the prototype for the pressure manifold system described in the previous section using brass fittings purchased from Home Depot. This design was later modified slightly to fit properly on the final system. However, Figure 35 shows a representation of one-half of the system to demonstrate how it works in principle.

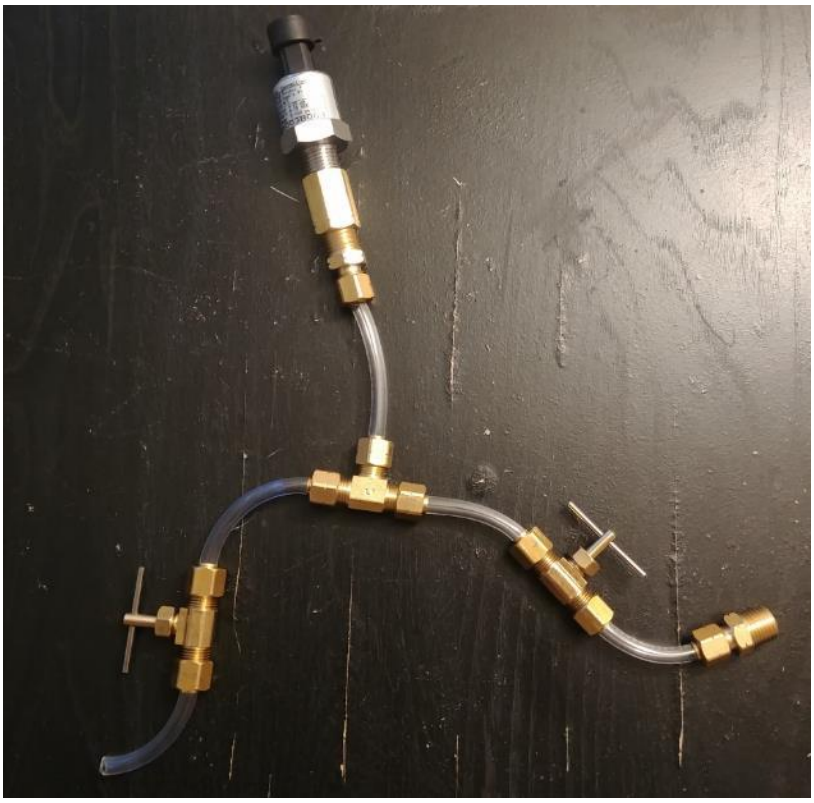

Figure 35: Pressure Measurement Manifold

Finally, the team assembled the utility cart that will be the base of the design. Two changes were made to the cart. First, we decided to invert the top tray of the cart to obtain a flat surface on which to mount the turbojet model and data acquisition equipment. This also allowed wiring to be hidden underneath, improving safety and aesthetics. We also decided to paint the cart in NAU colors. The painted and assembled cart is shown in Figure 36.

Figure 36: Painted Cart

7.2.3: Design Changes During Implementation and Final Manufacturing

After the cart was painted and the blades were printed, the team could begin assembling the entire system. We began by cutting the acrylic tube and the shaft to the correct length. Next, we collected and organized all blade sections into the acrylic tubing. Even after using the test piece, we found that all blades and rotor sections were slightly too big. We sanded each section by hand until a correct fit was achieved.

We next inserted all the blades and the shaft into the acrylic tubing. We found it was difficult to adjust the blades inside the tube to achieve the correct spacing. The team attempted to use an expansion fit by cooling the blades in a freezer, which made initial adjustment easier; however, once they reached room temperature again, they were very difficult to remove. To facilitate blade adjustment in the future, the team decided to cut the acrylic tube in half. This, coincidentally, increased the interactivity of the model, allowing students to open the casing to better see the inner workings. It also makes maintenance easier should any blades break in the future.

After cutting the tube in half, we needed a way to attach the two halves together to achieve a tight seal, while also allowing for easy opening and closing if needed. We decided to use small tool box hinges and a latch, with foam insulation tape along the seams. Next, we verified the two halves opened and closed properly, and the blades still fit inside and spun, and then marked holes for the pressure and temperature measurement systems and the air inlet for the combustion chamber. Holes were tapped to allow the proper adapters to be threaded into the tube, and small drilled holes accommodate the thermocouple wires.

After the tube was finalized, we began to arrange the layout of the cart. We set the tube and saddle on the top portion of the cart next to a computer to determine correct placement. Once situated correctly, we marked the location and secured the saddle to the cart with double-sided tape, and secured the tube to the saddle in the same manner.

We next needed to accommodate the pressure and temperature measurement systems on the top platform of the cart. The team wanted to group all controls together near the turbojet model for ease of operation. We thus decided to create a “control panel” where all the controls would be located. We spaced and measured the four pressure valves, and drilled holes to allow them to neatly pass through the top platform of the cart, so that only the valve handles were visible. We also grouped the thermocouples together next

to the valves so they could be easily plugged in and switched between states. Grommets were added to all holes to ensure a tight fit and to prevent damage to the tubing and wiring. This setup is shown in Figure 37.

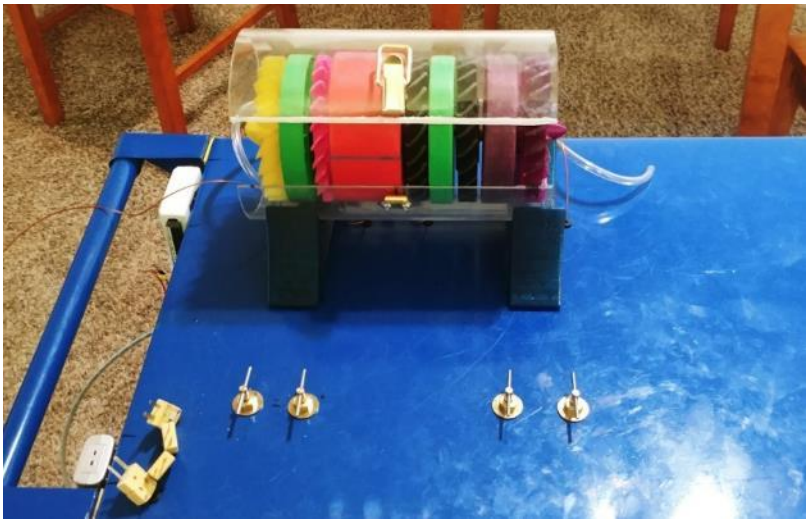

Figure 37: Initial Placement

After installing the valves, we had to adjust the lengths of the acrylic tubing from the initial pieces used in the prototype shown in Figure 35. We measured the necessary lengths needed and cut and installed each so there was no excess, and the tubing could be hidden away under the top platform of the cart. Zip tie mounts were used to affix the tubing, T-Valves, and transducers underneath the cart, shown in Figure 38.

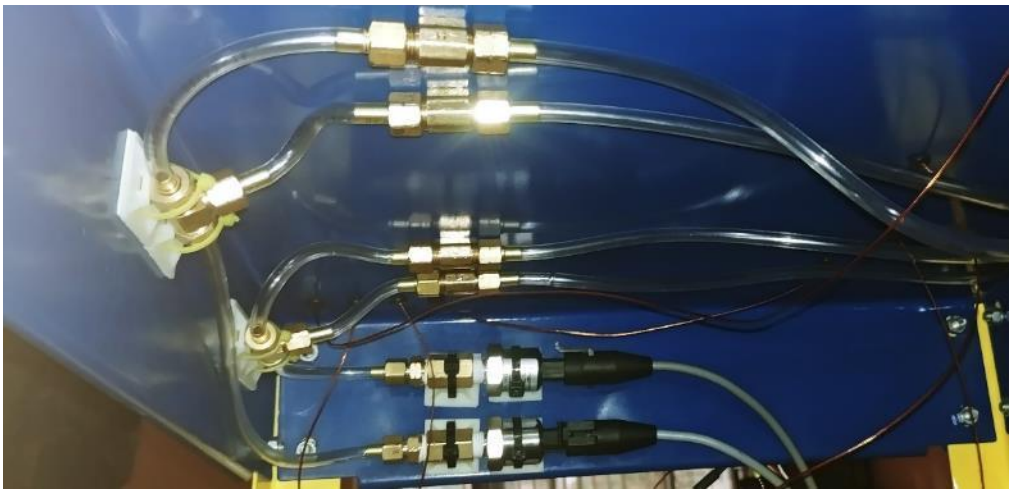

Figure 38: Underside of Cart

We then attached the system to the compressed air tank to see if everything was still working properly. The blades spun well and the combustion chamber design worked. However, the runtime was still only about 50 seconds, which was not long enough. Thus, we decided to add a second air tank to extend runtime, sourced used from the junkyard. We purchased hardware to mount the new tank to the cart, and painted everything to match. This is shown in Figures 39 and 40 below.

Figure 39: Air Tank as Purchased

Figure 40: Painted Tank and Hardware

After painting, the second tank was added to the cart, and connected to the first tank with an air hose so both would fill and empty at the same time. We also added a pressure release valve to the new air tank to allow a user to safely depressurize the tank should there be a problem.

The team also constructed a final heat exchanger using a 6-inch-long, 1.5-inch diameter steel pipe. The band heater was wrapped around this pipe along with a thermal fuse, which shuts the heater off at a specified temperature between 210 and 250 °F. This was mounted in line with the compressed air tank, so the air is heated before being injected into the combustion chamber; fittings were used to increase diameter from the 1/4-inch air hose to the 1 ½-inch pipe and back down again. The team decided to mount the heat exchanger underneath the top platform of the cart to better retain heat and to prevent anyone from accidentally contacting it during operation. It was placed on the side of the cart opposite the handle, just behind the computer platform. Two layers of thermal insulation tape were added to the cart around the heat exchanger to prevent the top platform from heating up, which could injure someone or damage a computer. This setup is shown below in Figure 41.

Figure 41: Heat Exchanger Mounted

After adding the new components, we also decided there should be an easier way to control everything. Previously, the compressed air hose needed to be unplugged when charging, and then plugged back in to start the turbine. To simplify this operation, we decided to add a ball valve on the control panel to control the compressed air. This allowed the hose to always remain plugged in, and also allows a user to precisely control the amount of air used in the experiment. Similarly, we added toggle switches to control the heater and pressure transducers. Originally, these were controlled simply by plugging them in. However, we felt switches would improve ease of use and theoretically speed up operation time. The final control panel with the ball valve and switches installed in shown in Figure 42. We also added a power strip as seen in Figure 43 so all the devices could be plugged in on the cart, and a single power cord plugged into the wall; this also allows a user to plug in their computer charger on the cart as well.

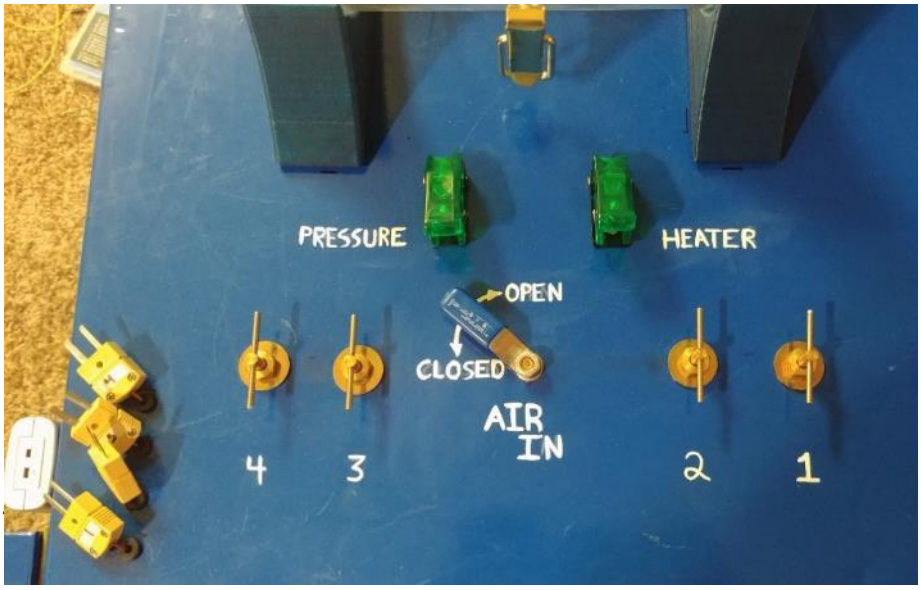

Figure 42: Control Panel

Figure 43: Power Strip

At this stage the team performed testing to test design decisions and reliability, which is detailed more in Section 8. However, during this testing, we experienced failure of the vinyl air hose between the heat exchanger and the combustion chamber. This section of tubing withstands the highest pressures and temperatures, so we decided to replace it with copper tubing for safety and reliability.

We also decided to reprint all the 3D-printed components for several reasons. First, we wanted to size them correctly so that sanding wouldn't be required for proper fitment, and to add space for more bearings. Additionally, we hoped to enhance the educational aspect of the device by color coding the sections: the rotating blade sections were printed in yellow, and the stators printed in green. This allows the instructor to distinguish between the sections during a lecture. Additionally, the combustion chamber was redesigned slightly; rather than splitting it in four quarters, the piece was split in half in the direction normal to the circular cross section, as seen in Figure 44, aiding the removal of support material and making final assembly simpler and more accurate. When reassembling, we also added washers in key locations to help keep the blade sections from contacting each other during operation.

Figure 44: New Combustion Chamber Design

Finally, the team worked on finishing touches. One team member painted on a few additional labels for the device, including a title on the front and a warning label on the back warning not to touch near the heater, shown in Figures 45 and 46. We also worked on neatly routing all wiring on the cart. We added a USB adapter so both USB cords could be plugged into a single port, and drilled a hole with a grommet so the USB cord can be easily inserted into a laptop. We also neatly mounted the air hose and all power cords. The completed device is shown in Figures 47-49.

Figure 45: Title Lettering

Figure 46: Heat Exchanger Warning Label

Figure 47: Final Product Front View

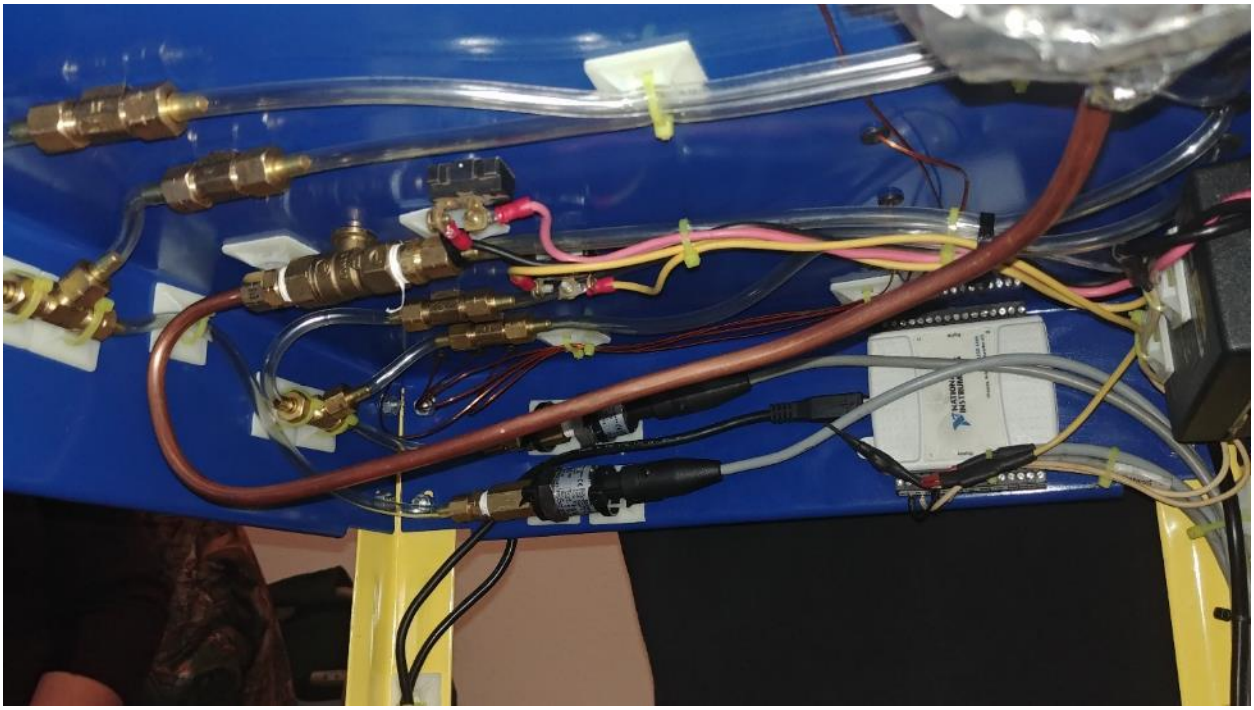

Figure 48: Underneath Cart Platform

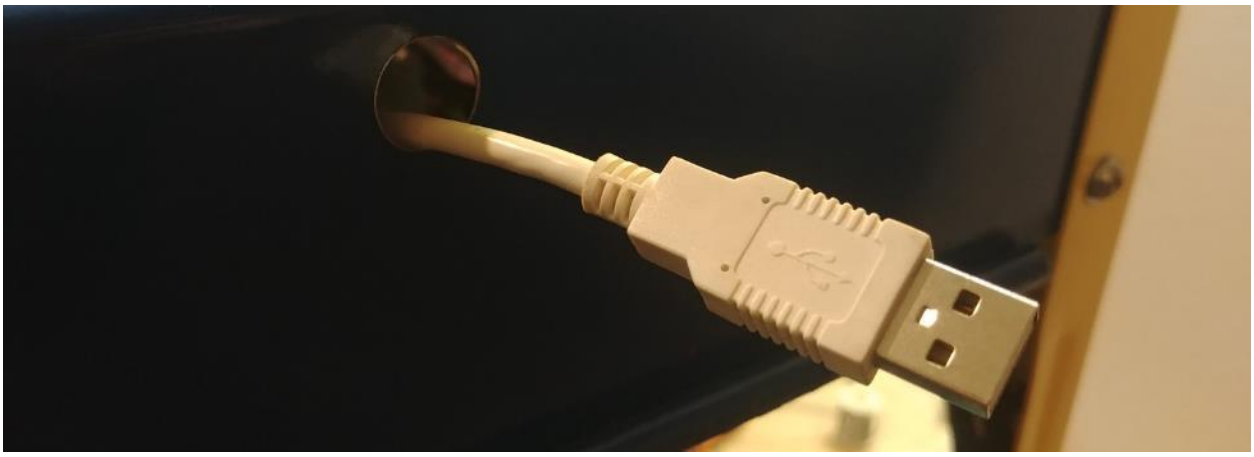

Figure 49: USB Cord for Data Acquisition

Additional photos of the final design can be viewed in Appendix I. The team finished the project slightly over the allotted $500 budget at approximately $530. However, after adding in the various components that were donated to the team, the total cost for this model is nearly double, at about $1030. The full Bill of Materials can be viewed in Appendix J.

8 TESTING

The team tested all aspects of the device to determine whether each of the original engineering requirements, detailed in Table 2, were met. Tests for each requirement are separated into individual sections below.

8.1 Fit in 2x3 Perimeter on Cart

Because this device is intended for use in a classroom, the client requested it be transportable by a single person. To accommodate this request, engineering requirements for size and weight were generated. To measure the size, the team simply used a tape measure, which verified the design is well within the 2-foot by 3-foot size constraint. As shown in Figures 50-51 below, the device measures about 16" wide by 30' long. The device is also entirely contained on a cart.

Figure 50: Width Measurement

Figure 51: Length Measurement

8.2 Total weight under 100lb

To check the weight, the device was weighed on a floor scale. The team placed a wooden platform on the scale so the wheels were lifted off the floor, then zeroed the scale with the wooden disk on it, so it wasn't accounted for in the total weight. The total system weight is 77.6 pounds, shown in Figures 52. This leaves adequate room for future adjustments by the client if desired.

Figure 52: weight measurement

8.3 Measure Pressure and Temperature at 4 States

This is the only design requirement that was not met completely. The device contains all necessary hardware to collect the requested data, but further software development is required to collect accurate measurements. Temperature measurements are accomplished using 4 J-Type thermocouples with attached miniplugs, and a National Instruments USB-TC01 temperature input device. Currently, all hardware is mounted on the cart, with the thermocouples and temperature input device clustered together as shown in Figure 53. A LabVIEW VI has been created which reports temperature measurements and saves them to an .lvm file which can be imported into Microsoft Excel for manipulation (Figure 54). This program should be updated for further automation so all four temperatures can be stored on a single file.

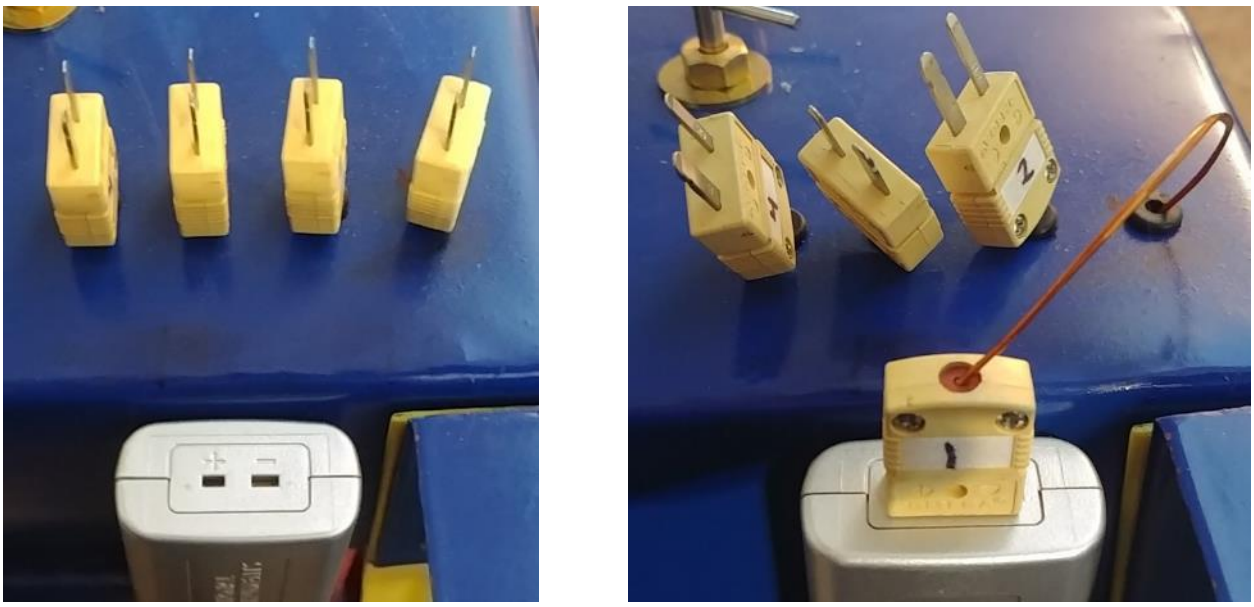

Figure 53: Temperature Measurement System

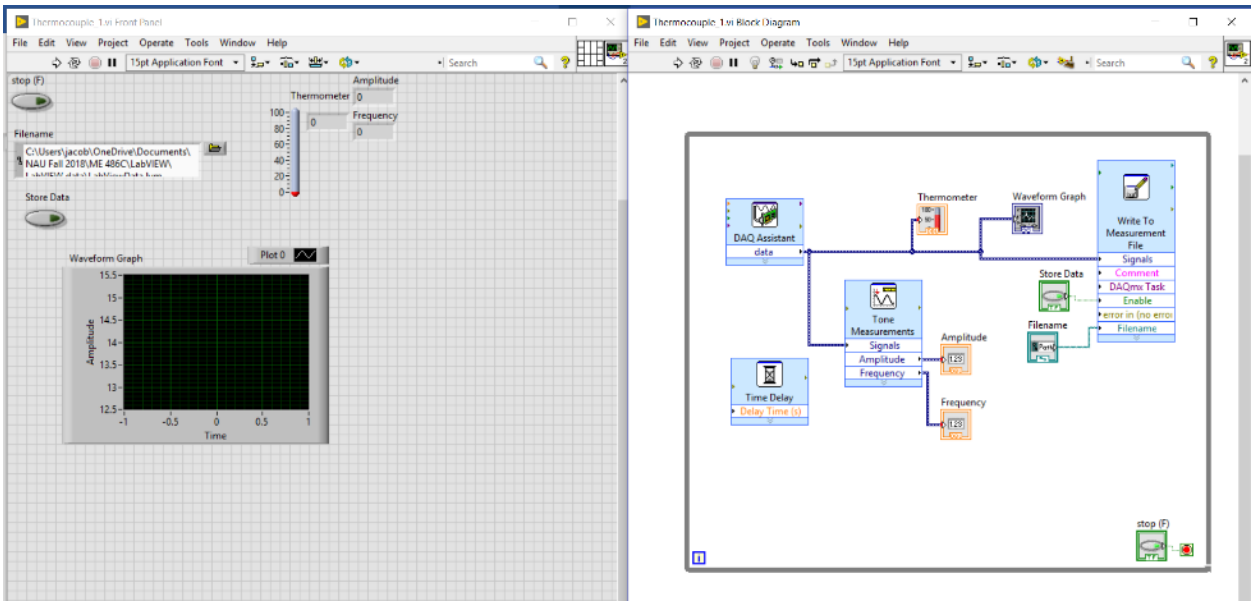

Figure 54: LabVIEW VI for Temperature Measurement

Pressure measurements are collected using two TDH30 Pressure transducers and a National Instruments USB 6009 DAQ. Because pressure measurements are required at 4 states, the team designed a manifold system with valves described previously to allow each transducer to measure pressure at two states. The first transducer measures pressure at states 1 and 2, and the second at states 3 and 4; both transducers are mounted out of sight underneath the cart. Switching between these states is accomplished by means of the four small valves on the control panel, labelled and grouped together in sets of two corresponding to the two states measured by each transducer. This is shown in Figure 55. Figure 38 in Section 7.2.2 shows a view of the plumbing underneath the cart.

Figure 55: Pressure Measurement Control Valves

To select a pressure measurement, first switch on the pressure measurement system. To do this, locate the left toggle switch labelled pressure, open the green cover, and flip the switch upward. This is shown below in Figure 56.

Figure 56: Turning on Pressure Measurement System

Next, locate the valve corresponding to the state number of the location of interest. Turn this valve counterclockwise until rotation stops. Then, turn the adjacent valve clockwise until rotation stops. For instance, if you wish to measure pressure at state 1, turn valve #1 all the way to the left, and valve 2 all the way to the right. This design allows one pressure from each pair to be measured simultaneously; i.e. pressure can be measured at states 1 and 3, 2 and 3, 1 and 4, or 2 and 4 simultaneously. The pressure transducers are correctly wired to a power source and the DAQ based on the wiring diagram for the 3 pin, 4-20 mA signal from the transducer data sheet seen in Figure 57. The LabVIEW coding was started (Figure 58), and receives measurements from the DAQ; however, further calibration is needed to obtain an accurate pressure reading.

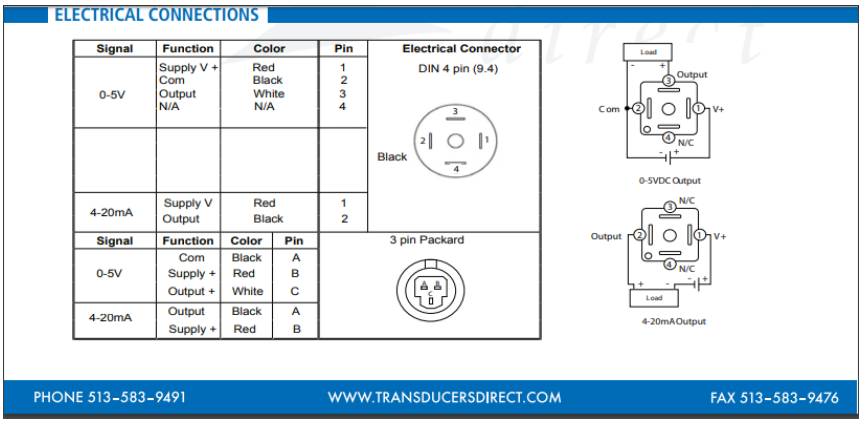

Figure 57: Pressure Transducer Wire Diagram

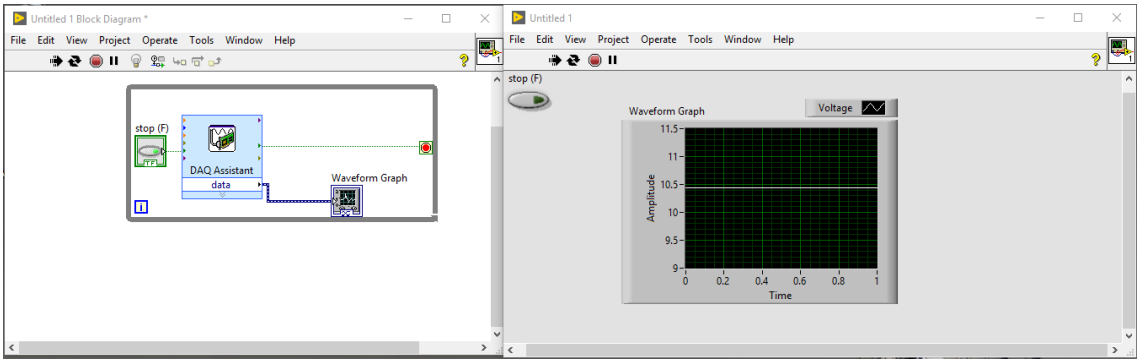

Figure 58: Pressure LabVIEW Coding

8.4 Outer Casing Must be Clear

Outer tubing is made with a clear acrylic tubing, Figure 59.

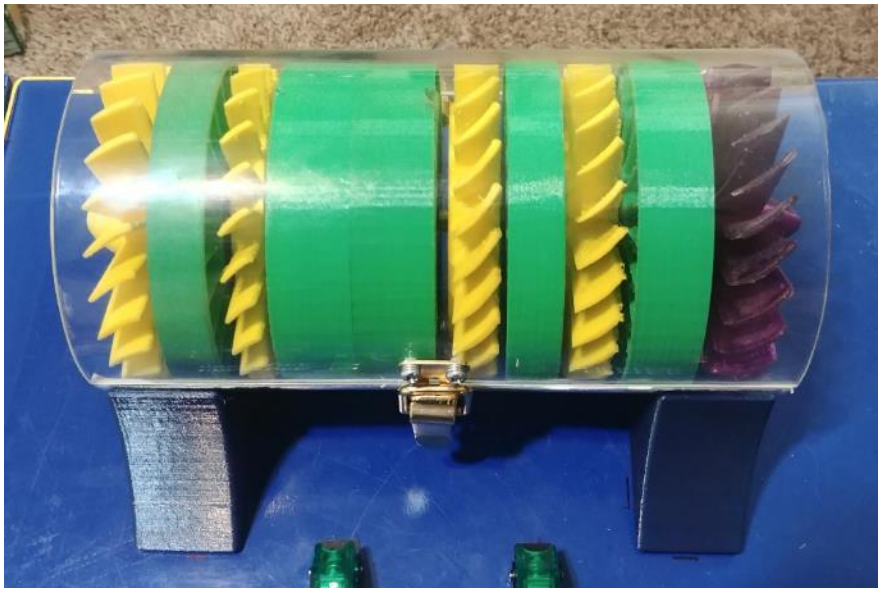
Figure 59: System Outer Casing

8.5 Use 120v 60Hz AC Power and/or Compressed Air

A 150-psi air compressor with two air tanks runs the system, in addition to three power cords which plug into a surge protector and thus a standard wall outlet, as demonstrated in Figures 60 and 61.

Figure 60: Compressed Air

Figure 61: Power

8.6 Minimize Exposure to Dangerous/Moving Parts

The team took numerous precautions to ensure the system protects the user from any parts that could be dangerous. The heat exchanger is likely the most dangerous component. This was mounted underneath the cart so it will not be touched by accident. There are two layers of insulation around the heat exchanger to prevent the metal surface of the cart from heating excessively. Further, the heat exchanger is controlled by a thermal fuse which shuts the heater off at a specified temperature. This set up is shown in Figure 62. There is also a warning label on the rear of the cart, shown in Figure 63.

Figure 62: Heat Exchanger Insulation

Figure 63: Heat Exchanger Warning Label

To test the effectiveness of the safety measures, the team performed several tests. First, the team verified the thermal fuse was operating properly by resting it on an electric stovetop and using a multimeter to see if it did, in fact, shut off, which was verified. The team also soldered all wire connections and covered junctions with heat shrink, shown in Figure 64. Next, the team monitored the heater temperature over time. While testing reliability, discussed later, the team ran the systems 25 times in succession. During these tests, temperature of both the heat exchanger and the top platform of the cart were measured during each trial. The team found that the heat exchanger temperature stabilized due to the thermal fuse, and the top surface of the cart never exceeded about 90 °F, even when left running for over an hour; plots of these results are shown in Figures 65 and 66. As shown in Figure 66, the top platform remains safe to touch even after extended operation. Full results of the temperature tests are available in Appendix K.


Figure 64: Heat Exchanger Wiring

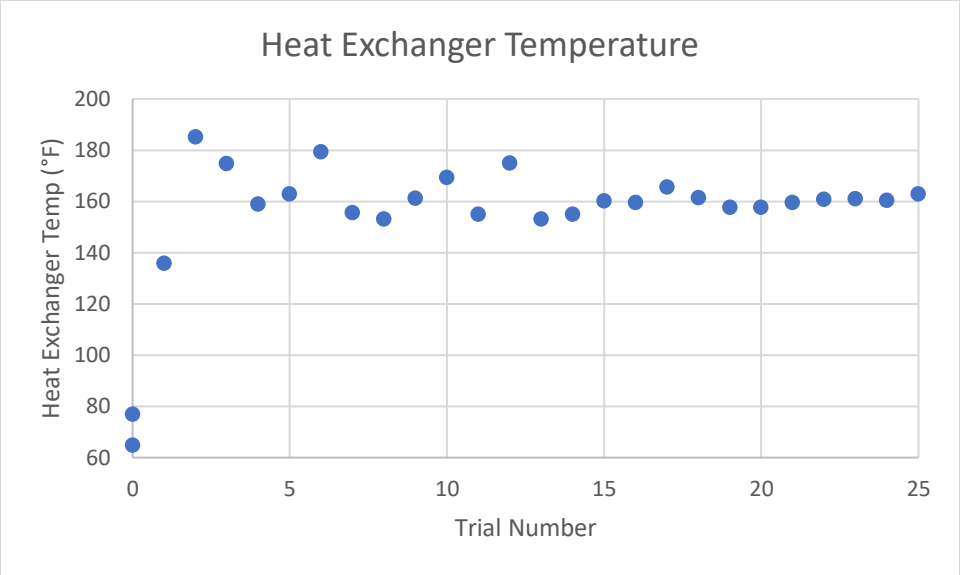

Figure 65: Heat Exchanger Temperature

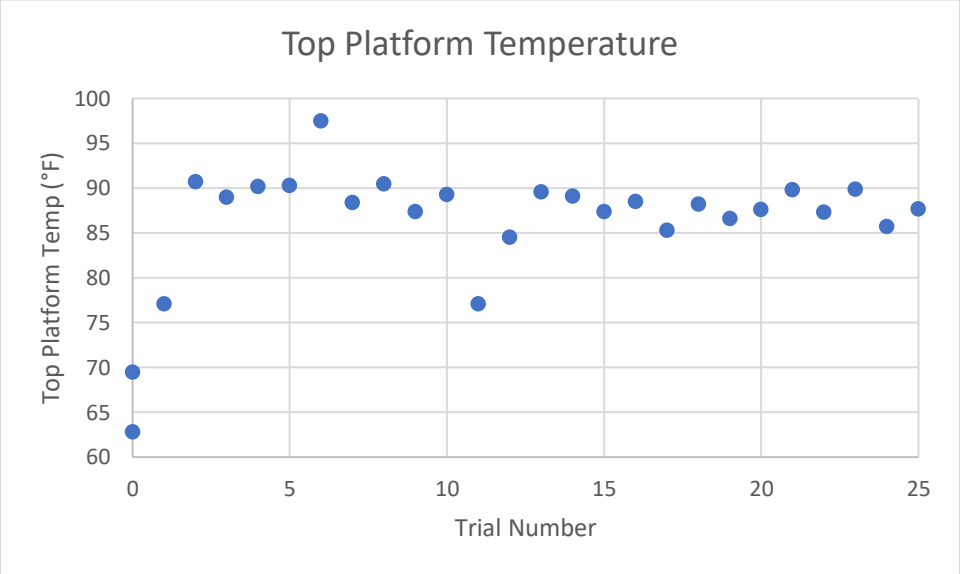

Figure 66: Temperature of the Cart Above Heat Exchanger

All the pressure lines are also contained underneath the cart so if failure does occur, the user will be shielded. The team did encounter failure of one of the vinyl tubes during durability testing. To remedy this, we replaced this line with copper piping as discussed earlier which should prevent any future failures and ensure reliability over extended usage. The tank also has a pressure release valve in case pressure needs to be relieved in an emergency; this is shown in Figure 67.

Figure 67: Pressure Release Valve

The design of the turbine model is such that it allows a user to open the outer casing to view the blade profiles and make repairs if necessary. To securely fasten the two halves together, the team used a locking latch, shown in Figure 68. This will prevent the system from opening during operating. Further, the turbine blades are mounted back from the tube edges, so they will not contact anything outside of the system.

Figure 68: Outer Casing Latch

8.7 Must Last 10 Semesters Minimum

The team conducted reliability testing twice: first with the original blades, as pictured in Figure 37, and again with the final green and yellow blades. These tests are separated into two sections. In order to test reliability, the team ran through numerous cycles with the device to monitor performance and look for points of failure. The team estimated that the device will likely be used about 4-5 times per semester, resulting in a target life of at least 50 cycles. Thus, the team decided to run through 25 cycles for initial testing. For each cycle, the team measured the time to fill the tank, as well as the time the turbine spun to monitor if performance deteriorated over time. Temperature was also measured as noted previously.

8.7.1 Testing with Initial System

In the first round of testing, the results revealed that the tank fill time remained very consistent, at about 5 minutes and 20 seconds. Run time actually increased over the testing period. This is likely because running

the device helped break in the bearings and resolved some clearance issues. Plots of these test results are shown in Figures 69 and 70, with full results available in Appendix K.

Given the consistency of these results, the team was confident that the device should last 10 semesters without issue, and small replacements that may need to be made are outlined in the operations manual if failure does occur. These tests also confirmed that demonstration time is under 15 minutes even if the test is run twice in sequence. However, the team still decided to repeat the 25-cycle test with the new blades to further prove reliability.

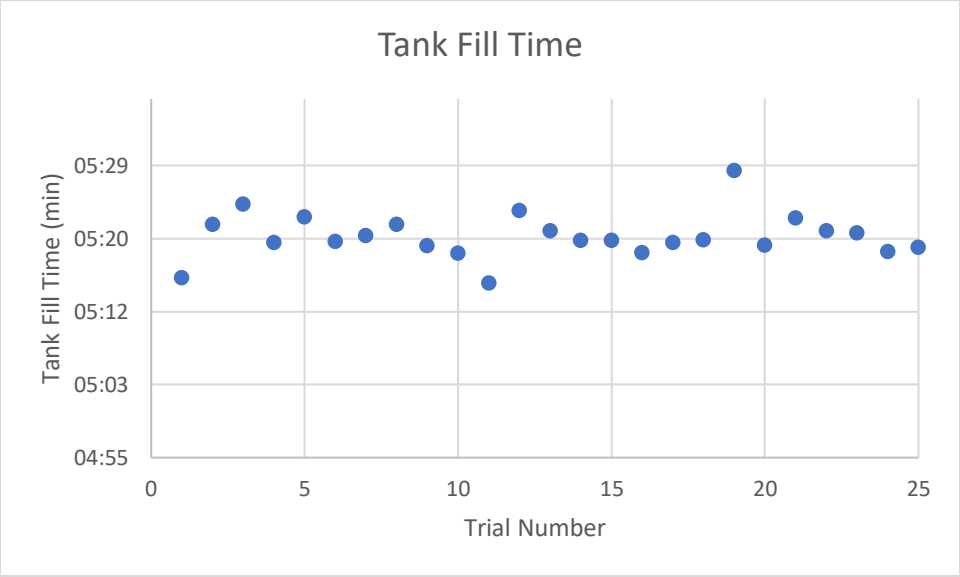

Figure 69: Air Compressor Charge Time

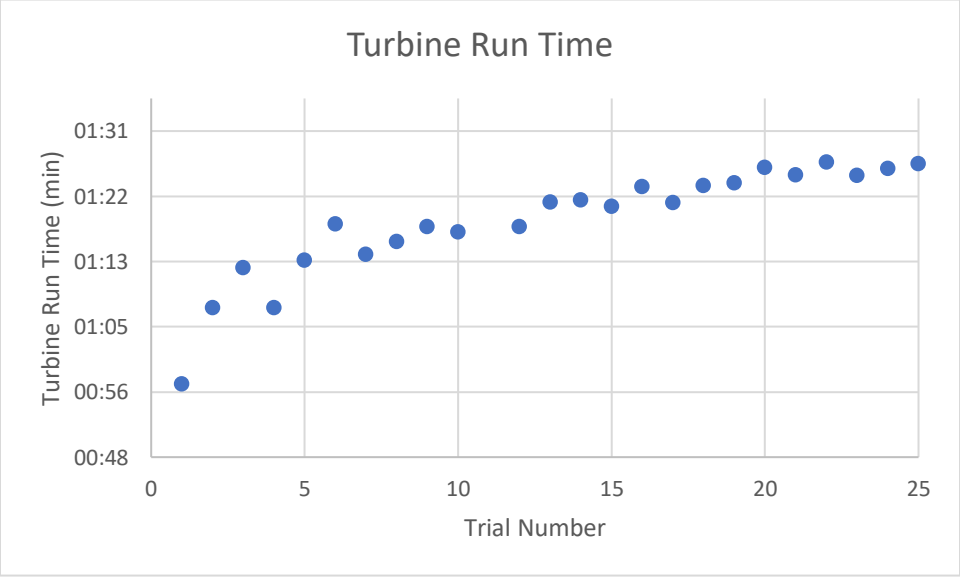

Figure 70: System Run Time

8.7.1 Testing with Final System

Testing with the final system had much more mixed results. Most notably, the team experienced heater failure during the second round of testing after trial 13 when we noted the heater temperature dropped dramatically. All wiring was checked with a multimeter, and it was determined that the switch was still

operating correctly and the heater was receiving power. Thus, the only explanation seems to be that the band heater broke. Before our team received the heater, it was used by another design team who deformed it to fit their design, which may have damaged it. Whatever the case, a new heater will need to be ordered. Despite the failure, the team continued testing the tank fill time and run time as shown in Figures 71 and 72 below. Again, tank fill time remained very consistent, but the run time of the device was shorter than in the previous testing. However, the turbine spun much more rapidly than in previous tests, and produced a noticeably greater amount of thrust, even after the heater stopped functioning. The team also had an issue around trials 6 and 7 where the blades started rubbing after the cart had been tipped over. This explains the variation of the data at this location, which was fixed in subsequent trials.

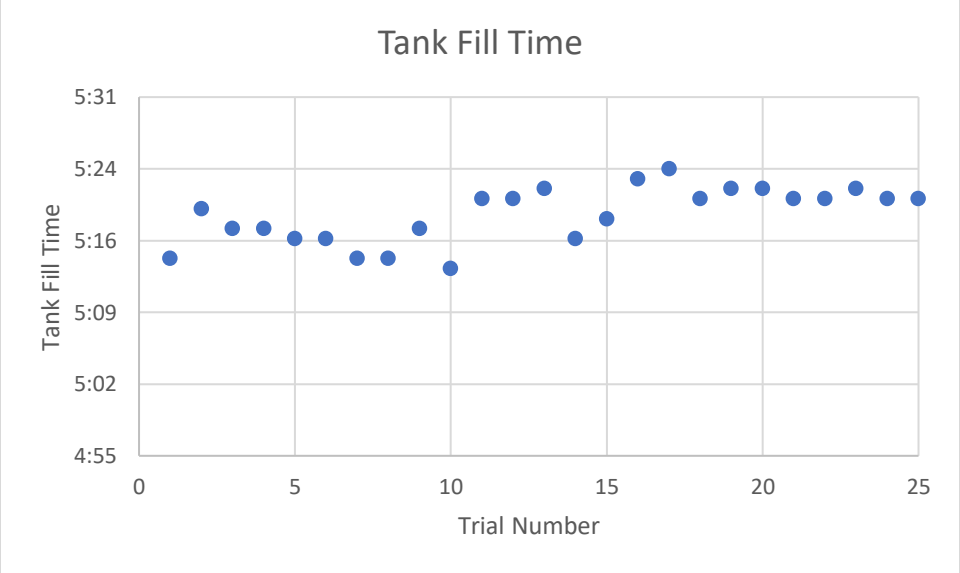

Figure 71: Air Compressor Charge Time (Final Blades)

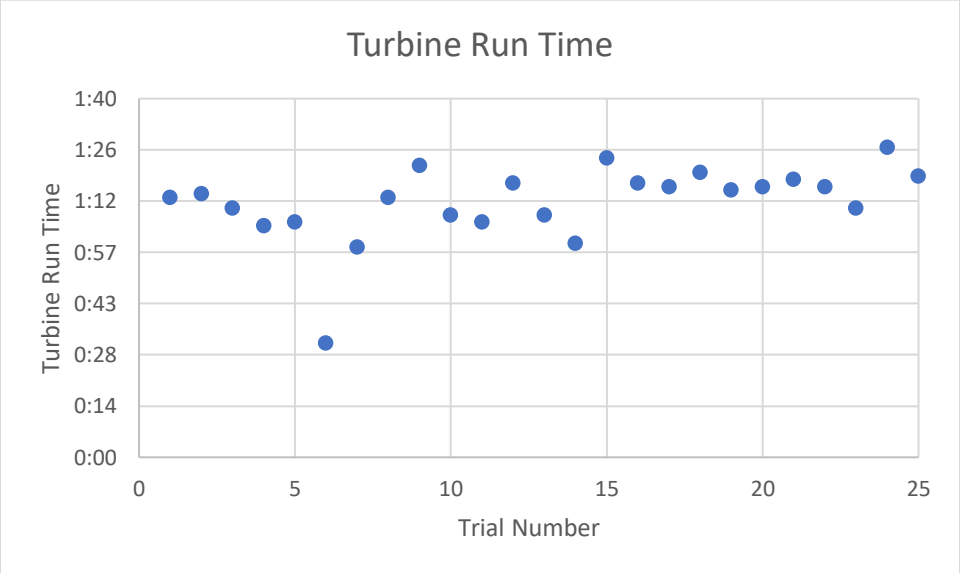

Figure 72: System Run Time (Final Blades)

8.8 Demo shouldn't take more than 15 minutes

As noted in the testing, charging the compressor with the added tank took approximately 5 minutes and 20 seconds. In addition, the system ran for less than 1 minute and 30 seconds on the compressed air. If the system had to be charged during class time, the total time to run the demonstration would be no longer than 7 minutes and could even be run twice for taking all of the desired measurements.

9 CONCLUSIONS

After finishing the project, the team had a final meeting to discuss the entire project, reflecting on what we had accomplished, what went well, and what we could improve upon were we to attempt this project again.

9.1 Contributions to Project Success

The team was able to accomplish many of the goals set out in the team charter when the project started. The overall device performs well and is an effective classroom demonstration tool. The model was safe for a classroom setting, due to the many considerations made by the team to meet this criterion. Combustion was replaced with a safer alternative, and dangerous components were shielded and labelled. The model was also completely self-contained on a cart, making it ideal for carrying in and out of a classroom meeting the goals of compactness and portability.

Another goal the team was able to meet was making the design aesthetically pleasing, by painting components to match and color coordinating the different blade sections. Messy wiring and tubing were also hidden underneath the cart to streamline the look of the device. The team also made significant improvements from the previous two iterations of this project. With this iteration, the blades spin at a much higher speed without having to manually manipulate the air flow, the run time is longer, and the measurement system is more sophisticated. Additionally, the new design is very user-friendly. All controls are grouped together in one area and clearly labelled, improving the user experience and overall product quality. Finally, the team was able to stay very close to the original budget even with numerous design changes made along the way, many of which were unexpected.

The team also worked well together over an entire year. The ground rules laid out in the team charter helped the team avoid many unnecessary conflicts during the project. One area in which the team was particularly successful was communication, which aided efficiency and time management.

Frequent communication was one tool the team relied heavily upon. Talking frequently through text, email, or phone call let the team know when problems arose and solutions were quickly devised. It also helped to keep everyone up to date on how personal schedules were changing and work was progressing. Team members only missed meetings on a small number of occasions; when this happened, the member always notified the team if they could not attend a meeting. The strong communication was likely aided by the fact that the team was smaller, but each team member's commitment to the project was also an important factor.

On that note, another ground rule that was useful to the team was completing assigned work on time. Work was split up amongst the three members and each member always got work done on time if not early. This allowed the whole team to provide feedback and look at documents before final submission. Work was generally divided based on the member roles laid out in the Team Charter, which were closely followed throughout the project, although some changes were made. Jacob was the Project Manager and Document Manager. He helped keep the team on schedule and ensured all assignments were submitted on time. He also consistently kept track of meeting minutes, making sure to record important details particularly for client meetings. Additionally, he generally completed final compiling, editing and formatting of written assignments. Samm was the Client Contact and Design and Manufacturing Lead. As such, he scheduled client meetings, and was responsible for CAD drawings and overseeing manufacturing. Ashley, the Budget Liaison and Website Developer, fulfilled her roles by completing and submitting all reimbursement forms and keeping the team website up to date. Following the original roles outlined in the team charter helped to break up the workload, which was particularly important for our small team, and gave each member an area of responsibility.

Surprisingly, the team did not experience much conflict during this year-long project. Again, this was probably due in part to the small size of the team. However, it was also because the team always addressed issues immediately; whether they were manufacturing problems, creative differences, or writing trouble, nothing was put off. Addressing issues immediately ensured that those problems did not grow and spiral out of control later. Ultimately, the team's effort in this area was very successful, as all team members are still on good terms at the end of the project, which is not always the case after projects such as this one.

9.2 Opportunities for Improvement

While the team accomplished many of its goals and generally worked together well, there are still several areas that could be improved. In terms of final product performance, there were a few goals the team didn't fully achieve. The main area in which the product fell short was data acquisition. The device had all physical measurement systems in place, but did not have the software capable of accurate data collection and manipulation that the client wanted.

There are several reasons why the team struggled to meet this goal. First, the team was simply too small. Having just three people increased individual workload dramatically, and members always had a lot of other considerations to address, so the data collection got set aside. However, even with the small size, the team could have done a better job planning ahead to meet this goal. From the beginning, the team decided that data acquisition would be the last consideration to address, as all members had used LabVIEW before and assumed it would be straightforward. However, we failed to consider the complexities of designing an entirely new data collection system, which turned out to be much more complicated than expected. Had we begun work on this earlier, we likely could have fulfilled this engineering requirement.

This leads to another area for potential improvement area: time management. This area was mixed; as noted before, the team did a good job of ensuring that all class deliverables were completed and submitted on time. Generally, the team also did well on these assignments. However, the class assignments often stalled progress on the actual construction of our product, which is likely also a contributing factor to our failure in completing a full data acquisition system.

Budget was also an area the team struggled with. As noted above, the team went over budget; however, it was only by a small amount, and this was not really an issue. The main problem area was budget management. Because our design team wanted to get started quickly, and because so many design changes were made during manufacturing, the team decided to make purchases out of pocket and submit reimbursement forms later. Unfortunately, the team did not do an adequate job keeping track of receipts. Generally, receipts were just grouped in a large collection and later submitted for reimbursement. No attempt was made at organizing the receipts or keeping copies for team records until the end of the assignment, which made creating the final Bill of Materials difficult, and meant that team members did not receive full reimbursement for what they had purchased.

Additionally, the team could improve on communication with the client. During the first semester, the team did a good job of checking in with the client at least once a week. However, for the second semester, meetings with the client were much more infrequent, and we often went several weeks without any communication. When we did communicate, we also failed to adequately express our progress, or more accurately our struggles, with the client. The team should have communicated with the client about the troubles with data acquisition earlier, but failed to do so for fear of disappointing him. However, had we reached out earlier, he likely could have provided helpful suggestions to guide the design team.

Finally, the team lacked an organized, set schedule. The team charter specified that the team should meet every Tuesday at 11 am, with other meetings scheduled as needed. This worked well in the first semester, but class schedules prevented this from working during the second semester. Rather than changing the scheduled meeting time, the team instead scheduled different meeting times every week as needed. As noted in the previous section, the team still met often and had productive meetings. However, the meetings were sporadic and varied greatly in length, and were often scheduled last minute. Having a fixed, scheduled meeting time every week would have helped to keep the team more organized.

Looking back, there are several actions the team could take to improve performance were the project to continue. First, the team should start data collection earlier. This was one of the client's biggest requests, so it should have been addressed first, even if it seemed simple. On that note, the team should communicate better with the client, to inform him of progress, but also to let him know when we are struggling to meet his requests and to discuss expectations.

The team should also work on better time management. Specifically, we should avoid letting class deadlines slow progress on the rest of the project. One method of accomplishing this would be setting a regular, permanent meeting time as discussed above. The meetings should also be set with a specific agenda. For example, one meeting could be scheduled to work on manufacturing, while the other set to work on class reports. This would ensure that class deliverables are completed without stopping the project's forward progress.

Finally, the team could improve performance by having a more organized budget. The team should carefully organize all receipts as soon as purchases are made, so they can be quickly referenced when needed. Additionally, the team should scan every receipt immediately after purchase to have a permanent record after submitting the original copy for reimbursement. This would help the team

to better stay within budget, have a more organized and up-to-date Bill of Materials, and ensure that each team member is reimbursed for exactly what they spent on the project.

Over the past year, the team learned numerous technical lessons as a result of this project. First of all, each team member gained substantial knowledge on the general principle behind turbines and how they work, far exceeding what was taught in Thermodynamics courses. The team also learned some basic aerodynamics principles which will likely prove useful in the future.

More generally, the team learned several important technical skills. Perhaps most important is the importance of design for manufacturing. Before beginning construction, we thought we had a good plan of how everything would work. However, manufacturing quickly revealed many issues with the original design that were previously unconsidered. As mentioned earlier, numerous changes had to be made to make the project feasible. The biggest change was the need to cut the acrylic tubing in half for proper assembly. But the team also ran into size and space constraints, and had particular difficulty mounting the pressure measurement system in the confined space underneath the cart. There were also issues in 3D printing, especially the combustion chamber, which were discussed in detail above. Again, these issues were never considered during the design stage, and only presented themselves after manufacturing began. This project demonstrated that designs that look great in principle may not always be feasible in practice.

The design team also learned the importance of effective budget management. While all team members have worked on several projects as students, this is the largest by far, and presented new challenges. Previous design projects were much shorter and had relatively small budgets, so budget was never given much thought in the past. This project's long timeline and large budget demonstrated the need for properly planning, implementing, organizing, and recording the budget.

Teamwork, delegation, and organization were also important lessons. As noted, all team members have substantial project experience from previous courses, which taught many skills that could be applied to this project. Even though this was the largest project undertaken by any of the members, it was also the smallest team we had ever worked on, which made these skills even more important. We did struggle in some areas, but over the past year, we managed to apply and refine these skills, allowing us to successfully complete a final product and preparing us for even bigger projects in our future careers.

References

[1] K. Hunecke, "Engine Classification," in *Jet Engines: Fundamentals of Theory, Design, and Operation*, Ramsbury, England: The Crowood Press Ltd, 1997, ch. 1, sec. 1.2, pp. 3-10.

[2] *The Market For Missle/Drone/UAV Engines* [Online]. Available: http://ww.forecastinternational.com/samples/F655_CompleteSample.pdf

[3] *MiniLab Gas Turbine Lab* [Online]. Available: http://www.turbinetechnologies.com/educational-labproducts/turbojet-engine-lab

[4] *Wren 50 Turbo Prop* [Online]. Available: http://www.wrenpowersystems.com/helitp.html.

[5] *RC Turboprop Model Jet Engines Explained* [Online]. Available: https://www.rc-airplanessimplified.com/model-jet-engines.html.

[6] N. Hall (2015, May 5). *Compressors* [Online]. Available: https://www.grc.nasa.gov/www/k12/airplane/compress.html.

[7] D. Newman (2003, Mar.). *Turbines and Compressors* [Online]. Available: http://ffden-2.phys.uaf.edu/212_fall2003.web.dir/Oliver_Fleshman/turbinesandcompressors.html.

[8] J. Escobar. (2003, May 1). *Turbine Engine Compressor Sections. Basic theory and operation* [Online]. Available: http://www.aviationpros.com/article/10387158/turbine-engine-compressorsections-basic-theory-and-operation

[9] S. Farokhi, "Axial Compressor Aerodynamics" in *Aircraft Propulsion*, 2nd ed., Chichester, United Kingdom: John Wiley & Sons Ltd, 2014, ch. 8, sec. 8.3, pp. 527-529.

[10] Q. Nagpurwala, *Design of Gas Turbine Combustors*, Bengaluru: M.S. Ramaiah School of Advance Studies.

[11] K. Hunecke, "Engine Classification," in *Jet Engines: Fundamentals of Theory, Design, and Operation*, Ramsbury, England: The Crowood Press Ltd, 1997, ch 5, sec 5.1, ppg 125-126

[12] K. Hunecke, "Turbine," in *Jet Engines: Fundamentals of Theory, Design, and Operation*, Ramsbury, England: The Crowood Press Ltd, 1997, ch. 6, sec. 6.1, pp. 137-145.

[13] *Jet Engine Design: The Turbine* [Online]. Available: http://aerospaceengineeringblog.com/jetengine-turbine/

[14] *Stator of Turbine* [Online]. Available: http://www.ekolenergo.cz/aktualitygb.html

[15] *Types of Turbines* [Online]. Available: http://www.idc-online.com/control/Types_of_Turbines.pdf

[16] S. Farokhi, "Aerothermo-dynamics of Gas Turbines," in *Aircraft Propulsion*, 2nd ed., Chichester, United Kingdom: John Wiley & Sons Ltd, 2014, ch. 10, sec. 10.2, pp. 685-713.

[17] *Angle of Attack* [Online]. Available: https://www.skybrary.aero/index.php/Angle_of_Attack.

[18] *Intex Quick-Fill Rechargeable Air Pump, 110-120 Volt, Max. Air Flow 21.2CFM* [Online]. Available: https://goo.gl/6HC12U

[19] *155 MPH 200 CFM 6 Amp Electric Handheld Leaf Blower Blue* [Online]. Available: https://goo.gl/JMt87v

[20] Cambered plate C=14% T=5% R=0.96 (cp-140-050-gn) [Online]. Available: http://airfoiltools.com/airfoil/details?airfoil=cp-140-050-gn

[21] W.W. Bathie. Fundamentals of Gas Turbines. New York, NY: John Wiley & Sons, 1996, pp. 248254.

Appendices

Appendix A: Concept Sketches

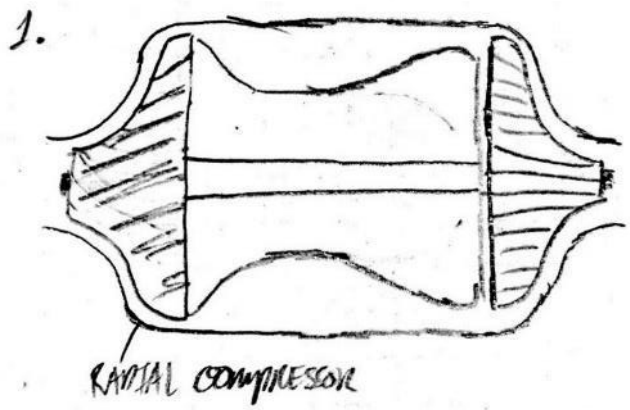

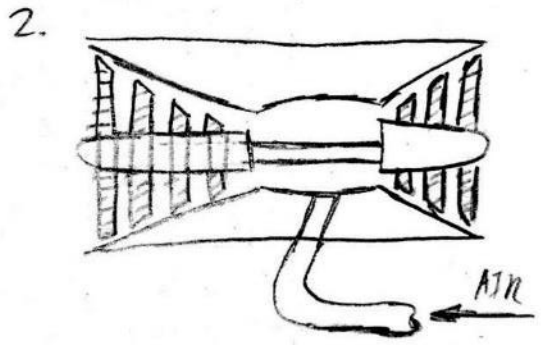

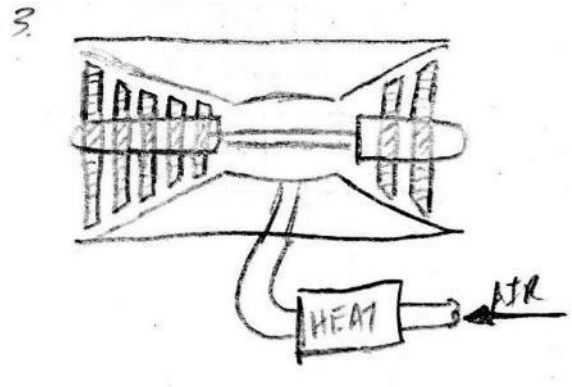

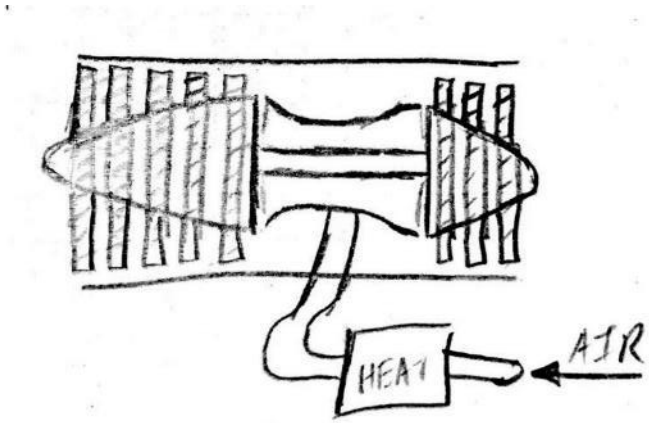

5.

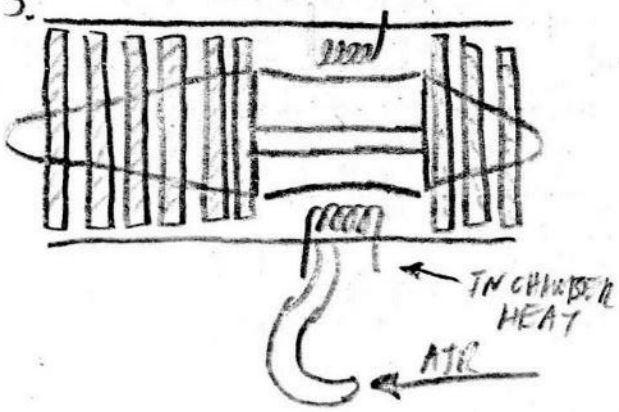

6.

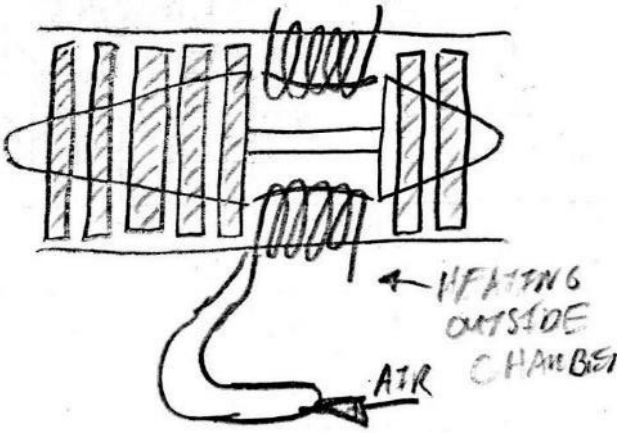

7.

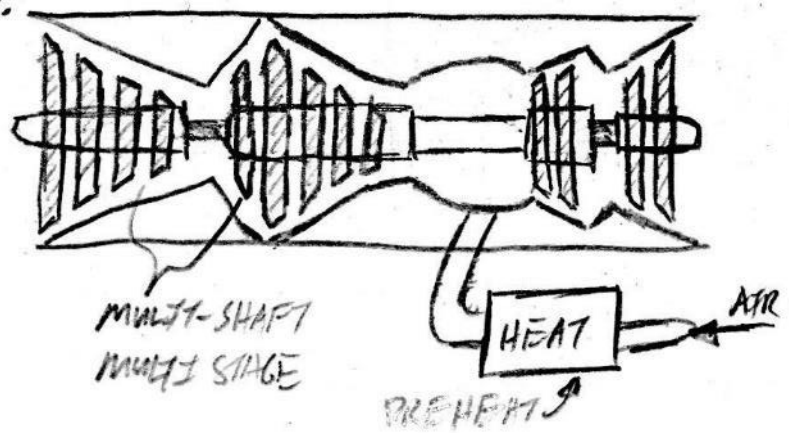
MULTI-SHAFT
MULTI STAGE
HEAT
AIR
PREHEAT

8.

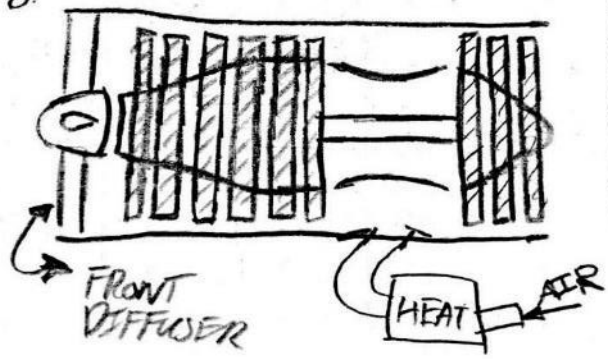
FRONT
DIFFUSER
HEAT
AIR

9.

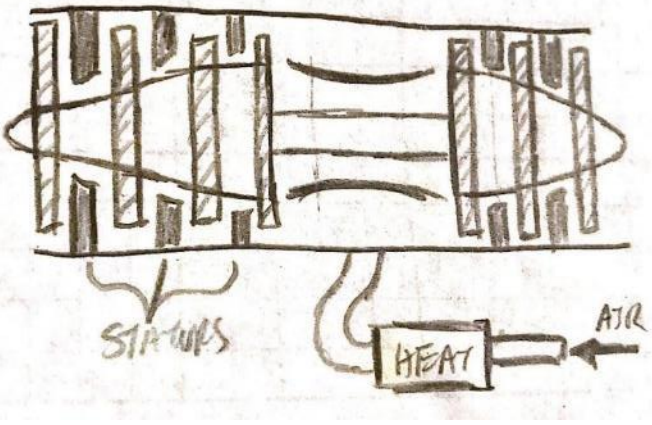
STATORS
HEAT
AIR

10.

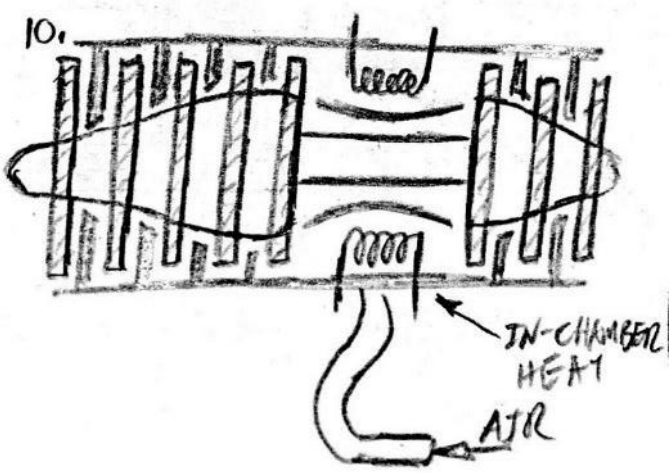
IN-CHAMBER
HEAT
AIR

11.

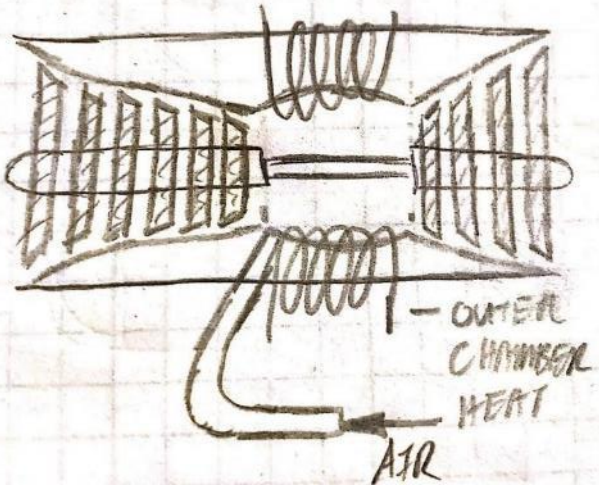
OUTER
CHAMBER
HEAT
AIR

12.

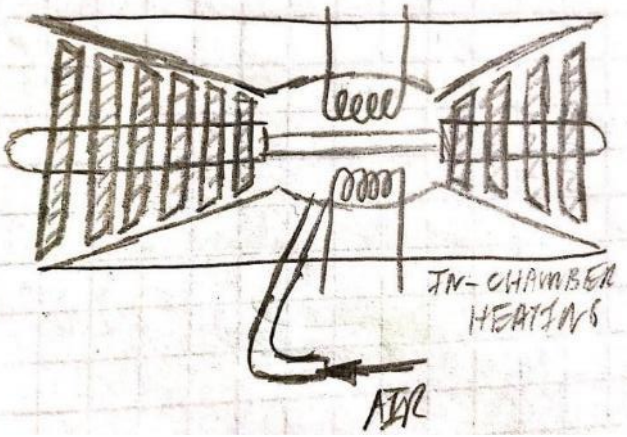
IN-CHAMBER
HEATING
AIR

13.

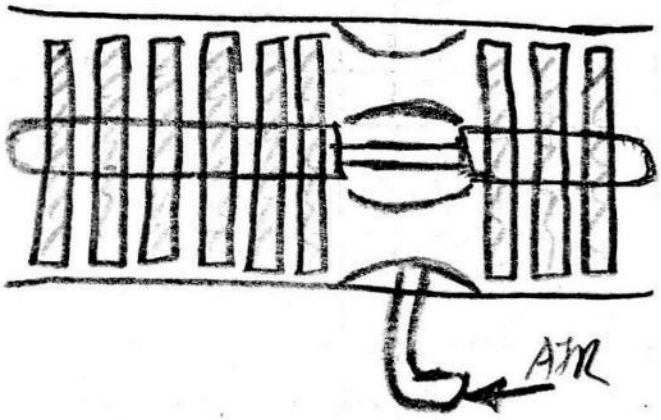

14.

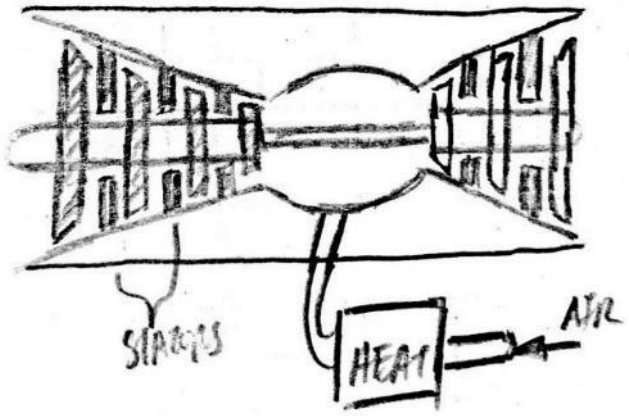

15.

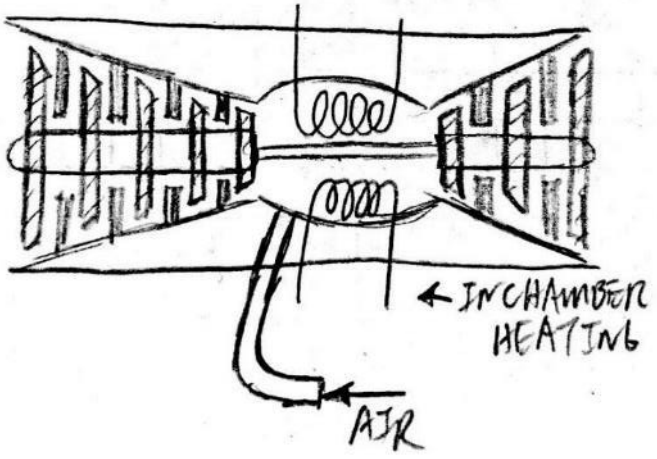

DESIGN 9

STATOR COMP. + TURBINE W/PREHEAT, COMPACT ANNEX DIAM.

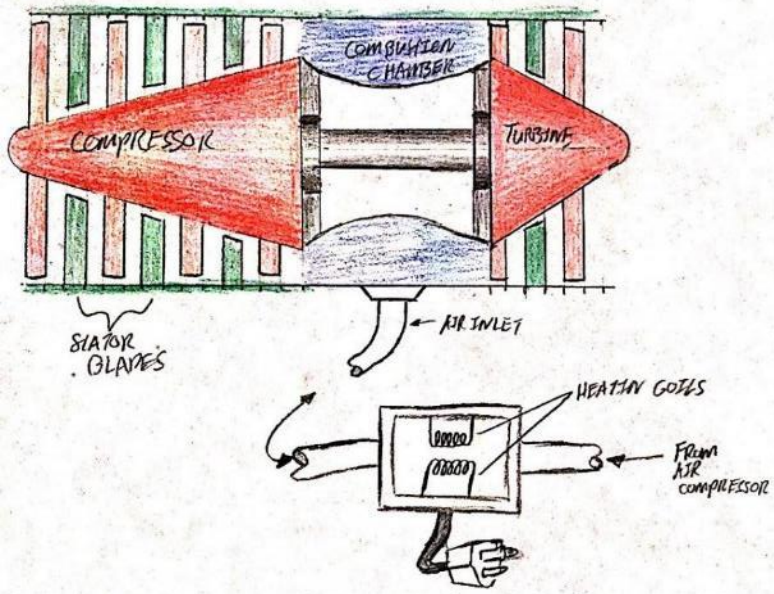

DESIGN 11

STATORLESS COMPRESSOR & TURBINE, W/PREHEAT, MIN. COMPACT DIAMETER

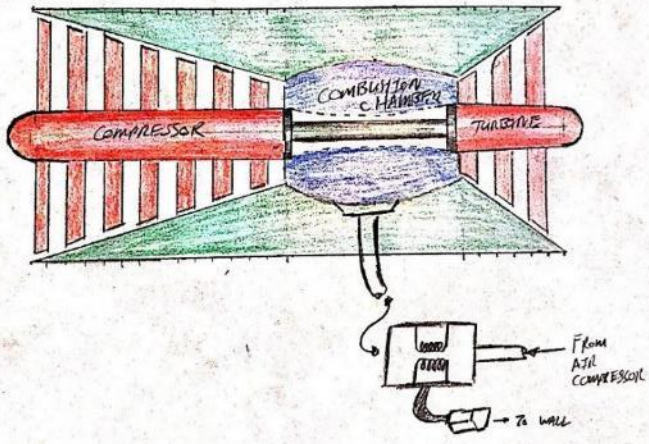

DESIGN 13

CONSTANT INER & OUTER DIAM, STATORLESS, NO HEAT

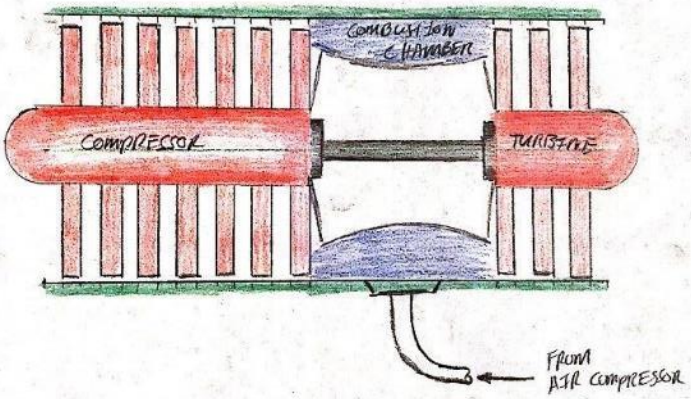

DESIGN 14

STATORLESS, CONST. OUTER DIAM, PREHEAT

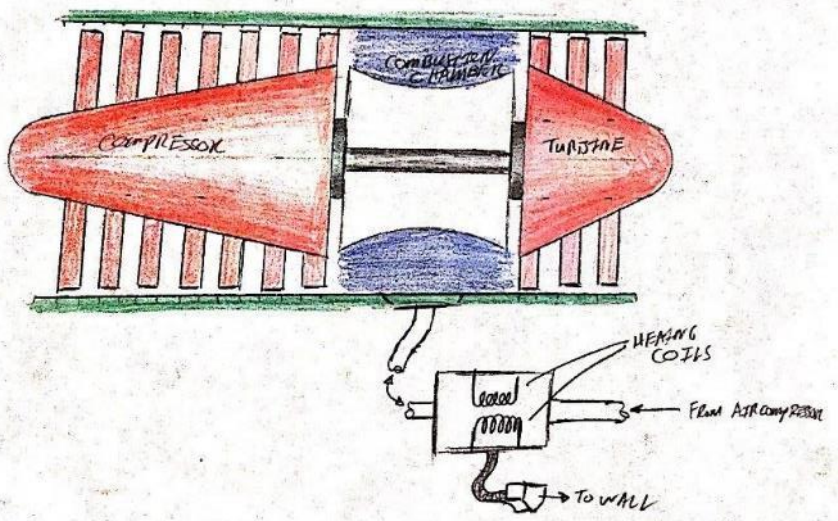

Appendix B: Pugh Chart

	1	2	3	4	5	6	7	8	9	10	11	12	13	14	15
Portable	-	s	s	s	s	s	s	s	s	s	s	s		-	s
Interactive	-	-	-	+	+	+	-	s	+	-	-	s		s	s
Educational	-	-	+	+	+	+	+	s	+	-	s	s	D	+	s
Durable	+	-	-	s	-	-	-	-	s	-	+	+		s	s
Reliable	-	s	-	-	-	-	-	-	-	-	s	s		-	-
Fit in 2x3 foot perimeter	s	s	s	s	s	s	s	s	s	s	s	s	A	s	s
Total weight < 100lbs	-	s	s	s	s	s	s	s	s	s	s	s		s	s
Demo < 15 minutes	s	s	-	-	-	-	-	-	-	-	-	-		-	-
Visability	-	-	-	s	s	s	-	-	s	-	-	-	T	-	s
120v AC, 60Hz, and/or compressed air	-	s	s	s	s	s	s	s	s	s	s	s		s	s
Minimize exposure	-	s	s	s	s	s	s	s	s	s	s	s		s	s
Feasibility	-	-	-	-	-	-	-	s	-	-	s	-		-	s
Efficiency	-	+	+	+	+	+	+	+	+	+	s	s	U	+	+
Cost	-	-	-	-	-	-	-	-	-	-	-	-		-	-
Total -	11	6	7	4	5	5	7	5	4	8	4	4		6	3
Total +	1	1	2	3	3	3	2	1	3	1	1	1	M	2	1
Total s	2	7	5	7	6	6	5	8	7	5	9	9		6	10

Figure B1: Pugh Chart

Appendix C: Part Drawings

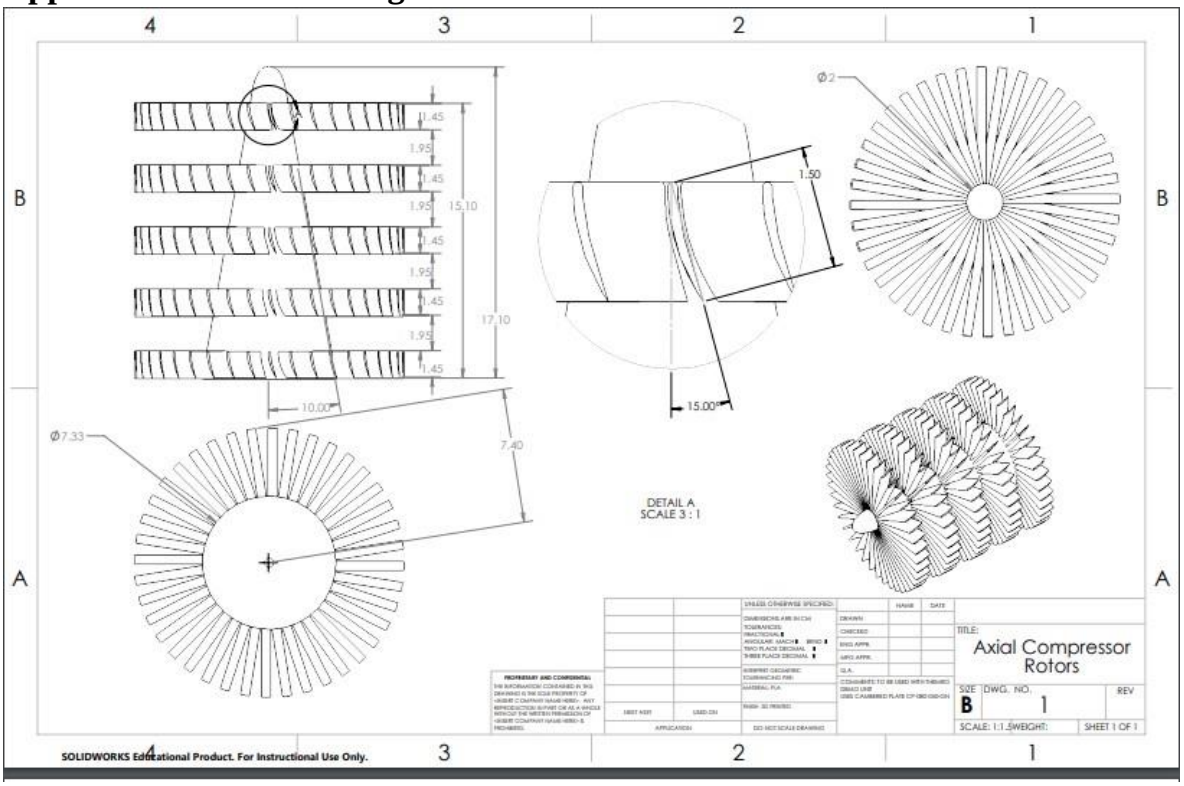

Figure C1: Compressor Rotors

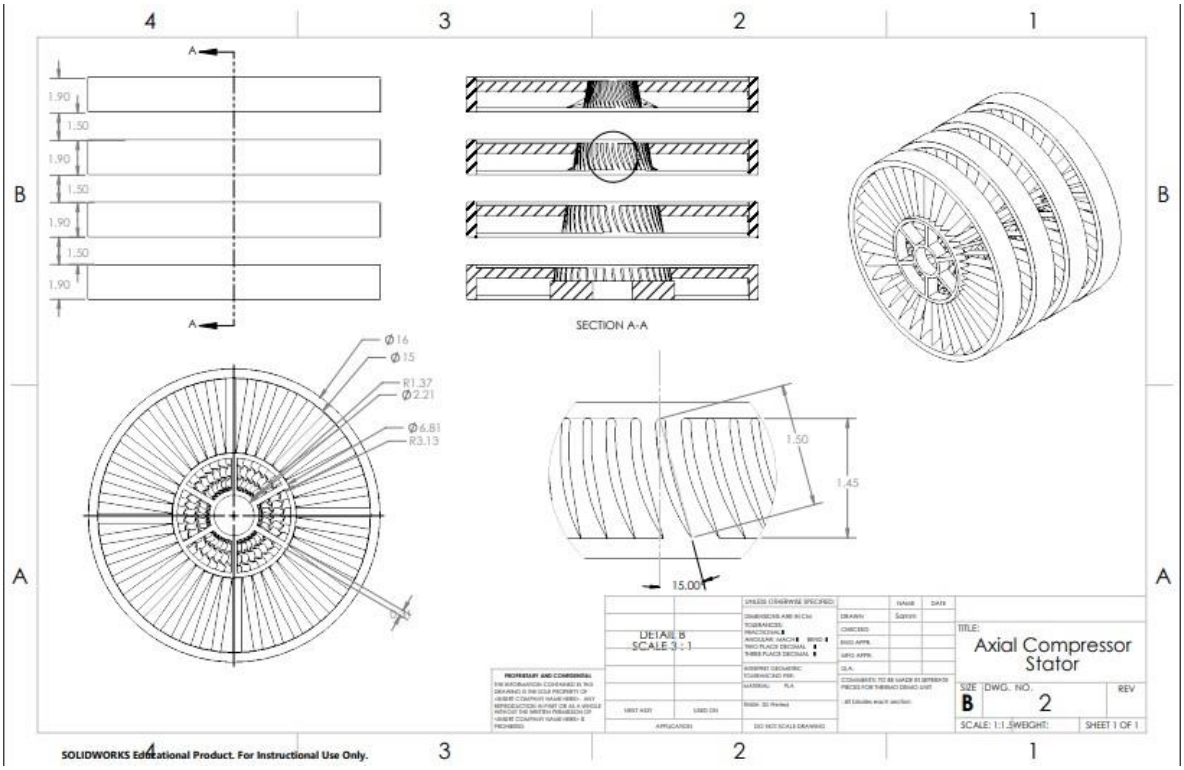

Figure C2: Compressor Stators

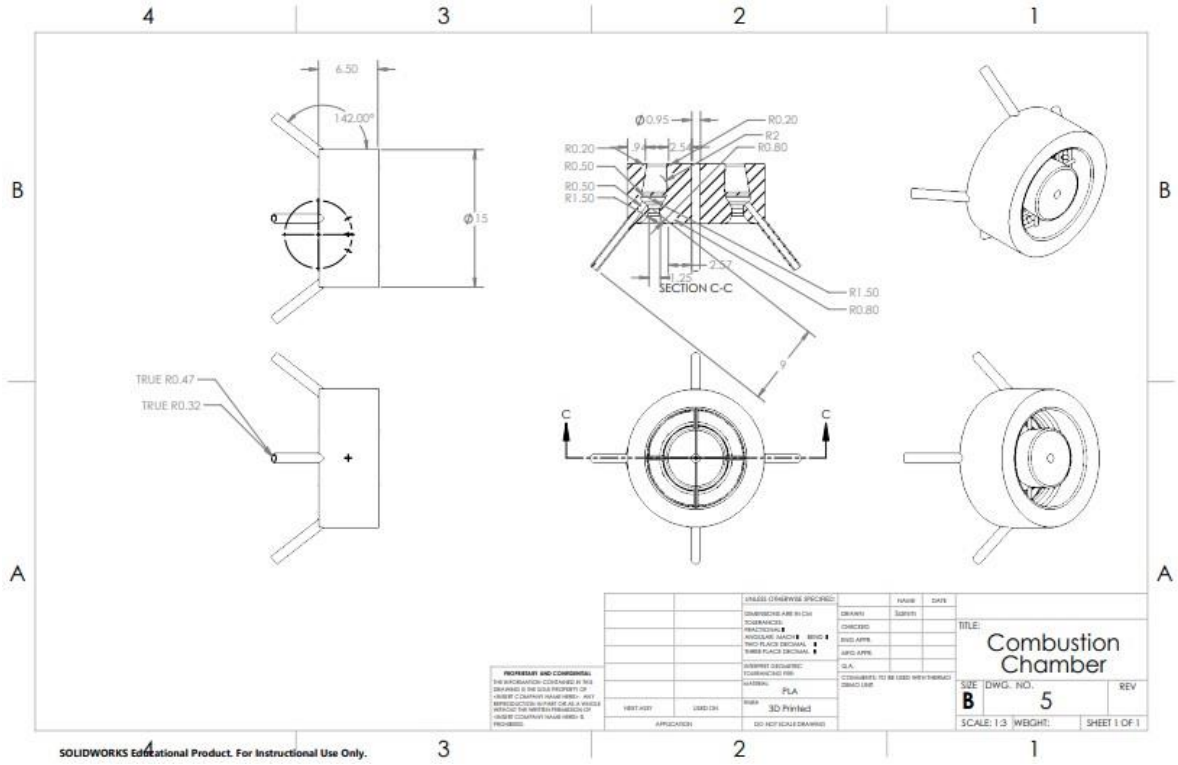

Figure C3: Combustion Chamber

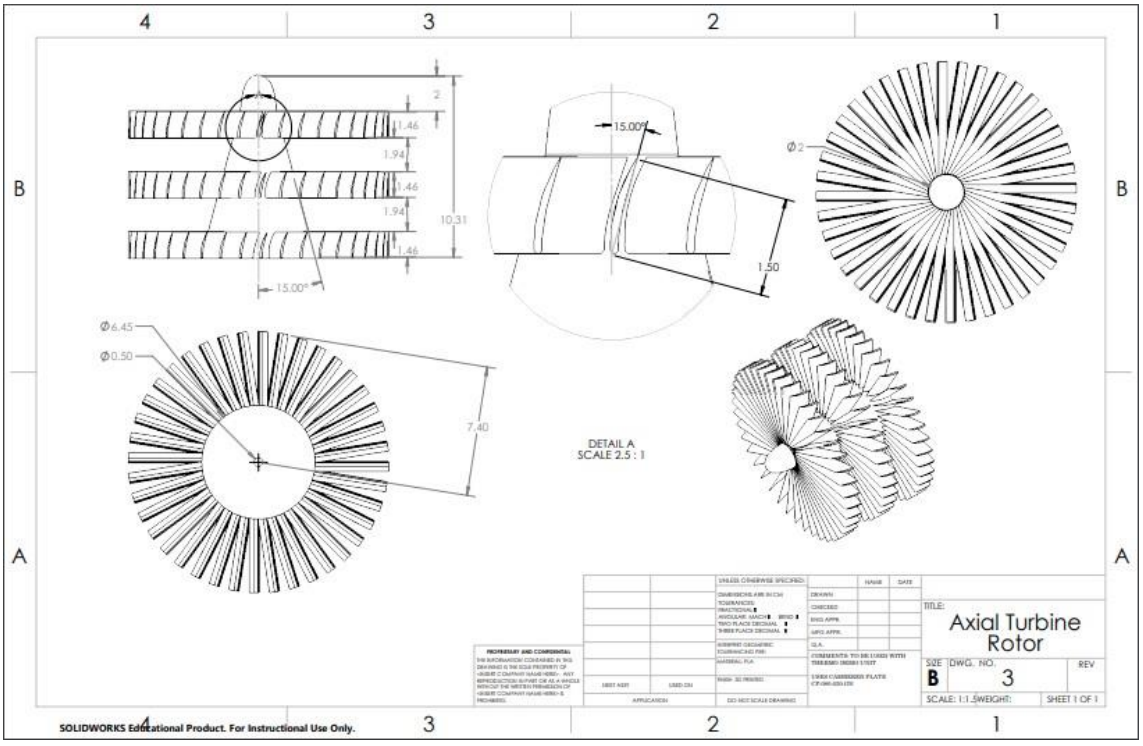

Figure C4: Turbine Rotors

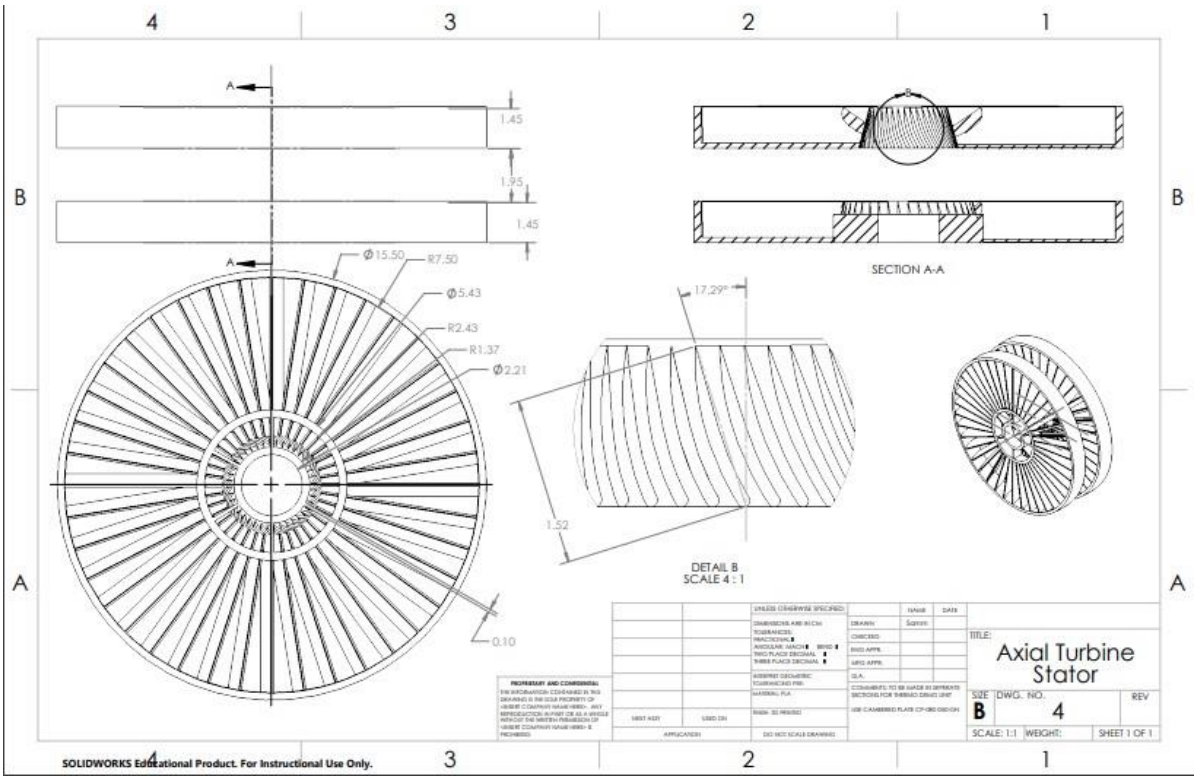

Figure C5: Turbine Stators

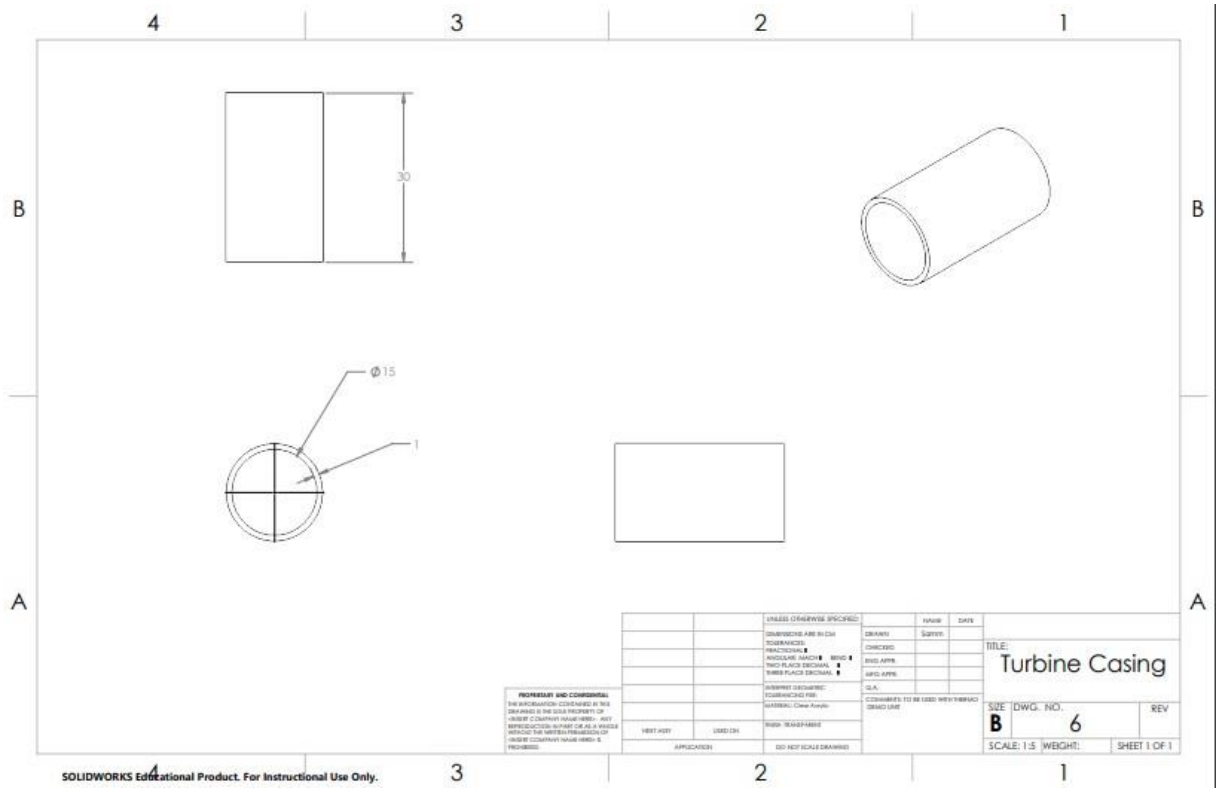

Figure C6: Outer Housing

Appendix D: Engineering Calculations—Compressor

The most important part of the calculations was the assumptions we were going to make do we could continue forward. We assumed a turbulent flow at the inlet to ensure an even velocity profile at the inlet, and because everyday jet engines experience turbulent flow at the inlet as well. Based on that, the Reynolds number for a turbulent internal flow must be above 4000: we assumed an inlet Reynold's number of at least 4500. From that we were able to find an inlet velocity using equation D1 below.

$$v_{inlet} = Re^{inlet} * \mu / \rho D \qquad (D1)$$

Re_{inlet} is the Reynold's number at the inlet, μ is the dynamic viscosity of the fluid, in this case it is air, ρ is the density of the fluid, and D is the diameter of the inlet. Assuming standard temperature and pressure, and an inlet size of 15 centimeters the minimum inlet velocity of .4510 m/s was calculated. That is almost exactly 1 mile per hour. Seeing as how the unit will be stationary for demonstration and that the inlet velocity is very low, the unit should be able to operate in a room with no inlet velocity aside from the suction it will create as it operates.

To start analyzing the blades, a 2cm hub radius was assumed at the first stage of the compressor, yielding a blade length of 6.4 cm leaving a 1 mm clearance between the blade and inner wall of the acrylic pipe. Using this information, the Reynold's number at the blades was calculated from equation D2 below.

$$Re_{blade} = \rho v_{inlet} L / \mu \qquad (D2)$$

The chord is the length of the line connecting the leading and trailing edges of an airfoil [3]. I assumed this to be 1.5 cm because it seemed like a reasonable length, and most likely will be adjusted later. The Reynold's number I calculated at the blades was 450. These numbers were much lower than I saw on recommended Reynold's number for the airfoil on *airfoiltools.com*, but they will still work for initial calculations.

The next step was to assume a speed that the model will rotate at. From our initial research about the project I had found the Wren 50 model engine [4]. This engine uses real combustion and has similar dimensions to our design. The engine idles at 55,000 rpm and because our design is slightly larger I used that speed in my calculations. I converted that speed to radians per second and used that value to find the angular velocity of the blades using equation D3 below.

$$U_1 = r * \omega \qquad (D3)$$

The radius of the blades is represented by r, and omega is the speed in radians per second of the blades. Figure 2 below shows the structure of the velocity triangles and how they will be solved

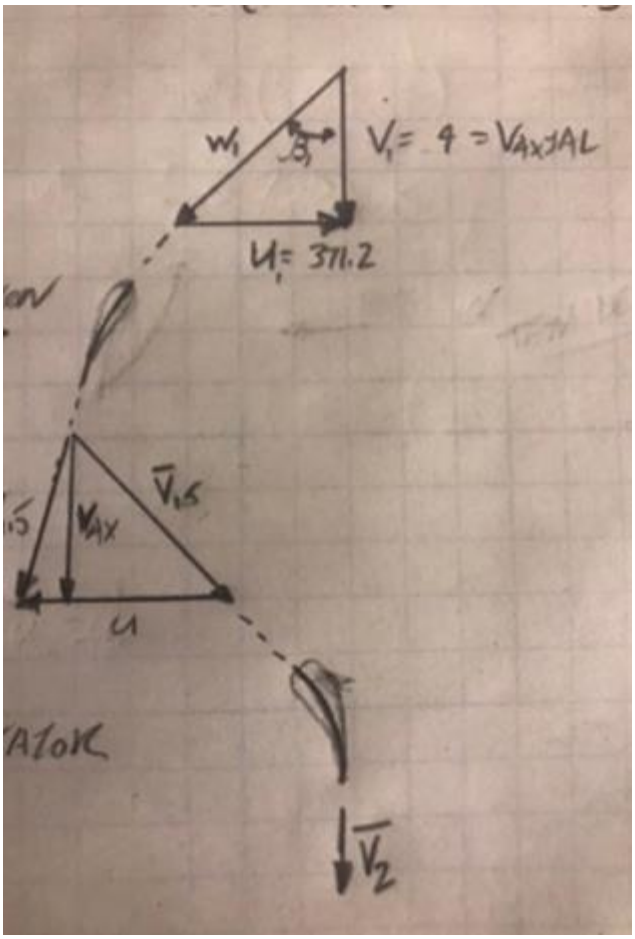

Figure D1: *velocity triangle and blade diagram*

The lower blade is the stator, and the upper triangle is the rotor. Both of these together make up stage 1. The equations and processes for finding β_1, $\beta_{1.5}$, $\alpha_{1.5}$, and v_2 can be seen below in figures D3 and D4.

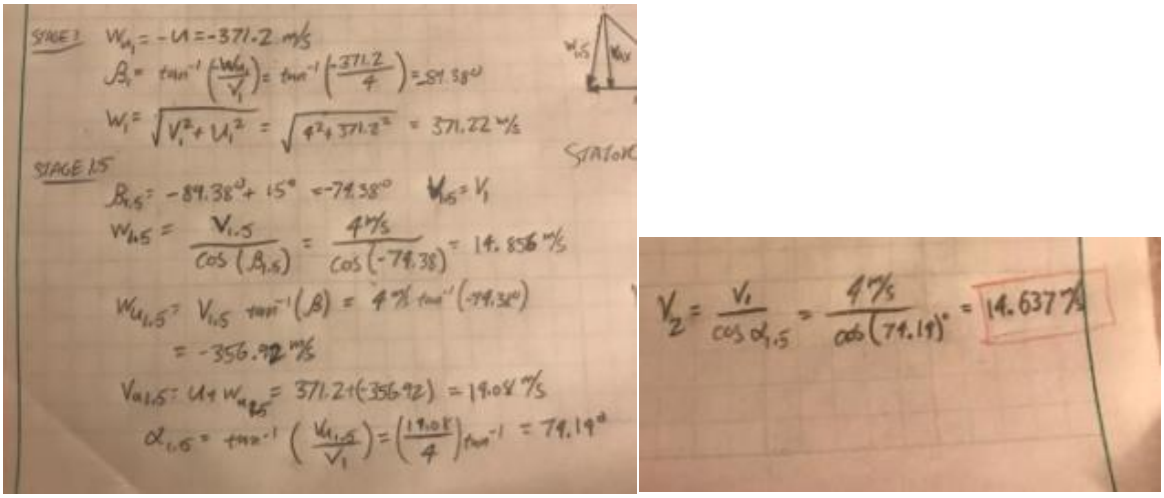

Figure D3,4: *velocity diagram calculations*

Appendix E: Engineering Calculations—Combustion Chamber

The following equations were used in the analysis of the combustion chamber:

$$Re_D = \frac{U_\infty D}{v} \quad (1)$$

$$\dot{m} = \rho u_m A$$

$$q = h\Delta T$$

$$q = \dot{m}\, C_p \Delta T$$

Appendix F: Engineering Calculations—Turbine

Airfoil selection

To maximize the efficiency of a turbine, it is important to maintain the optimal angle of attack over the blades. As shown in Figure F1, the angle of attack refers to the angle between the "relative wind", or the relative velocity of the incoming flow, and the Chord line of the airfoil.

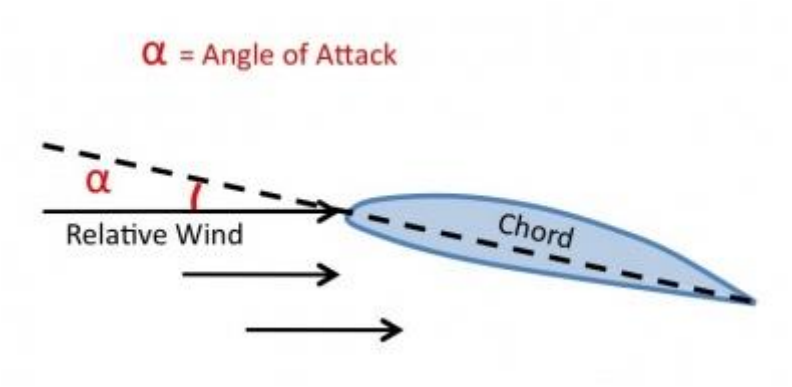

Figure F1: Airfoil Geometry [17]

The optimal angle of attack will provide the maximum ratio of lift and drag and depends on the airfoil profile selected. Thus, the first step in the design process was to select an airfoil profile. Dr. Acker suggested that a "cambered plate" type profile would be ideally suited in this application, due to the small scale and low Reynolds numbers. The website airfoiltools.com provides numerous cambered plate profiles as well as their best-suited Reynolds number ranges. To choose the initial profile, a very rough Reynolds number was estimated.

At this stage the team estimates that the model will have a diameter of about ten centimeters. The blades should occupy most of this space and will likely have a Chord length of around one centimeter. Unfortunately, it is difficult to estimate the mass flow rate in the final system. As a starting point, I researched the volumetric flow rate of a typical air mattress pump, which is about 21 cubic feet per minute (CFM), or approximately 0.01 cubic meters per second, and a leaf blower, which has a volumetric flow rate of about 200 CFM, or 0.1 cubic meters per second. [18, 19]. I estimate that our model will have a volumetric flow rate somewhere between these two. For this analysis, we will assume 0.05 m^3/s, but this is just a ballpark starting point which can easily be adjusted in the final MATLAB code.

Assuming this volumetric flow rate, and a turbine rotational velocity of about 5000 rpm (again this can be adjusted), we estimated the average Reynolds number of the center of the airfoil to be approximately 8000. The calculation is detailed below.

$$\vec{V} = \vec{W} + \vec{U}$$

Where V = absolute (incoming) velocity, W = relative velocity, and U = blade velocity. W is the important velocity here, as it is the velocity that the blade experiences. It is important to note that this expression is a vector sum.

$$\dot{\forall} = V * A; V = \frac{\dot{\forall}}{A}$$

Where $\dot{\forall}$ = volumetric flow rate and A = cross sectional area.

$$A = \frac{\pi}{4}(D)^2 = \frac{\pi}{4}(0.1m)^2$$

Where D = casing diameter.

$$V = \frac{0.05\ m^3/s}{\frac{\pi}{4}(0.1m)^2} = 6.36\frac{m}{s} \approx 6.5\ m/s$$

$$U_{avg} = r_{avg}\omega = (0.025m)\left(5000\frac{rev}{\min}\right)\left(2\pi\frac{rad}{rev}\right) = 13.1\frac{m}{s} \approx 13\ m/s$$

r_{avg} = midpoint radius, ω = angular velocity

$$W = \sqrt{V^2 + U^2} = \sqrt{\left(6.5\frac{m}{s}\right)^2 + \left(13\frac{m}{s}\right)^2} = 14.53\frac{m}{s} \approx 14.5\frac{m}{s}$$

$$Re = \frac{\rho V c}{\mu}$$

Re = Reynolds Number, ρ= fluid density, c= chord length, μ = dynamic viscosity.

$$At\ 7000\ ft\ (\sim 2000\ m), \frac{\rho}{\rho_{SL}} = 0.8217\ \Rightarrow\ \rho \approx 1.007\frac{kg}{m^3}$$

$$Re = \frac{\left(1.007\frac{kg}{m^3}\right)\left(14.5\frac{m}{s}\right)(0.01m)}{(1.81E-5\frac{Ns}{m^2})} \approx 8067$$

Most standard airfoils operate at significantly higher Reynolds numbers. Dr. Acker suggested that airfoil design is not as critical at low Reynolds numbers, so for this analysis we selected a standard cambered plate airfoil at the lowest Reynolds number range, which is 50,000. The selected airfoil is a cp-140-050gn cambered plate, shown below in Figure F2. This airfoil has an optimal angle of attack of 13.25 degrees [20].

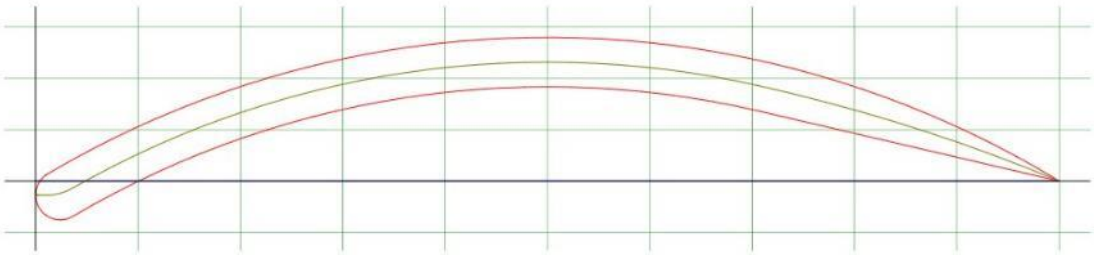

Figure F2: Selected Airfoil Profile [20]

Angle of Attack Calculation

As noted previously, the goal is to maintain this angle of attack over the entire length of the blade. As shown in Figure F1, this is the angle between the relative wind and the Chord line of the airfoil. *Fundamentals of Gas Turbines* provides an excellent diagram illustrating the geometry of the flow entering a rotor stage, illustrated in Figure F3. In this example, V_1 is the incoming axial flow, W_1 is the relative velocity, and β is

the angle of the relative velocity with respect to the axial direction. In this example, it is assumed that the axial velocity is one dimensional in the axial direction, and the relative velocity enters the rotors at the Chord line angle, meaning the angle of attack is zero. This type of diagram is known as a velocity triangle.

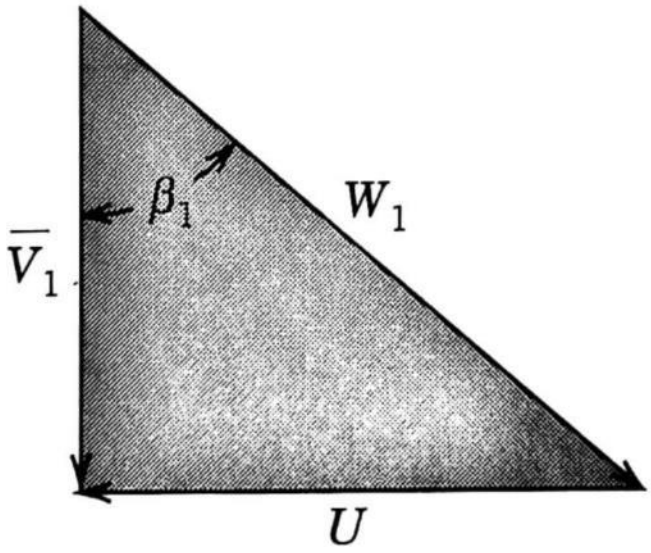

disc

Figure F3: Velocity Triangle [21]

This example can be expanded to demonstrate a flow with a positive angle attack. Figure F4 illustrates this theory using the selected airfoil profile. In the figure, γ is the angle between the chord line and the axial direction, which will be defined as the pitch angle, and α is the angle between the chord line and the relative wind, which is the angle of attack.

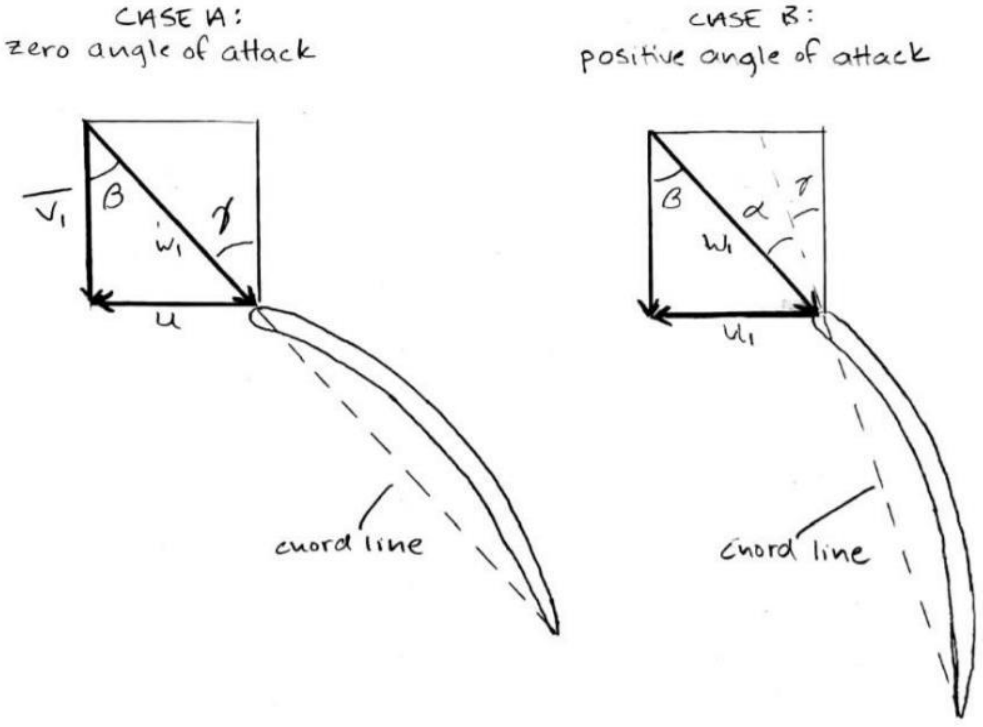

Figure F4: Airfoils with Velocity Triangles

Case A is the same as in Figure F3, where the flow enters at the same angle as the chord line, and the angle of attack is zero. In Case B, the incoming velocity is identical to Case A. This time, however, the blade is oriented differently to create a positive angle of attack. By inspection, the angles β and $\alpha + \gamma$ constitute alternate interior angles, meaning $\beta = \alpha + \gamma$.

However, as noted previously, the blade velocity U will vary depending on radial location along the blade. As a result, β will also change. To maintain a constant angle of attack, the pitch angle γ must be continuously varied radially along the blade profile. This angle can be calculated at each location using the equation $\gamma = \beta - \alpha$. Since this value continuously changes, the best way to calculate parameter is by creating a MATLAB script which discretizes the blade profile into finite elements and calculates γ for each element.

MATLAB Program

The MATLAB script for this analysis prompts a user to input the volumetric flow rate in CFM, angular velocity in RPM, casing diameter in centimeters (cm), and desired angle of attack in degrees. It also asks the user how many elements they would like the blade to be discretized into. Using this information, the program makes necessary unit conversions, then calculates axial velocity using the method detailed in the Airfoil Selection section. Next, it calculates blade velocity at each point along the blade based on the radial location of each blade element. It then calculates the relative flow angle and the necessary pitch angle to maintain the desired angle of attack at each location. The final output is a plot which displays pitch angle in degrees vs. the radial location in meters. Figure F5 below shows an example output using a flow rate of 100 CFM, an angular velocity of 5000 RPM, a casing diameter of 10 cm, an angle of attack of 13.25 degrees, and 100 blade elements.

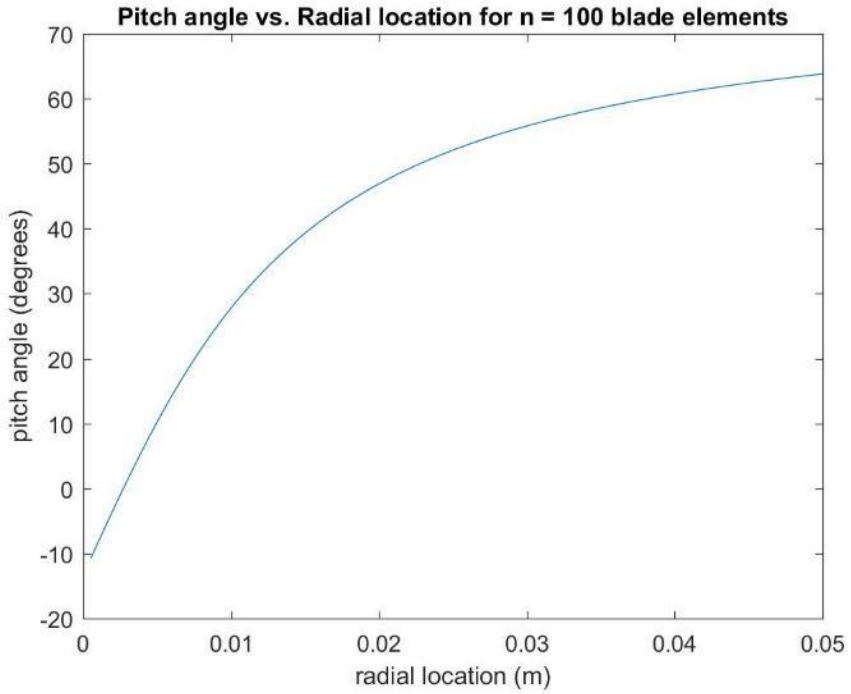

Figure F5: Pitch Angle vs. Radial Location

This code makes several assumptions. First, it assumes the incoming axial velocity is one dimensional and enters parallel to the axial direction. It also assumes that each blade occupies half the inner diameter (ignoring the shaft at the center). The script is presented below in its entirety

```
% Programmer: Jacob Barker
% Date: 03/09/18
%%%%%%%%%%%%%%%%%%%%%%%%%%%%%%%%%%%%%%%%%%%%%%%%%%%%%%%%%%%%%%%%%%%%%%%%%%%%%%%

clear; clc; close all;

%prompt user for volumetric flow rate
Vdot1 = input('Enter volumetric flow rate (CFM): ');

%prompt user for angular velocity
RPM = input('Enter angular velocity (RPM): ');

%prompt user for desired number of blade elements n = input('Enter desired number of
blade elements: n = ');

%prompt user for desired angle of attack
alpha = input('Enter angle of attack (degrees): ');

%Prompt user for outer diameter
d1 = input('Enter housing diameter (cm): d = ');

%convert units
Vdot = Vdot1*(1/60)*(12^3)*(2.54^3)*(100^(-3)); %m^3/s

omega = RPM*2*pi/60; %rad/s
  d = d1/100; %m
  r = d/2; %m
%ignores shaft diameter, assumes blades occupy entire cross section

%distance between blade element "nodes" dx = r/(n-1);

%blade element "node" locations. "Off the edge" configuration as
%blade tip angle important. Starts at dx as there is no blade velocity
%at zero (shaft location) x = dx:dx:r;

%caclulate axial velocity Va = Vdot/(pi/4*d^2);

%Create blank vectors for U, W, beta, gamma to be populated in for loop
U = zeros(1,length(x)); W = zeros(1,length(x)); beta = zeros(1,length(x));
gamma = zeros(1,length(x));

for i = 1:length(x)
    U(i)=x(i)*omega;

    W(i)=sqrt((x(i)^2)+Va^2);

    beta(i)=radtodeg(atan(U(i)/Va));

    gamma(i)=beta(i)-alpha;
     end  plot(x,gamma) xlabel('radial location (m)')
ylabel('pitch angle (degrees)') title(['Pitch angle vs. Radial
location for n = ' num2str(n) ' blade elements'])
```

Appendix G: Updated Bill of Materials, Version 1

Table G1 shows the midpoint Bill of Materials for the project. The items highlighted in yellow indicate that they were purchased by the previous capstone team, and thus are not part of our $500 allotted budget.

Table G1: Updated Bill of Materials

Item	Quantity	Cost per unit	Subtotal	Manufacturer	Item #	Vendor	Hyperlink
Acrylic Tubing	23 7/8 in	$17.99	$17.99	estreetplastics	ET0450042524	estreetplastics	https://goo.gl/rmKMEm
3D Printed Compressor Blades	255 g	$0.10	$25.50	MakerBot	N/A	NAU Cline Library	n/a
3D Printed Compressor Stator Blades	292 g	$0.10	$29.20	MakerBot	N/A	NAU Cline Library	n/a
3D Printed Turbine Blades	152 g	$0.10	$15.20	MakerBot	N/A	NAU Cline Library	n/a
3D Printed Turbine Stator Blades	213 g	$0.10	$21.30	MakerBot	N/A	NAU Cline Library	n/a
3D Printed Combustion Chamber	208 g	$0.10	$20.80	MakerBot	N/A	NAU Cline Library	n/a
3D Printed Test Fitting #1	77.58 g	$0.10	$7.76	MakerBot	N/A	NAU Cline Library	n/a
3D Printed Test Fitting #2	64.28 g	$0.10	$6.43	MakerBot	N/A	NAU Cline Library	n/a
Aluminum Shaft	2 ft	$5.62	$5.62	MetalsDepot	R3516	Metals Depot	https://goo.gl/CezFTP
Ceramic 608 Bearings	2	$3.33	$6.66	VXB	608-2RS-DRY	VXB	https://goo.gl/zPNP8M
Air compressor with tank	1	$89.00	$89.00	Porter Cable	C2002	CPO Commerce	https://goo.gl/KRQu8p
Band Heater	1	$28.50	$28.50	Tempco	NHL00100	Grainger	https://goo.gl/WnqnU8
K Type Thermocouple Wire	25 ft	$0.86	$21.50	TIP Industries	TIPWRK004	TIP Industries	https://goo.gl/AETaH8
Thermocouple Connectors	4	$2.30	$9.20	Omega	OST-U-M	Omega	https://goo.gl/mftfh2
Thermocouple DAQ	1	$107.00	$107.00	National Instruments	USB-TC01	National Instruments	https://goo.gl/U5soAU
1/4 in. x 1/4 in. MIP Brass Compression Adapter	2	$4.40	$8.80	Everbilt	801079	Home Depot	https://goo.gl/z6qf8e
Brass Pipe Coupling 1/4 in. FIP	2	$4.16	$8.32	Everbilt	801889	Home Depot	https://goo.gl/VR7m58
Brass Compression Tee 1/4 in	2	$7.51	$15.02	Everbilt	800849	Home Depot	https://goo.gl/Nh2w24
1/4 in. Compression Angle Needle Valve	4	$8.80	$35.20	Everbilt	800539	Home Depot	https://goo.gl/NpVaUW
1/4 in. O.D. x 0.170 in. I.D. x 10 ft. PVC Clear Vinyl Tube	1	$2.82	$2.82	Everbilt	701906	Home Depot	https://goo.gl/pECLr4
Pressure Transducer	2	$49.00	$98.00	Transducers Direct	TDH30BG025003B004	Transducers Direct	https://goo.gl/ZAUC21
Pressure Transducer DAQ	1	$250.00	$250.00	National Instruments	USB-6009	National Instruments	https://goo.gl/xaw9sP
Cart	1	$37.99	$37.00	US General	5107	Harbor Freight	https://goo.gl/gR9cP3
		Total:	**$866.82**				
		Our Cost:	$401.32				

Appendix H: Blade Deflection MATLAB Program

```
% turbine blade beam analysis
%Author: Jacob Barker

clear;
clc;
close all;

%%%%%%%%%%%%%%%%%%%%%%%%%%%%%%%%%%%%%%%%%%%%%%%%%%%%%%%%%%%%%%%%%%%%%%%%%%%%%%%

%prompt user to enter cross-sectional diameter (in)
d = input('Enter the cross-sectional diameter in inches: ');

%prompt user for volumetric flow rate
Q = input('Enter volumetric flow rate in CFM: ');

%prompt user for angular velocity
RPM = input('Enter angular velocity in RPM: ');

%prompt user to specify blade size
L = input('Enter length of blade in inches: ');
t = input('Enter blade thickness in inches: ');
c = input('Enter blade chord length in inches: ');

%prompt user to enter air density (will change based on elevation)
rho = input('Enter air denisty in slugs per cubic ft: ');

%prompt user to enter modulus of elasticity in ksi
E = input('Enter modulus of elasticity, E, in ksi: ');

%prompt user to enter material density in slugs per cubic ft
rho2 = input('Enter blade material density in slugs per cubic ft: ');

Ax = ((pi()/4)*d^2)/144;

Va = (Q/Ax)*(1/60);

Vt = L*(1/12)*RPM*(1/60)*(2*pi());

w1 = (1/2)*rho*(Vt^2)*c*(1/12);

w2 = (1/2)*rho*(Va^2)*t*(1/12);

It = (1/12)*c*(t^3);
Ia = (1/12)*t*(c^3);

d1 = ((11*w1*(L^4))/(120*E*It))*(1/12)*(1/1000);

d2 = ((w2*(L^4))/(8*E*Ia))*(1/12)*(1/1000);

dtot = sqrt(d1^2+d2^2);

sigma = rho2*((RPM*(1/60)*(2*pi()))^2)*((L^2)/2)*(1/144);


fprintf('The total deflection is %f inches\n', dtot)

fprintf('The stress due to centripetal acceleration is %f psi', sigma)
```

Appendix I: Final Device Photos

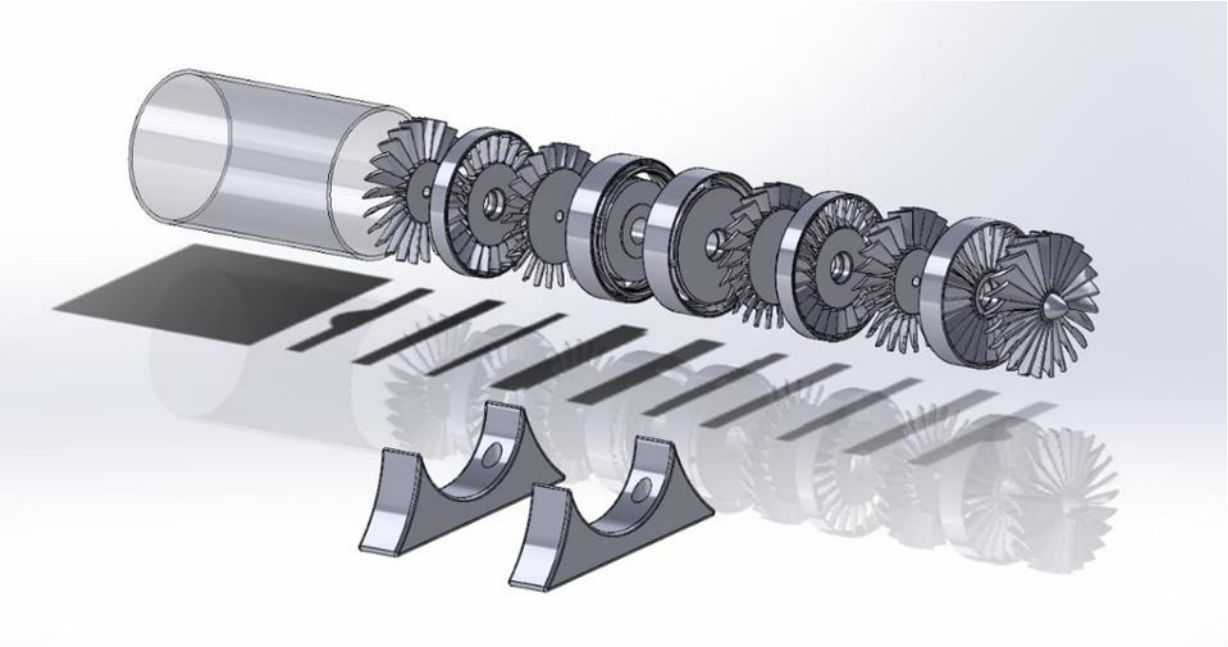

Figure I1: Final Turbojet Model Exploded View

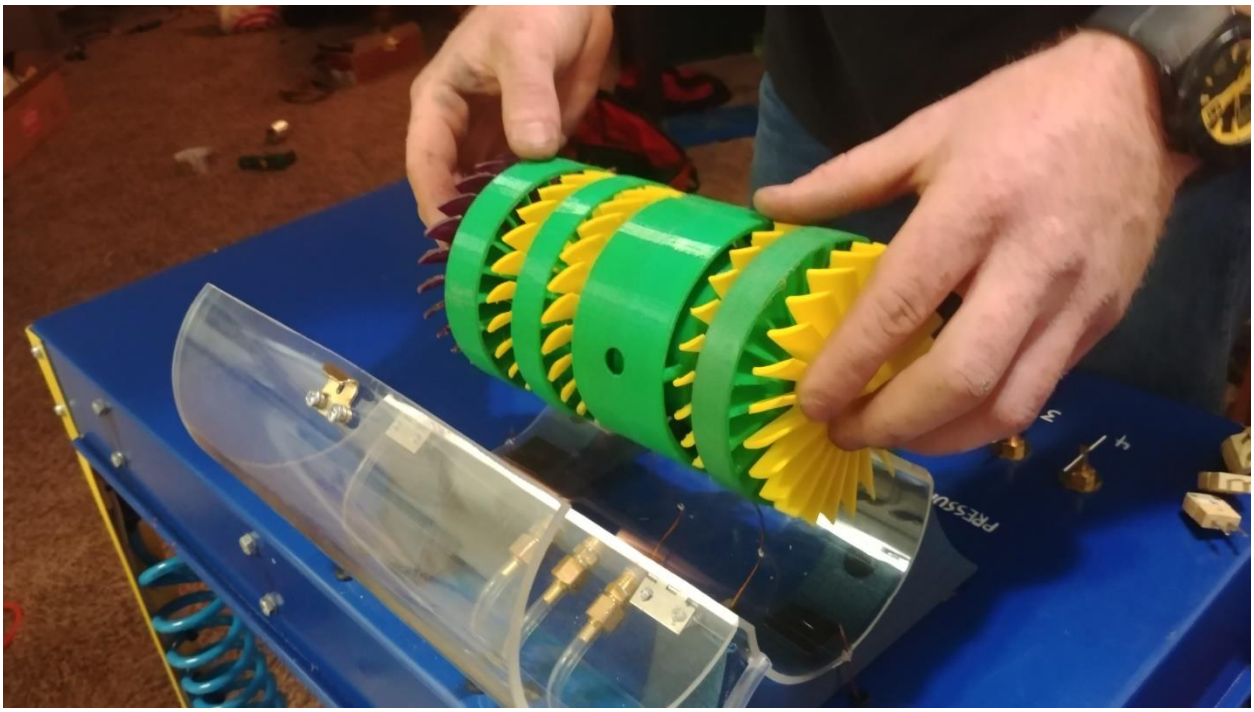

Figure I2: Turbojet Blade Removal Process

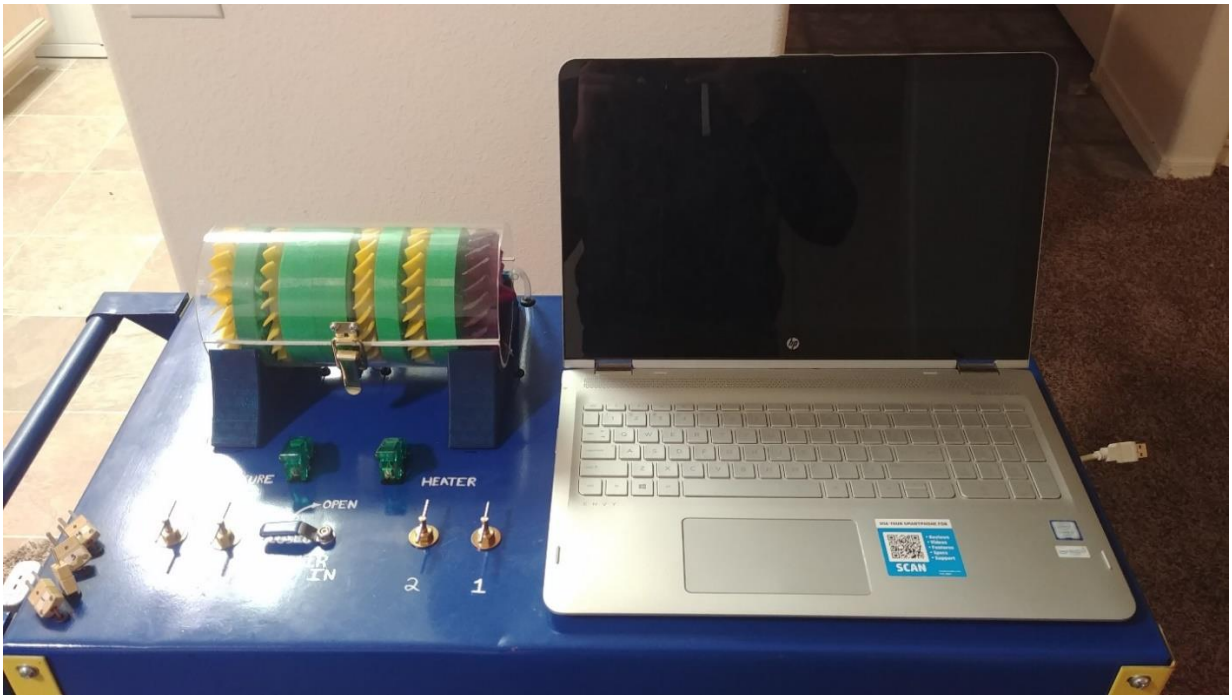

Figure I3: “Benchtop” View

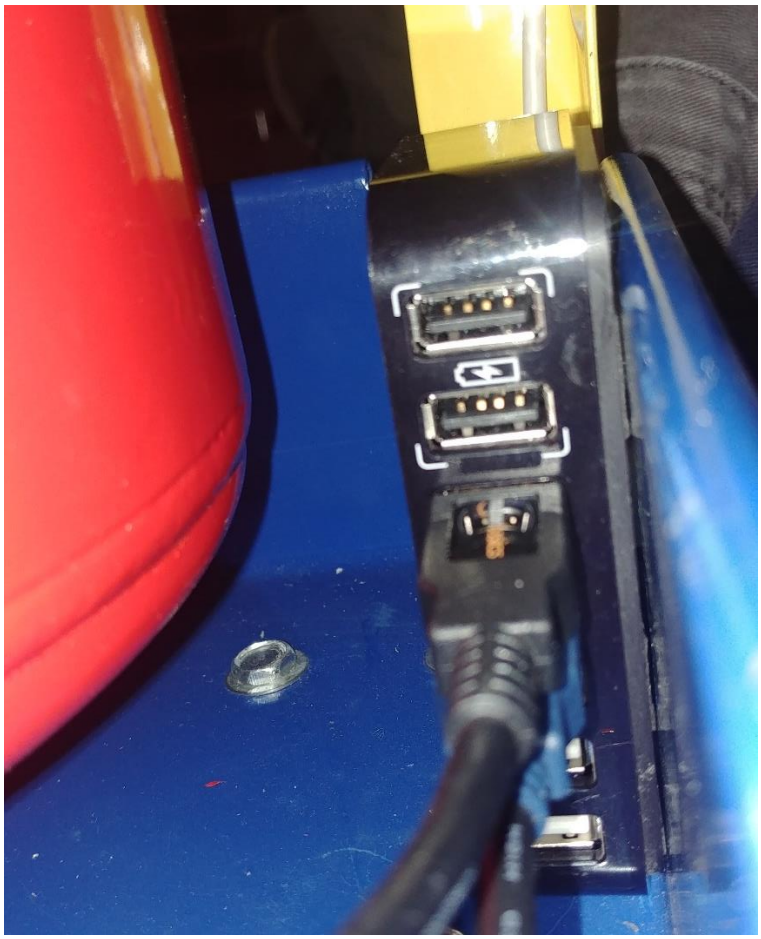
Figure I4: USB Adapter

Appendix J: Final Bill of Materials

Bill of Materials							
Item	**Quantity**	**Cost per unit**	**Subtotal**	**Manufacturer**	**Item #**	**Vendor**	**Hyperlink**
Acrylic Tubing	23 7/8 in	$0.10	$17.99	estreetplastics	ET0450042524	estreetplastics	https://goo.gl/rmKMEm
Compressor Chamber Side 1	77.5 g	$0.10	$7.75	MakerBot	N/A	NAU Cline Library	N/A
Compressor Chamber Side 2	88.1 g	$0.10	$8.81	MakerBot	N/A	NAU Cline Library	N/A
Compressor Stator 1	82.7 g	$0.10	$8.27	MakerBot	N/A	NAU Cline Library	N/A
Compressor Blade 1	69.3 g	$0.10	$6.93	MakerBot	N/A	NAU Cline Library	N/A
Compressor Blade 2	51.2 g	$0.10	$5.12	MakerBot	N/A	NAU Cline Library	N/A
Compressor Blade 3	57.3 g	$0.10	$5.73	MakerBot	N/A	NAU Cline Library	N/A
Compressor Stator 2	255 g	$0.10	$6.68	MakerBot	N/A	NAU Cline Library	N/A
Turbine Blade 1	292 g	$0.10	$4.27	MakerBot	N/A	NAU Cline Library	N/A
Turbine Blade 2	53.8 g	$0.10	$5.38	MakerBot	N/A	NAU Cline Library	N/A
Turbine Stator	62.8 g	$0.10	$6.28	MakerBot	N/A	NAU Cline Library	N/A
Saddle	142 g	$0.10	$14.22	MakerBot	N/A	NAU Cline Library	N/A
3D Printed Test Fitting #1	77.58 g	$0.10	$7.76	MakerBot	N/A	NAU Cline Library	N/A
3D Printed Test Fitting #2	64.28 g	$0.10	$6.43	MakerBot	N/A	NAU Cline Library	N/A
Aluminum Shaft	2 ft	$5.62	5.62	MetalsDepot	R3516	Metals Depot	https://goo.gl/CezFTP
Ceramic 608 Bearings	4	$3.33	$13.32	VXB	608-2RS-DRY	VXB	https://goo.gl/zPNP8M
Air compressor with tank	1	$89.00	$89.00	Porter Cable	C2002	CPO Commerce	https://goo.gl/KRQu8p
Band Heater	1	$28.50	$28.50	Tempco	NHL00100	Grainger	https://goo.gl/WnqnU8
Thermal Fuse	1	$17.60	$17.60	Grainger	Unknown	Unknown	Unknown
K Type Thermocouple Wire	25 ft	$0.86	$21.50	TIP Industries	TIPWRK004	TIP Industries	https://goo.gl/AETaH8
Thermocouple Connectors	4	$2.30	$9.20	Omega	OST-U-M	Omega	https://goo.gl/mftfh2
Thermocouple DAQ	1	$107.00	$107.00	National Instruments	USB-TC01	National Instruments	https://goo.gl/U5soAU
1/4 in. x 1/4 in. MIP Brass Compression Adapter	2	$4.40	$8.80	Everbilt	801079	Home Depot	https://goo.gl/z6qf8e
Brass Pipe Coupling 1/4 in. FIP	3	$4.16	$12.48	Everbilt	801889	Home Depot	https://goo.gl/VR7m58
Brass Compression Tee 1/4 in	2	$7.51	$15.02	Everbilt	800849	Home Depot	https://goo.gl/Nh2w24
1/4 in. Compression Angle Needle Valve	4	$8.80	$35.20	Everbilt	800539	Home Depot	https://goo.gl/NpVaUW
1/4 in. O.D. x 0.170 in. I.D. x 10 ft. PVC Clear Vinyl Tube	1	$2.82	$2.82	Everbilt	701906	Home Depot	https://goo.gl/pECLr4
1-1/2 in. x 6 in. Galvanized Steel Nipple	1	$6.36	$6.36	Mueller	567-060HN	Home Depot	https://goo.gl/UXY4mM
1-1/2 in. x 1 in. Galvanized FPT x FPT Reducing Coupling	2	$7.28	$14.56	Southland	511-375HN	Home Depot	https://goo.gl/Ce8sVk
1 in. x 1/2 in. Black Malleable Iron Hex Bushing	2	$3.18	$6.36	Mueller	521-953HN	Home Depot	https://goo.gl/9MQn86
5/16 in. Stainless Steel Flat Washer (5-Pack)	2	$1.18	$2.36	Everbilt	800351	Home Depot	https://goo.gl/fDHng4
1/2 in x 3/8 in Galvanized Bushing	2	$2.57	$5.14	Southland	182311	Home Depot	https://goo.gl/6aWxvy
Nylon Lock Nut 2-Pack	1	$2.36	$2.36	Everbilt	245218	Home Depot	https://goo.gl/BtqP9H
3/8 in Galvanized Plug	3	$2.20	$6.60	Southland	182052	Home Depot	https://goo.gl/WKZ5bR
1/2" Galvanized Plug	1	$1.98	$1.98	LDR Industries	182060	Home Depot	https://goo.gl/U5fNrW
Catch Latch	1	$5.69	$5.69	National Hardware	7161383	HomCo	N/A
Hinges 4 Pack	1	$2.99	$2.99	National Hardware	7174469	HomCo	N/A
Machine Screws	14	$0.11	$1.54	Unknown	999	HomCo	N/A
Foam Insulation Tape	1	$2.99	$2.99	Frost King	5343686	HomCo	N/A
Pressure Transducer	2	$49.00	$98.00	Transducers Direct	TDH30BG025003B004	Transducers Direct	https://goo.gl/ZAUC21
Pressure Transducer DAQ	1	$250.00	$250.00	National Instruments	USB-6009	National Instruments	https://goo.gl/xaw9sP
Cart	1	$37.99	$37.99	US General	5107	Harbor Freight	https://goo.gl/gR9cP3
Corner Bracket	2	$1.19	$2.38	Unknown	2049625	HomeCo	N/A
Air Tank	1	$10.00	$10.00	Ford	N/A	U-Pick-It	N/A
1/4 Brass Drain Cock	1	$2.99	$2.99	Merlin	63556	Harbor Freight	https://goo.gl/SAHF55
Teflon Tape	1	$0.79	$0.79	HTF	63944	Harbor Frieght	https://goo.gl/6rcRAd
Air Hose (Blue)	1	$14.98	$14.98	Husky	1000055182	Home Depot	https://goo.gl/WUUP4M
Air Hose (Black)	1	$4.99	$4.99	Central Pneumatic	91294	Harbor Frieght	https://goo.gl/pfgsWb
Copper Refrigeration Tube	1	$9.98	$9.98	Everbilt	647788	Home Depot	https://goo.gl/hwf21z
Power strip	1	$5.97	$5.97	Hyper Tough	564052687	Walmart	https://goo.gl/9nAJDc
1/4 in. Lead Free Brass Threaded FPT x FPT Ball Valve	1	$7.90	$7.90	Everbilt	870561	Home Depot	https://goo.gl/tnRoz9
Toggle switch	2	$4.49	$8.98	Gardner Bender	218779	Home Depot	https://goo.gl/n6yAYG
Toggle switch cover	2	$0.89	$1.78	Unknown	70412	JPM Supply	https://goo.gl/RUyeBu
Zip Ties	1	$2.97	$2.97	Hyper Tough	571708690	Walmart	https://goo.gl/gptBUK
Zip tie mounts (100 pack)	1	$14.97	$14.97	Commercial Electric	295956	Home Depot	https://goo.gl/WM3nd9
16 gauge wire	10	$0.18	$1.80	Pacer Marine	WUL16RD	Apex Lighting	https://goo.gl/45yywv
Blue spray paint	2	$3.98	$7.96	Rust-Oleum	615627	Home Depot	https://goo.gl/g2TNg7
Yellow spray paint	1	$3.98	$3.98	Rust-Oleum	619323	Home Depot	https://goo.gl/2ZrorH
Red spray paint	1	$3.98	$3.98	Rust-Oleum	1002239955	Home Depot	https://goo.gl/ScAYmL
		Total:	**$1,029.00**				
*Donated to our team		Our Cost:	$530.92				

Appendix K: Testing Results

Testing Round 1: Prototype Blades				
Trial	**Charge Time (min)**	**Run Time (min)**	**Heater Temp (°F)**	**Top Platform Temp (°F)**
0	----------	----------	64.8	62.8
1	05:16	00:57	135.7	77.1
2	05:22	01:07	185.1	90.7
3	05:25	01:13	174.8	89
4	05:20	01:07	158.8	90.2
5	05:23	01:14	162.8	90.3
6	05:20	01:18	179.2	97.5
7	05:21	01:14	155.5	88.4
8	05:22	01:16	153	90.5
9	05:20	01:18	161.2	87.4
10	05:19	01:17	169.2	89.3
INTERMISSION	----------	----------	76.8	69.5
11*	05:15	52:48	155	77.1
12	05:24	01:18	175	84.5
13	05:21	01:21	153	89.6
14	05:20	01:22	155	89.1
15	05:20	01:21	160.2	87.4
16	05:19	01:23	159.4	88.5
17	05:20	01:21	165.5	85.3
18	05:20	01:23	161.3	88.2
19	05:28	01:24	157.6	86.6
20	05:20	01:26	157.7	87.6
21	05:23	01:25	159.6	89.8
22	05:21	01:27	160.7	87.3
23	05:21	01:25	161	89.9
24	05:19	01:26	160.4	85.7
25	05:19	01:26	162.9	87.7
*Blades adjusted				

Testing Round 2: Final Blades				
Trial	**Charge Time (min)**	**Run Time (min)**	**Heater Temp (°F)**	**Top Platform Temp (°F)**
Initial			61.8	66.4
1	5:15	1:13	202	70.8
2	5:20	1:14	176	84.3
3	5:18	1:10	184	87.5
4	5:18	1:05	205	90.4
5	5:17	1:06	210	85.8
6*	5:17	0:32	211	89.5
7	5:15	0:59	176	88.7
8	5:15	1:13	189	88.4
9	5:18	1:22	200	91.3
10	5:14	1:08	162	69.5
11	5:21	1:06	182	80.6
12	5:21	1:17	211	83.4
13	5:22	1:08	183	78
14**	5:17	1:00	101	
15	5:19	1:24		
16	5:23	1:17		
17	5:24	1:16		
18	5:21	1:20		
19	5:22	1:15		
20	5:22	1:16		
21	5:21	1:18		
22	5:21	1:16		
23	5:22	1:10		
24	5:21	1:27		
25	5:21	1:19		
*Rubbing Issue				
**Heater malfunction				